Mississippi Transportation Research Center

U.S. Department
of Transportation
Federal Highway
Administration

HOT MIX ASPHALT (HMA) CHARACTERIZATION FOR THE 2002 AASHTO DESIGN GUIDE

REPORT NO.
FHWA/MS-RD-07-166

Prepared by
Dr. Thomas D. White, Joshua C. Littlefield,
Jamie Pittman, Robert C. Plummer
Jonathan R. Easterling and James R. Owens
Department of Civil and Environmental Engineering
Construction Materials Research Center (CMRC)
Mississippi State University
Mississippi State, MS
and
Dr. M. Shane Buchanan
Vulcan Materials
Birmingham, AL

September 30, 2008

JAMES WORTH BAGLEY COLLEGE OF ENGINEERING
MISSISSIPPI STATE UNIVERSITY
CIVIL & ENVIRONMENTAL ENGINEERING

Mississippi Transportation Research Center

HOT MIX ASPHALT (HMA) CHARACTERIZATION FOR THE 2002 AASHTO DESIGN GUIDE

REPORT NO. FHWA/MS-RD-07-166

Prepared by
Dr. Thomas D. White, Joshua C. Littlefield,
Jamie Pittman, Robert C. Plummer
Jonathan R. Easterling and James R. Owens
Department of Civil and Environmental Engineering
Construction Materials Research Center (CMRC)
Mississippi State University
Mississippi State, MS
and
Dr. M. Shane Buchanan
Vulcan Materials
Birmingham, AL

September 30, 2008

1.Report No.	2. Government Accession No.	3. Recipient's Catalog No.
FHWA/MS-DOT-RD-07-166		

4. Title and Subtitle	5. Report Date
Hot Mix Asphalt (HMA) Characterization for the 2002 AASHTO Design Guide	December 2007
	6. Performing Organization Code

7. Author(s)	8. Performing Organization Report No.
Thomas D. White, Joshua C. Littlefield, Jamie Pittman, Robert C. Plummer, Jonathan R. Easterling, and James R. Owens	MS-DOT-RD-07-166

9. Performing Organization Name and Address	10. Work Unit No. (TRAIS)
Mississippi State University Department of Civil Engineering P.O. Box 9546 Mississippi State, MS 39762	11. Contract or Grant No.

12. Sponsoring Agency Name and Address	13. Type Report and Period Covered
Federal Highway Administration Mississippi Department of Transportation	Final Report
	14. Sponsoring Agency Code

15. Supplementary Notes

16. Abstract The two study objectives were to conduct dynamic modulus and APA rutting tests of selected Mississippi HMA mixtures. A total of twenty-five mixtures were tested including aggregate combinations of gravel and gravel/limestone; 9.5mm, 12.5mm and 19.0mm NMAS gradations; asphalt binder grades of PG 67-22, PG 76-22 and 82-22; and compaction N_{design} levels of 50, 65 and 85. Twenty-four of the mixtures were designed for four percent air voids and one was designed for three percent air voids.

Sample preparation proved to be problematic. Target air void content for the dynamic modulus samples was 7.0±0.5 percent. Results (air voids) for a given compaction level can vary with gradation, aggregate type, asphalt content and mass of mix compacted. Another problem is the density gradient of Superpave gyratory compacted cylindrical samples. Developers of the test method minimized the density gradient by cutting a 100mm core from the larger, original 150mm sample. To achieve the target air void content of 7.0±0.5 percent for cored dynamic modulus test specimens, the 150mm samples were compacted to an air void level of approximately 8.0±0.5 percent. Because of uncertainty in the air void level that would be produced, four to five 150mm samples of a mixture were compacted with a goal of producing three with the target air void level. The cored 100 mm diameter test specimens were checked that the target 7.0±0.5 percent air void level was achieved. In some cases, new samples and cored specimens had to be prepared with an adjusted air void level.

After compaction, specimen preparation for dynamic modulus testing requires fixtures, coring equipment and saw rugged enough to produce specimens meeting required geometric tolerances. Some end spalling during sawing was largely stopped by wrapping duct tape around the specimen's ends.

Results of the study were parameters of the fitted sigmoid functions and associated shift factors of the master curve for twenty-fine HMA mixtures. MDOT will use these functions to estimate HMA dynamic modulus as input for calibrating the 2002 pavement design guide.

Asphalt Pavement Analyzer rutting test results for the twenty-five mixtures are compared with MDOT rutting criteria.

17. Key Words	18. Distribution Statement
Hot Mix Asphalt, Dynamic Modulus, Specimen Preparation, Master Curves, Shift Factors, APA	Unclassified

19. Security Classif. (of this report)	20. Security Classif. (of this page)	21. No. of Pages	22. Price
Unclassified	Unclassified		

Form DOT F 1700.7 (8-72) Reproduction of completed page authorized

TABLE OF CONTENTS

LIST OF TABLES

LIST OF FIGURES

CHAPTER 1 INTRODUCTION

1.1 INTRODUCTION

The Mississippi Department of Transportation (MDOT) currently uses the *1972 AASHTO Interim Guide for the Design of Pavement Structures*. This guide is empirically based and relates pavement serviceability (roughness, cracking, patching or rutting as is appropriate to the type of pavement surface) to layer structural capacity. Structural capacity in terms of structural number (SN) was defined by performance under controlled traffic of test sections with different layer combinations and thicknesses. The test sections were built and tested on the AASHO Road Test conducted from 1958 to 1961. As defined during analysis of the road test results, structural number is "an abstract number expressing the structural strength of pavement required for a given combination of soil support value, total equivalent 18-kip single-axle loads, terminal serviceability index, and regional factor. The required SN must be converted to actual thickness of surfacing, base, and subbase by means of appropriate layer coefficients representing the relative strength of the material to be used for each layer."

Currently the AASHTO 2002 *Guide for Design of New and Rehabilitated Pavement Structures* is being developed. This guide will potentially be adopted by the Mississippi Department of Transportation (MDOT) to design pavement structures. Ongoing research has focused on identifying laboratory tests producing results that can be correlated with pavement performance. In the case of flexible pavements, one focus has been a test of hot mix asphalt (HMA), the results of which correlate with field performance with respect to rutting, fatigue cracking, etc. A number of tests were evaluated for this relationship. Currently, the dynamic modulus test is being applied in the 2002 design guide. The test is run in accordance with AASHTO TP 62-03, *Standard Test Method for Dtermining Dynamic Modulus of Asphalt Concrete Mixtures.*

In application, the laboratory dynamic modulus test results are used to characterize HMA stiffness for pavement thickness design. During testing a sinusoidal compressive stress is applied to either unconfined or confined HMA sample. The dynamic modulus ($|E^*|$) is determined by dividing the peak dynamic stress by the peak recoverable axial strain. An additional parameter, the phase angle (ϕ) is defined as the

time lag between the applied stress and the resulting strain. A phase angle of 0 and 90 degrees indicates pure elastic and viscous materials, respectively.

Mississippi DOT is interested in developing dynamic modulus relationships for typical MDOT HMA mixtures. These relationships will facilitate MDOT's calibration and implementation of the new 2002 AASHTO Pavement Design Guide.

1.2 OBJECTIVES

Objectives of the research are to conduct dynamic modulus characterization of selected Mississippi HMA mixtures. As a result of these tests, MDOT will have functions to estimate HMA dynamic modulus as input to the 2002 pavement design guide. In addition, APA tests will be conducted on the HMA mixtures to provide MDOT a relative comparison of the mixture's potential inservice performance.

1.3 APPROACH

Mississippi DOT will identify candidate HMA mixtures to be tested. These mixtures will be characterized using the dynamic modulus test procedure. Three coarse-graded HMA mixes comprised of gravel and gravel / limestone aggregate will be evaluated. The gradations include three nominal maximum aggregate sizes of 9.5, 12.5, and 19.0 mm, respectively. Aggregate testing will include fine angularity and flat and elongated particle count.

The contribution of asphalt binder stiffness to the dynamic modulus will be evaluated by using PG 67-22 (unmodified), PG 76-22, and PG 82-22 asphalt binders. The PG 76-22 and 82-22 asphalt binders will be modified with styrene butadiene styrene (SBS) polymer.

Mix designs will be conducted for each factor level combination at N_{design} levels of 50, 65, and 85 gyrations. This will allow the effect of compactive effort, and thus varying asphalt content, to be determined for a given mixture type.

Dynamic modulus will be determined on triplicate test specimens, approximately 100 mm in diameter and 150 mm in height. The dynamic modulus results will be used to develop a database for use in the 2002 design guide. This database will enable the

pavement designer to readily retrieve dynamic modulus information for a specific mixture(s) and for a given design application.

Tested mixtures will also be evaluated using the asphalt pavement analyzer (APA) for comparison purposes. Mississippi DOT has performed APA testing on many mixes and a side-by-side comparison of the dynamic modulus and APA will be useful.

CHAPTER 2 MATERIALS AND MIXTURE DESIGNS

2.1 INTRODUCTION

Selection of mixtures for the study was based primarily on those combinations of materials routinely used on Mississippi highways. These included mixtures used for low, medium and high traffic volume pavements. There were adjustments in the actual mixtures tested as the study progressed. Mixtures were designed using MDOT Superpave mixture design procedures.

2.2 MIXTURE COMBINATIONS

In this study, selected Mississippi Department of Transportation coarse-graded HMA mixes comprised of gravel and limestone/gravel aggregate were tested to determine dynamic moduli and APA rutting. Within the two aggregate types, mixtures considered for testing included three nominal maximum aggregate sizes of 9.5 mm, 12.5 mm, and 19.0 mm and three performance grade (PG) asphalt binders, PG 67-22, PG 76-22, and PG 82-22. The various N_{design} levels used in the mix designs were 50, 65, and 85. Mississippi DOT Superpave procedures were utilized for mixture designs. Initially, twenty-four mixtures were designed for the standard 4 percent air voids. One of the twenty-four mixtures was also designed for 3 percent air voids. Table 2.1 shows the matrix of mixture combinations that were designed and tested.

2.3 ASPHALTS

Quantities of all three grades of asphalt, PG 67-22, PG 76-22, and PG 82-22 were provided by Ergon from their Vicksburg, MS facility.

2.4 AGGREGATES

All gravel and limestone aggregates were acquired from APAC Inc., Columbus, Mississippi. Aggregate quality tests were conducted and consisted of gradation analysis (AASHTO T 27), specific gravity and absorption (AASHTO T 84, AASHTO T 85), uncompacted voids for fine aggregates (AASHTO T 304), and percentage of fractured particles for coarse aggregates (ASTM D 5821-01). Each blended gradation is shown in

Table 2.2 and Figure 2.1 through Figure 2.3. Stockpile percentages for each aggregate blend are shown in Table 2.3. Blend specific gravity and absorption are shown in Table 2.4. Results for uncompacted voids and percentage of fractured particles testing are shown in Table 2.5 and Table 2.6, respectively.

2.5 MIX DESIGN

Mississippi Superpave mix design procedures (MDOT TMD 11-78) were utilized to determine design asphalt contents at four percent air voids for mixes 1 through 24. Mix 25 was designed for three percent air voids. Specimen bulk specific gravity was determined in accordance with AASHTO T-166. Theoretical maximum specific gravity tests were conducted on duplicate specimens in accordance with AASHTO T-209.

In preparation for mixing, aggregate batches to be mixed with the PG 67-22 binder were heated for four hours at 171ºC (340ºF). Aggregate batches to be mixed with the PG 76-22 and PG 82-22 asphalt binders were heated for four hours at 188ºC (370ºF). Concurrently, the PG 67-22 asphalt binder was heated for four hours at 155ºC (310ºF) prior to mixing with the aggregate. The PG 76-22 and PG 82-22 asphalt binders were heated at 171ºC (340ºF) for four hours followed by stirring with a low shear mixer for one hour prior to mixing with the aggregate. After mixing, mixtures prepared with PG 67-22 binder were short-term aged (cured) at 145ºC (294ºF) for 1.5 hours prior to compaction while mixtures with PG 76-22 and PG 82-22 binders were cured at 155ºC (311ºF). Mixing and compaction temperatures used for the study are shown in Table 2.7. After aging, mixtures were compacted to the target N_{design} using a Pine Gyratory Compactor.

Summary HMA mix design volumetric properties at design content are shown in Table 2.8. Data for each mix design are shown in Appendix A.

Table 2.1 Mixture Test Matrix

Gradation	Aggregate Type	Binder PG	NMAS Gradation	N_{design}	No. Dynamic, Modulus Replicates
Coarse	Gravel	67-22	9.5	50	3
				65	3
			12.5	50	3
				65	3
			19.0	50*	3 (3)
				65	3
				85	3
		76-22	9.5	85	3
			12.5	85	3
			19.0	85	3
		82-22	9.5	85	3
			12.5	85	3
	Limestone / Gravel	67-22	9.5	50	3
				65	3
			12.5	50	3
				65	3
			19.0	50	3
				65	3
				85	3
		76-22	9.5	85	3
			12.5	85	3
			19.0	85	3
		82-22	9.5	85	3
			12.5	85	3

* Mix Designed at 4% and 3% Air Voids

75

Table 2.2 Blended Aggregate Gradations

Sieve Size (mm)	Sieve Size (in)	Percent Passing, %					
		Gravel			Limestone/Gravel		
		9.5GR	12.5GR	19.0GR	9.5L/GR	12.5L/GR	19.0L/GR
25.0	1"	100.0	100.0	100.0	100.0	100.0	100.0
19.0	3/4"	100.0	100.0	99.5	100.0	100.0	97.4
12.5	1/2"	99.9	95.6	86.8	100.0	92.5	83.5
9.5	3/8"	94.5	87.0	73.3	96.8	79.6	69.6
4.75	# 4	60.7	51.8	43.4	62.7	49.9	46.2
2.36	# 8	40.7	33.2	28.4	38.4	34.2	33.5
1.18	# 16	29.8	23.5	20.9	26.5	25.9	26.3
0.600	# 30	23.4	18.1	16.5	20.4	20.5	21.4
0.300	# 50	12.3	10.5	9.9	11.4	12.4	12.7
0.150	#100	6.1	6.1	6.0	6.1	7.6	7.6
0.075	#200	4.5	4.7	4.7	4.4	5.9	5.9

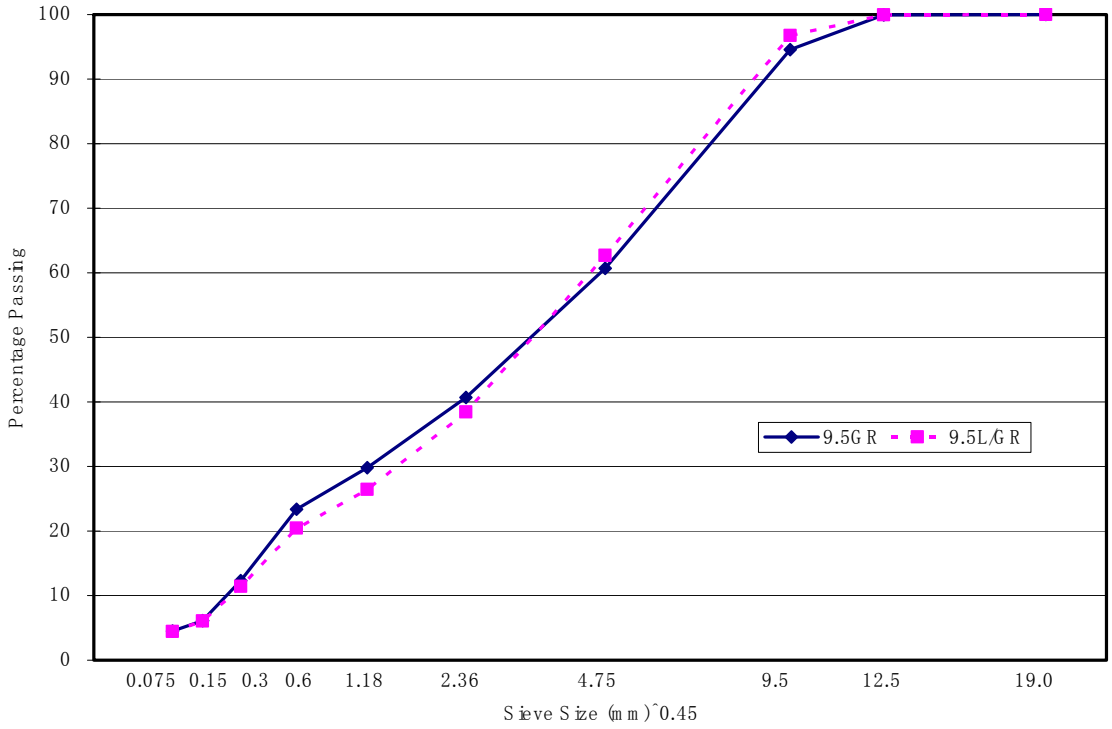

Figure 2.1 Blended 9.5 mm NMAS Gradations

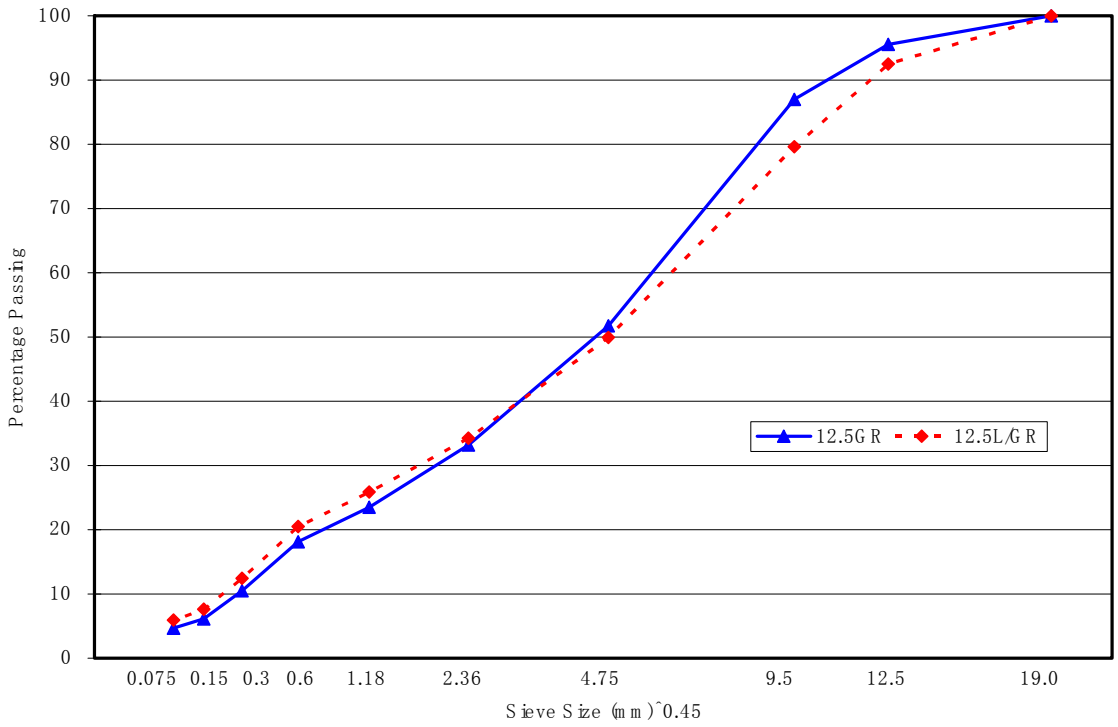

Figure 2.2 Blended 12.5 mm NMAS Gradations

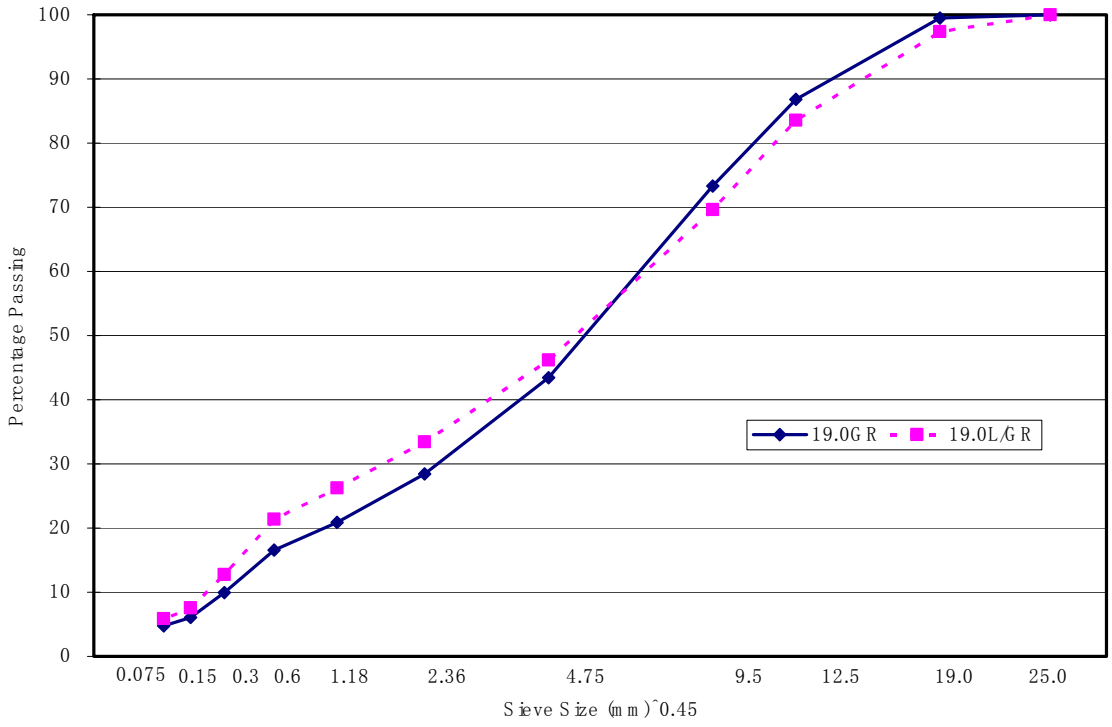

Figure 2.3 Blended 19.0 mm NMAS Gradations

Table 2.3 Stockpile Percentages for Blended Aggregate Gradations

Aggregate Stockpile		Percent Passing, %					
		Gravel			Limestone/Gravel		
mm	Designation	9.5GR	12.5GR	19.0GR	9.5L/GR	12.5L/GR	19.0L/GR
25.0	1" Gravel	0.0	0.0	25.0	0.0	0.0	0.0
19.0	3/4" Gravel	0.0	20.0	50.0	0.0	26.0	40.0
12.5	1/2" Gravel	79.0	67.0	14.0	40.0	21.0	0.0
9.5	3/8" Gravel	0.0	0.0	0.0	0.0	0.0	0.0
4.75	#57 Limestone	0.0	0.0	0.0	0.0	0.0	10.0
2.36	#78 Limestone	0.0	0.0	0.0	0.0	22.0	15.0
1.18	#89 Limestone	0.0	0.0	0.0	34.0	0.0	0.0
0.600	#8910 Limestone	0.0	0.0	0.0	10.0	18.0	20.0
0.300	Coarse Sand	20.0	12.0	10.0	15.0	12.0	14.0
0.150	Hydrated Lime	1.0	1.0	1.0	1.0	1.0	1.0

Table 2.4 Aggregate Blend Specific Gravity and Absorption

Aggregate Blend	Apparent Specific Gravity (Gsa)	Bulk Specific Gravity (Gsb)	Absorption (%)
9.5GR	2.637	2.435	3.15
12.5GR	2.634	2.422	3.32
19.0GR	2.63	2.411	3.45
9.5L/GR	2.668	2.519	2.22
12.5L/GR	2.677	2.523	2.28
19.0L/GR	2.682	2.538	2.12

Table 2.5 Fine Aggregate Uncompacted Voids

Mix Type	Uncompacted Voids, %
9.5GR	42.3
12.5GR	43.6
19.0GR	42.5
9.5L/GR	40.6
12.5L/GR	40.9
19.0L/GR	41.4

Table 2.6 Coarse Aggregate Percentage of Fractured Surfaces

Mix	No. of fractured surface	Count	Percentage, %	Weight	Percentage, %
9.5 GR	0	5	3.0	5.7	2.7
	1	15	9.1	14.3	6.9
	2	145	87.9	187.9	90.4
12.5 GR	0	8	2.3	8.3	3.2
	1	27	7.9	30.0	3.2
	2	307	89.8	220.0	85.2
19.0 GR	0	10	3.0	3.4	1.5
	1	33	9.9	25.1	11.2
	2	291	87.1	196.1	87.3
9.5 L/GR	0	6	1.1	2.8	1.2
	1	3	0.5	2.0	0.9
	2	553	98.4	221.4	97.9
12.5 L/GR	0	8	2.7	15.4	6.8
	1	7	2.4	4.5	2.0
	2	280	94.9	208.0	91.3
19.0 L/GR	0	5	1.6	9.2	3.6
	1	10	3.2	10.5	4.1
	2	295	95.2	233.4	92.2

Table 2.7 Mixing, Curing and Compaction Temperatures

Asphalt Binder	Temperature, ºC (ºF)		
	Mixing	Curing	Compaction
PG 67-22	155ºC (310ºF)	145ºC (294ºF)	145ºC (294ºF)
PG 76-22	171ºC (340ºF)	155ºC (310ºF)	155ºC (310ºF)
PG 82-22	171ºC (340ºF)	155ºC (310ºF)	155ºC (310ºF)

Table 2.8 Mixture Design Asphalt Content and Volumetric Properties

Mix Type		Design Asphalt Content (%)	Gmm	VMA (%)	VFA (%)	Pba (%)	Pbe (%)	Air Voids (%)	Dust/Effective Asphalt
1	9.5GR67-50	7.30	2.3054	15.7	74.6	0.9	6.5	4.0	0.7
2	9.5GR67-65	6.70	2.3054	15.2	73.7	0.9	5.9	4.0	0.8
3	9.5GR76-85	7.02	2.3312	14.5	72.5	1.4	5.7	4.0	0.8
4	9.5GR82-85	6.77	2.3438	13.9	71.1	1.6	5.2	4.0	0.9
5	12.5GR67-50	7.30	2.3019	15.4	74.1	1.0	6.4	4.0	0.7
6	12.5GR67-65	7.01	2.3019	15.2	73.6	1.0	6.1	4.0	0.8
7	12.5GR76-85	6.73	2.2983	15.0	73.4	0.9	5.8	4.0	0.8
8	12.5GR82-85	7.04	2.3159	14.7	72.7	1.3	5.8	4.0	0.8
9	19.0GR67-50	6.36	2.3035	14.1	71.7	1.2	5.2	4.0	0.9
10	19.0GR67-65	6.27	2.3035	14.0	71.5	1.3	5.1	4.0	0.9
11	19.0GR67-85	6.00	2.3035	13.8	71.0	1.3	4.8	4.0	1.0
12	19.0GR76-85	6.00	2.2874	14.4	72.2	0.9	5.1	4.0	0.9
13	9.5L/GR67-50	5.11	2.3991	13.2	69.8	1.3	3.9	4.0	1.1
14	9.5L/GR67-65	5.63	2.3991	13.7	70.8	1.3	4.4	4.0	1.0
15	9.5L/GR76-85	5.54	2.3890	14.0	71.4	1.1	4.5	4.0	1.0
16	9.5L/GR82-85	6.37	2.3898	14.7	72.8	1.1	5.3	4.0	0.8
17	12.5L/GR67-50	5.15	2.3745	14.3	72.0	0.8	4.4	4.0	1.3
18	12.5L/GR67-65	4.95	2.3745	14.1	71.7	0.8	4.2	4.0	1.4
19	12.5L/GR76-85	5.00	2.3748	14.2	71.7	0.8	4.3	4.0	1.4
20	12.5L/GR82-85	6.66	2.3897	15.1	73.6	1.1	5.7	4.0	1.0
21	19.0L/GR67-50	4.26	2.3846	13.6	70.7	0.7	3.6	4.0	1.7
22	19.0L/GR67-65	4.06	2.3846	13.5	70.3	0.7	3.4	4.0	1.8
23	19.0L/GR67-85	4.37	2.3846	13.7	70.9	0.7	3.7	4.0	1.6
24	19.0L/GR76-85	4.06	2.3796	13.6	70.7	0.6	3.5	4.0	1.7
25	19.0GR67-50	6.76	2.3035	15.3	73.9	2.3	4.6	3.0	1.0

As shown in Table 2.1, mix designs were conducted at different N_{design} levels. The process for determination of the design asphalt content is as follows:

- Find maximum specific gravity, G_{mm}, for each mix at 5.5% asphalt content.
- Find effective specific gravity, G_{se}, of the aggregate utilizing the G_{mm} found for 5.5% asphalt content.
- Find maximum specific gravity, G_{mm}, for each mix with asphalt contents of 4.5%, 5.5%, and 6.5%.
- Find bulk specific gravity, G_{mb}, for each mix at 4.5%, 5.5%, and 6.5% asphalt content after compaction at N_{design}.

- Find percent air voids, VTM, for each of the samples: $VTM = 100 \times (1 - \frac{G_{mb}}{G_{mm}})$
- Plot VTM versus asphalt content for each mix.
- Fit a line to the data and project at which asphalt content VTM is 3% or 4%, as required for each mixture.

CHAPTER 3 DYNAMIC MODULUS AND APA SPECIMEN PREPARATION AND TESTING

3.1 INTRODUCTION

Two types of tests were conducted on mixtures in this study, dynamic modulus and Asphalt Pavement Analyzer (APA) rutting. In the dynamic modulus test, cyclic loads over a range of frequencies are applied to a cylindrical specimen at each of a set of temperatures. Three replicate specimens of each mixture are tested and dynamic modulus results averaged. Separate cylindrical specimens were prepared and tested in the APA. The APA is a laboratory wheel test device to evaluate rutting potential. The Mississippi DOT has an experience base and criteria for APA rutting results. Four replicate specimens of each mixture were tested in the APA device.

3.2 DYNAMIC MODULUS SPECIMEN PREPARATION

In preparing specimens for dynamic modulus testing, the Superpave gyratory compactor is utilized to produce cylindrical specimens approximately 170mm high and 150mm in diameter. The resulting cylinders have a density gradient that varies from the periphery to the cylinder's axis with the outside of the cylinder being less dense. To minimize the effect of the density gradient in dynamic modulus test results, compacted specimens are cored with a 100mm core barrel centered on and parallel to the axis of the larger, original cylinder. Subsequently, both ends of the cored specimen are sawn so they are parallel. The resulting test specimen has a relatively uniform density. The average diameter of the cored test specimens is required to be between 100 and 104 mm with an average height between 147.5 and 152.5 mm. The air voids for each specimen is required to be between 6.5 and 7.5 %.

A Pine Superpave Gyratory Compactor Specimens was used to compact all specimens. The compaction process is not straight-forward as in compacting specimens for a mix design where the number of revolutions (N_{design}) is a set value. Target air void content for dynamic modulus test specimens is 7.0±0.5 percent. However, the 150mm Superpave Gyratory Compactor sample cannot be compacted directly to this air void level. When this is done the cored and sawn 100mm diameter test specimen had an air

void level approximately one percent lower than the required 7.0±0.5 percent (about 6 percent ±).To overcome this problem, the 150mm samples were compacted to an air void level of approximately 8.0±0.5 percent. To further complicate the problem, the air voids relation varies from mix to mix.

Because of the above problems, a trial and error process evolved where 150mm diameter samples were first compacted to a height of roughly 170mm. Bulk specific gravity and air void content for each sample were then measured. The target air void level for the samples after compaction was 8.0±0.5 percent. Because of uncertainty in the air void level that would be produced, four to five specimens of a mixture would be compacted with the hope three would prove to have the requisite target air void level. For each mixture, the air void level for each set of compacted specimens was determined; the mix mass was increased or decreased if the air void content was low or high, respectively, and a new set of specimens compacted. Limited calibration was achieved, but the process was repeated for each new mixture. There was improvement with experience.

When three samples with the appropriate air void content were produced, the 150 mm diameter samples were cored to obtain a 100 mm diameter test specimen and approximately 10 mm was sawed off each end producing a core 150 mm tall. Bulk specific gravity and air void content for each test specimen was measured after coring and sawing to ensure the target air void level of 7.0±0.5 percent. In some cases, new samples had to be compacted with an adjusted air void level and then cored and sawn to produce test specimens meeting the target test air voids.

The coring and sawing operations are shown in Figures 3.1 through 3.5. Both operations require positive specimen restraint and equipment powerful enough and rugged enough to smoothly cut the specimens. In the current study, a new, replacement saw was purchased and jigs fabricated to insure specimens meeting geometric tolerances could be prepared. As shown in Figures 3.3 and 3.5, duct tape was wrapped around the specimen's ends prior to sawing. The tape confined the ends, reducing spalling.

Figure 3.1. Preparing to Core Compacted Sample to Produce Dynamic Modulus Test Specimen

Figure 3.2. Cored Dynamic Modulus Test Specimen

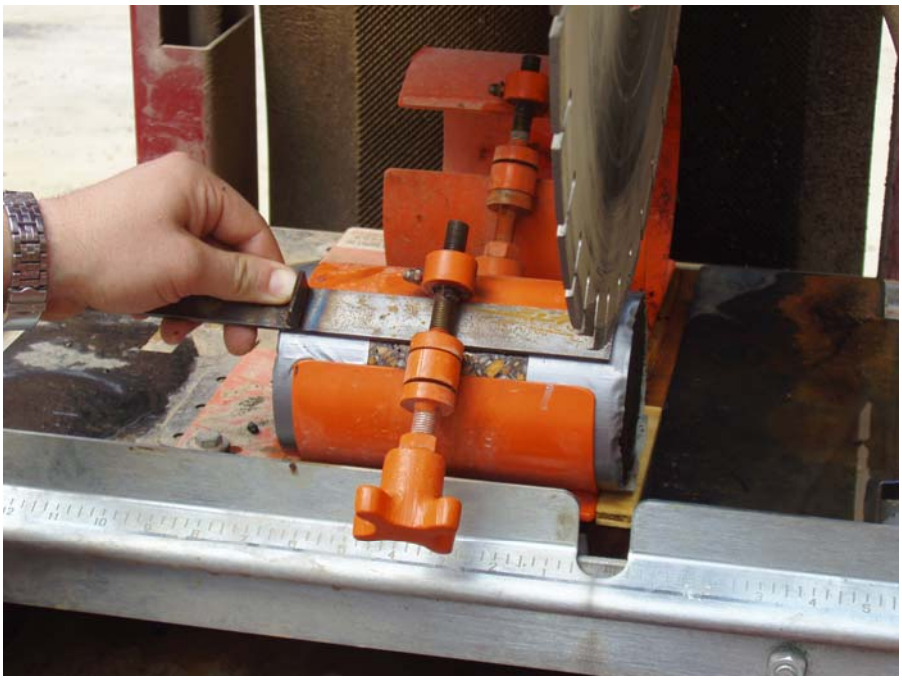

Figure 3.3. Preparing to Saw First End of Dynamic Modulus Test Specimen

Figure 3.4. Sawing End of Dynamic Modulus Test Specimen

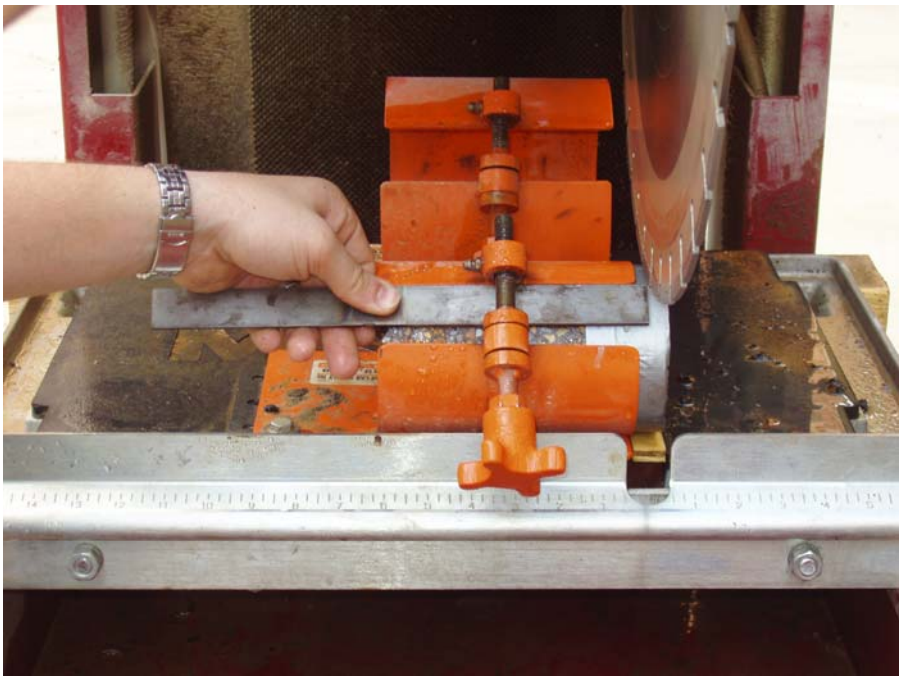

Figure 3.5. Preparing to Saw Opposite End of Dynamic Modulus Test Specimen

3.3 ASPHALT PAVEMENT ANALYZER SPECIMEN PREPARATION

Test specimens 150mm in diameter and 75±5 mm high were compacted using the Pine Superpave Gyratory Compactor for testing in the Asphalt Pavement Analyzer (APA). The same approach was taken in preparing APA specimens for testing as was used in preparing samples for dynamic modulus tests. To account for the density gradient of 150mm diameter gyratory compacted samples, the samples were compacted to a target air void level approximately one percent higher than the test air void level of 7.0±0.5 percent. Rutting is measured at the center of the test cylinder surface where the air void level would be expected to be at the 7.0±0.5 percent level.

Asphalt Pavement Analyzer total aggregate batch weight was determined by forming a simple ratio of the APA specified specimen height of 75 mm + 1.5 mm (an offset that is built into the Pine Gyratory Compactor) to the average height of the three specimens used for the dynamic modulus tests. This ratio was multiplied times the total aggregate batch weight used in the original specimen for the dynamic modulus test. This result is used as the total aggregate batch weight for the APA specimens.

With batch weights determined, aggregates and binder were heated, mixed, cured and compacted at temperatures used for preparing the dynamic modulus samples. Bulk

specific gravity and air voids were determined to insure the APA specimens were at the same air void level as samples for the dynamic modulus tests. A tolerance of ±0.5 percent for matching APA Specimen air voids with the air voids of the dynamic modulus sample was adopted. If specimens did not meet the tolerance they were remade until they did.

A more detailed explanation of the Asphalt Pavement Analyzer and its development and uses are given by Buchanan, et al.

3.4 DYNAMIC MODULUS TESTS

Dynamic Modulus tests were conducted on three replicate cores of each of the twenty-five mixtures in this study. Each specimen was tested at five temperatures: -10, 4, 21, 37, and 54ºC. A load producing an axial strain from between 50 and 150 microstrain is applied at five frequencies: 25, 10, 5, 1, 0.5, and 0.1 Hz (AASHTO TP 62-03). For some mixtures there were high temperature-load combinations that resulted in strain higher than the above strain criteria. In these cases new specimens were prepared and tested with reduced load. Mixture 25 failed to carry load at 54°C and loading frequencies of 0.1Hz and 0.5Hz (Highest temperature and two lowest frequencies of loading). The author had the same experience in running the test in the late 1960s when similar mixtures failed under self-weight at 40°C.

In preparation for testing, three vertical lines were marked at equal spacing (120°) around the circumference of each specimen. Subsequently, the specimens were placed in a jig and pairs of reference studs attached with epoxy. Figures 3.6 to 3.8 show the marking and stud attachment.

Figure 3.6 Marking Reference Lines

Figure 3.7 Placing epoxy on Studs

Figure 3.8 Attaching Studs to Specimen Using Jig

After the epoxy holding the studs cured the set of three specimens were placed in an environmental chamber set at the test temperature. The environmental chamber and closed loop electro-hydraulic test system used in the study are shown in Figure 3.9. A thermocouple was installed in a dummy specimen also in the environmental chamber to monitor temperature during conditioning and tests. Specimens were tested from lowest to highest temperature. After the set of specimens reached a target temperature, the strain gages (Asphalt Model 3910 Extensometers from Epsilon Technology Corporation) were attached to each pair of studs and connected to the data acquisition system as shown in Figure 3.10. Through control software, a static seating load was applied and then the periodic haversine load was applied automatically starting with the highest frequency. Load, deformation and temperature data were recorded and stored automatically. After subjecting each specimen to the loading sequence, the temperature of the environmental chamber was set to the next highest temperature and the procedure repeated until the set was tested for all temperatures.

The load and strain data are used to calculate a dynamic modulus and phase angle for each temperature frequency combination for the three replicate specimens. Average amplitude of load and average deformation of the three extensometers over the last five loading cycles are used to determine the specimen stress and strain (AASHTO TP 62-03).

$$\sigma_0 = \frac{\overline{P}}{A}$$

where

σ_0 = Average peak stress

$\overline{P}$ = Average amplitude of load over the last five loading cycles

A = Specimen cross sectional area.

Three extensometers were mounted on each specimen. Therefore three sets of deformation measurements are made with time and are the response to the sinusoidal loading. The average of these three deformations for the last five loading cycles is used to compute specimen strain (ε_0).

$$\varepsilon_0 = \frac{\overline{\Delta}}{GL}$$

where

$\overline{\Delta}$ = Average peak deformation for the three strain gauges for the last five lad cycles

GL = Initial gauge length

Specimen dynamic modulus (|E*|) for each for each loading frequency ($\boldsymbol{\omega}$) is computed

$$\left|E^*\right| = \frac{\sigma_0}{\varepsilon_0}$$

The phase angle (ϕ) is the lag in strain in response to load. Phase angle is computed for each strain gage for each cycle set of the dynamic modulus test.

$$\phi = \frac{t_i}{t_p}(360)$$

t_i = Average lag time between a cycle of stress (load) and corresponding cycle of deformation (strain)

t_p = Average time for a stress (load) cycle

Subsequently, the average phase angle is computed for each set of dynamic modulus tests, i.e. each temperature and frequency combination.

In summary, corresponding data sets of time, stress and strain are used to calculate dynamic modulus [|E*(ω)|] at a test frequency, ω, for each specimen tested. From the same data set an average phase angle, ϕ, between the load and strain is determined for the last five loading cycles. Table 3.1 shows the summary of dynamic modulus data for Mix 1. Data for all mixes are in Appendix B.

Figure 3.9 Environmental Chamber and Test Equipment

Figure 3.10 Attaching Extensometers

Table 3.1 Mix 1 Dynamic Modulus Summary

Temperature, °C	Frequency, Hz	Dynamic Modulus, psi			
		A	B	C	Average
-10	25	2637304	1761973	2387725	2262334
	10	2529084	1670636	2306228	2168649
	5	2438805	1614603	2229588	2094332
	1	2240194	1464418	2037050	1913887
	0.5	2141993	1396979	1943819	1827597
	0.1	1891148	1241528	1702177	1611618
4	25	1825279	1447866	1741300	1671482
	10	1657567	1279496	1569146	1502070
	5	1546643	1189964	1459427	1398678
	1	1272673	991296	1196245	1153405
	0.5	1152306	907609	1070749	1043555
	0.1	876746	705849	788478	790358
21	25	838131	802233	508602	716322
	10	685207	643618	643095	657307
	5	569005	545852	554946	556601
	1	359648	345229	359410	354762
	0.5	281586	278091	284038	281238
	0.1	294560	162568	161735	206288
37	25	406667	385005	304619	365431
	10	276736	240085	172388	229736
	5	205601	174511	132748	170953
	1	100004	79635	59608	79749
	0.5	76283	64253	46644	62393
	0.1	47587	39774	30387	39249
54	25	127529	115039	81451	108006
	10	62529	54685	45985	54400
	5	34171	28451	23846	28822
	1	20496	16884	13860	17080
	0.5	16903	14273	12407	14528
	0.1	13265	11306	10018	11530

3.5 APA TESTS

Asphalt Pavement Analyzer tests were conducted on four replicate cores of each of the twenty-five mixtures in this study. Prepared specimens are shown in Figure 3.11. The APA has three wheels and each can traverse two of specimens in sequence during a stroke. Specimens are inserted in preformed cylindrical holes so specimens are at the same elevation of the surrounding surface and alignment is maintained during testing. Figure 3.12 shows the APA interior. All four specimens of a mix were tested at the same time by using the middle and right wheels. Tests were conducted following procedures described by Buchanan, et al.. Test temperature was 64ºC (147°F). Hose pressure and load were 690 kPa (100psi) and 445 N (100 lbs), respectively. Tests were stopped when a total of 8000 wheel passes were applied to specimens. Back and forth stroke of the driving mechanism applies two wheel passes. Figure 3.13 shows specimens after testing.

The APA has automatic data recording. Average rutting of the two specimens tested by each wheel are recorded and plotted as deformation versus rutting as shown in Figure 3.14 for Mix 1. Rutting is plotted by wheel because there is a difference from wheel to wheel. Table 3.2 presents summary results of the average rutting for both wheels as well as specimen height and air voids for all mixtures tested. Rutting plots for all mixtures are in Appendix C.

Figure 3.11 Prepared APA Specimens

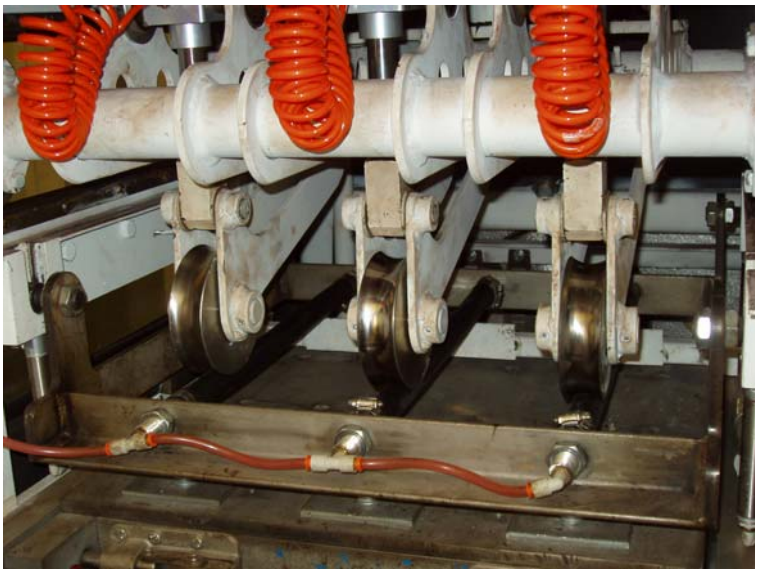

Figure 3.12 APA Test Chamber

Figure 3.13 Tested APA Specimens

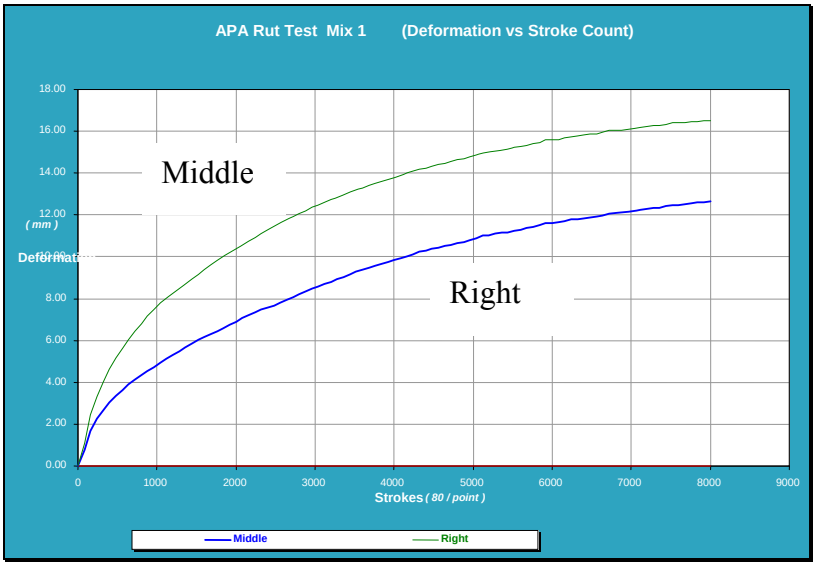

Figure 3.14 APA Rutting, Mix 1 (9.5GR67-22, N50)

Table 3.2 Summary APA Test Results

Sample ID	Aggregate Type	Binder Type	N_{design}	Binder Content, %	VMA, %	Height, mm	Air Voids, %	Average Air Voids, %	Rut Depth mm @64°C (147°F)
1A	9.5 GR	67-22	50	7.86	21.54	75.0	7.81	8.11	14.585
1B	9.5 GR	67-22	50			75.3	8.15		
1C	9.5 GR	67-22	50			75.2	8.12		
1D	9.5 GR	67-22	50			75.2	8.34		
2A	9.5 GR	67-22	65	7.18	20.44	75.5	8.22	8.33	13.559
2B	9.5 GR	67-22	65			75.6	8.25		
2C	9.5 GR	67-22	65			75.5	8.31		
2D	9.5 GR	67-22	65			75.6	8.56		
3A	9.5 GR	76-22	85	7.55	20.19	75.3	10.59	8.39	3.383
3B	9.5 GR	76-22	85			75.6	7.79		
3C	9.5 GR	76-22	85			75.6	7.32		
3D	9.5 GR	76-22	85			75.6	7.87		
4A	9.5 GR	82-22	85	7.27	19.29	75.7	8.30	8.21	3.740
4B	9.5 GR	82-22	85			75.7	8.66		
4C	9.5 GR	82-22	85			75.6	7.84		
4D	9.5 GR	82-22	85			75.6	8.05		
5A	12.5 GR	67-22	50	7.88	21.25	75.4	7.95	8.04	14.279
5B	12.5 GR	67-22	50			75.4	8.13		
5C	12.5 GR	67-22	50			75.5	7.49		
5D	12.5 GR	67-22	50			75.5	8.61		
6A	12.5 GR	67-22	65	7.52	20.70	75.5	8.27	8.12	13.494
6B	12.5 GR	67-22	65			75.5	7.82		
6C	12.5 GR	67-22	65			75.6	7.70		
6D	12.5 GR	67-22	65			75.5	8.68		
7A	12.5 GR	76-22	85	7.21	20.30	76.0	8.73	8.54	4.058
7B	12.5 GR	76-22	85			76.3	8.72		
7C	12.5 GR	76-22	85			76.4	8.63		
7D	12.5 GR	76-22	85			76.2	8.10		
8A	12.5 GR	82-22	85	7.59	20.31	75.7	8.15	7.96	3.262
8B	12.5 GR	82-22	85			75.6	8.14		
8C	12.5 GR	82-22	85			75.6	7.82		
8D	12.5 GR	82-22	85			75.6	7.72		
9A	19 GR	67-22	50	6.78	19.05	75.6	7.29	7.71	7.380
9B	19 GR	67-22	50			75.6	8.00		
9C	19 GR	67-22	50			75.6	7.50		
9D	19 GR	67-22	50			75.6	8.04		
10A	19 GR	67-22	65	6.68	18.82	75.6	8.64	8.19	9.320
10B	19 GR	67-22	65			75.7	7.56		
10C	19 GR	67-22	65			75.7	7.89		
10D	19 GR	67-22	65			75.6	8.69		
11A	19 GR	67-22	85	6.39	18.30	76.5	7.84	7.58	8.340
11B	19 GR	67-22	85			76.5	7.62		
11C	19 GR	67-22	85			76.5	7.12		
11D	19 GR	67-22	85			76.4	7.76		
12A	19 GR	76-22	85	6.36	18.91	75.6	8.55	7.65	3.859
12B	19 GR	76-22	85			75.6	8.59		
12C	19 GR	76-22	85			75.7	5.93		
12D	19 GR	76-22	85			75.6	7.55		
13A	9.5 GR/LMS	67-22	50	6.20	18.34	76.0	8.42	9.20	11.655
13B	9.5 GR/LMS	67-22	50			75.9	9.40		
13C	9.5 GR/LMS	67-22	50			75.9	9.19		
13D	9.5 GR/LMS	67-22	50			75.9	9.78		

Table 3.2 (continued)

Sample ID	Aggregate Type	Binder Type	N_{design}	Binder Content, %	VMA, %	Height, mm	Air Voids, %	Average Air Voids, %	Rut Depth mm @ 64°C (147°F)
14A	9.5 GR/LMS	67-22	65	5.98	17.92	76.1	8.19	8.17	8.389
14B	9.5 GR/LMS	67-22	65			76.2	8.29		
14C	9.5 GR/LMS	67-22	65			76.2	8.27		
14D	9.5 GR/LMS	67-22	65			76.2	7.95		
15A	9.5 GR/LMS	76-22	85	5.86	18.08	75.5	8.63	8.02	3.974
15B	9.5 GR/LMS	76-22	85			75.7	7.96		
15C	9.5 GR/LMS	76-22	85			75.7	8.08		
15D	9.5 GR/LMS	76-22	85			75.6	7.43		
16A	9.5 GR/LMS	82-22	85	6.80	19.71	76.6	7.91	8.57	3.159
16B	9.5 GR/LMS	82-22	85			76.3	8.57		
16C	9.5 GR/LMS	82-22	85			76.3	8.65		
16D	9.5 GR/LMS	82-22	85			76.3	9.17		
17A	12.5 GR/LMS	67-22	50	5.44	17.94	75.9	8.54	8.11	9.202
17B	12.5 GR/LMS	67-22	50			75.9	8.08		
17C	12.5 GR/LMS	67-22	50			75.9	7.91		
17D	12.5 GR/LMS	67-22	50			75.8	7.92		
18A	12.5 GR/LMS	67-22	65	5.20	17.51	75.9	7.30	7.35	8.404
18B	12.5 GR/LMS	67-22	65			76.0	7.62		
18C	12.5 GR/LMS	67-22	65			75.9	7.25		
18D	12.5 GR/LMS	67-22	65			75.9	7.24		
19A	12.5 GR/LMS	76-22	85	5.25	17.59	76.4	8.41	8.52	1.688
19B	12.5 GR/LMS	76-22	85			76.4	8.97		
19C	12.5 GR/LMS	76-22	85			76.2	8.53		
19D	12.5 GR/LMS	76-22	85			76.3	8.15		
20A	12.5 GR/LMS	82-22	85	7.14	20.41	75.3	7.08	7.80	3.405
20B	12.5 GR/LMS	82-22	85			75.0	8.48		
20C	12.5 GR/LMS	82-22	85			75.3	7.27		
20D	12.5 GR/LMS	82-22	85			75.2	8.40		
21A	19 GR/LMS	67-22	50	4.44	16.23	75.5	7.91	7.75	6.048
21B	19 GR/LMS	67-22	50			75.2	7.54		
21C	19 GR/LMS	67-22	50			75.2	7.48		
21D	19 GR/LMS	67-22	50			75.1	8.07		
22A	19 GR/LMS	67-22	65	4.22	15.81	75.6	7.15	8.09	7.040
22B	19 GR/LMS	67-22	65			75.6	9.28		
22C	19 GR/LMS	67-22	65			75.6	7.98		
22D	19 GR/LMS	67-22	65			75.6	7.96		
23A	19 GR/LMS	67-22	85	4.58	16.47	75.5	7.23	7.89	7.096
23B	19 GR/LMS	67-22	85			75.5	8.43		
23C	19 GR/LMS	67-22	85			75.6	7.60		
23D	19 GR/LMS	67-22	85			75.6	8.28		
24A	19 GR/LMS	76-22	85	4.22	15.99	75.6	8.93	8.71	3.252
24B	19 GR/LMS	76-22	85			75.6	7.91		
24C	19 GR/LMS	76-22	85			75.5	9.07		
24D	19 GR/LMS	76-22	85			75.6	8.92		
25A	19 GR	67-22	50	4.43	12.39	75.8	7.60	8.01	9.105
25B	19 GR	67-22	50			75.7	8.34		
25C	19 GR	67-22	50			75.7	8.00		
25D	19 GR	67-22	50			75.7	8.10		

CHAPTER 4 RESULTS

4.1 INTRODUCTION

Dynamic modulus test results from Chapter 3 are utilized to fit a master curve, produce shift factors [α(T)], and develop predictive equations from which dynamic moduli can be estimated for Mississippi HMAs. The shift factors provide the magnitude of data shift for tests at different temperatures relative to a reference temperature. A sigmoid function is fitted to the shifted data to produce the master curve.

4.2 MASTER CURVE AND SHIFT FACTORS

Within limits HMA has been defined as viscoelastic which means it is a time and temperature dependent material. Dynamic modulus is used in the 2002 Design Guide to characterize HMA stiffness for varying temperature and time (rate of loading). Laboratory dynamic moduli data as described in Chapter 3 can be utilized to produce functions estimating HMA dynamic modulus for use in the 2002 Design Guide. In developing the functions for a given HMA a master curve and shift factors are required. The master curve accounts for time (rate of loading) effects and shift functions account temperature effects.

From the laboratory data dynamic modulus is computed for each loading frequency for each temperature for which tests were conducted. The master curve is a semi-log plot of dynamic modulus versus log reduced time as shown in Figure 4.3. The master curve is developed by selecting a reference temperature (21°C) and reference frequency (1Hz) and shifting the data sets at other temperatures right and left until a single smooth curve is produced. The shift magnitudes for each temperature are used to produce a shift factor function. A sigmoid function is fitted to the experimental master curve that then provides an estimate of dynamic modulus for varying temperature and rate of loading.

The sigmoid function fitting the master curve is (Witzcak and Sotil):

$$\log(|E^*|) = \delta + \frac{\alpha}{1 + e^{\beta + \gamma \log(t_r)}}$$

where

$|E^*|$ = dynamic modulus, psi
δ = Minimum value of |E*|
$\delta + \alpha$ = Maximum value of |E*|
β, γ = empirical coefficients describing the shape of the sigmoidal function
t_r = reduced time of loading at reference temperature

The shift factor provides a relationship between temperature and time of loading and is given by:

$$\alpha(T) = \frac{t}{t_r}$$

$$t_r = \frac{t}{\alpha(T)}$$

and

$$\log(t_r) = \log)t) - \log[\alpha(T)]$$

where

$\alpha(T)$ = shift factor as a function of temperature
t = time of loading at target temperature
t_r = reduced time of loading at reference temperature

The above relation allows the time of loading at any temperature can be translate to a reduced time of loading at the reference temperature.

The shift factor, α(T), as a function of temperature, can be a linear or non-linear function. Recommendations (Witczak and Sotil) are to fit a second order polynomial to account for either case. For example,

$$\alpha(T) = aT^2 + bT + c$$

where
T = target temperature
a, b, c = regression coefficients

In application, after the function for estimating |E*| is fitted to the master curve and the function for the shift factor fitted, |E*|, can be estimated for target temperatures and rates of loading. A value of the shift factor, α(T), is determined at a temperature T. Then log(t), log of time of loading at the target temperature (1/f), and log[α(T)], log of shift factor, are used to obtain log(t_r), log of reduced time at reference temperature. Subsequently, |E*| is determined.

The process of fitting the master curve and determining the shift factors utilizes a series of Excel spreadsheets involving the Excel solver routine. Application of the spreadsheets in solving for the shift factors and coefficients for the predicting equation is given as a set of numbered steps:

1. In Figure 4.2, the average dynamic moduli values (|E*|) from Figure 4.1 are entered in column D for each temperature-loading frequency combination shown in columns B and C, respectively.
2. The log of measured dynamic modulus is entered in column G.
3. Time of loading is shown in column E and is the reciprocal of the loading frequency (1/f).
4. In determining the log of reduced time, data is normalized to a reference temperature and loading frequency. For the current data, the reference temperature and loading frequency are 21°C and 1 Hz, respectively. In Figure 4.2, the log of reduced times in cells 22F to 27F for the reference temperature of 21°C are the log of time in columns 22E to 27E..
5. Log reduced times at loading times for other than the reference temperature of 21°C are obtained by adding the incremental log reduced time between 1Hz, 21°C (0.0000) and some other frequency at 21°C to the log reduced time at 1 Hz for any other temperature. This process is part of fitting the sigmoid function to the experimental data. For example, in the solution for mix 1 in Figure 4.2, log reduced time for 5 Hz, -10°C is log reduced time for 1 Hz, -10°C plus log reduced time for 5 Hz, 21°C (-4.7215-0.6990 = -5.4205)
6. In the Excel solver routine, coefficients for the predicting equation and the shift factors are varied to minimize the error term. . The squares of the differences in the log of the

measured dynamic moduli (column G) and the log of the predicted dynamic moduli (column H) represents the error produced by the predicting equation and are shown in column I..

7. The Excel solver routine is based upon trial and error. As a result, initial values of the predicting equation coefficients must be estimated. They can be estimated from previous tests or test results reported in the literature (Witczak and Sotil). Also, once the coefficients are determined for one mixture they can be used as starting points for the other mixtures. Initial values are entered and final values shown in cells L10 to O10.
8. For Mix 1, the shift factors, [α(T)] (log reduced time), for 1 Hz, any temperature shown in Table 4.1 are plotted in Figure 4.3. Similarly, predicted and measured dynamic modulus values are plotted against log reduced time to obtain the master curve shown in Figure 4.4.

.

A summary of the empirical coefficients and shift factors for each mixture are given in Table 4.2. Data and master curves for each mix are provided in Appendix B. Note that arrows on each master curve are drawn to emphasize the shift from the measured values of dynamic modulus to the predicted values of dynamic modulus.

	A	B	C	D	E	F	G	H
1								
2		Temperature, °C	Frequency, Hz	Dynamic Modulus, psi				
3				A	B	C	Average	
4		-10	25	2637304	1761973	2387725	2262334	
5			10	2529084	1670636	2306228	2168649	
6			5	2438805	1614603	2229588	2094332	
7			1	2240194	1464418	2037050	1913887	
8			0.5	2141993	1396979	1943819	1827597	
9			0.1	1891148	1241528	1702177	1611618	
10		4	25	1825279	1447866	1741300	1671482	
11			10	1657567	1279496	1569146	1502070	
12			5	1546643	1189964	1459427	1398678	
13			1	1272673	991296	1196245	1153405	
14			0.5	1152306	907609	1070749	1043555	
15			0.1	876746	705849	788478	790358	
16		21	25	838131	802233	508602	716322	
17			10	685207	643618	643095	657307	
18			5	569005	545852	554946	556601	
19			1	359648	345229	359410	354762	
20			0.5	281586	278091	284038	281238	
21			0.1	294560	162568	161735	206288	
22		37	25	406667	385005	304619	365431	
23			10	276736	240085	172388	229736	
24			5	205601	174511	132748	170953	
25			1	100004	79635	59608	79749	
26			0.5	76283	64253	46644	62393	
27			0.1	47587	39774	30387	39249	
28		54	25	127529	115039	81451	108006	
29			10	62529	54685	45985	54400	
30			5	34171	28451	23846	28822	
31			1	20496	16884	13860	17080	
32			0.5	16903	14273	12407	14528	
33			0.1	13265	11306	10018	11530	
34								

Raw Data | Master Curve

Figure 4.1 Dynamic Modulus Spreadsheet

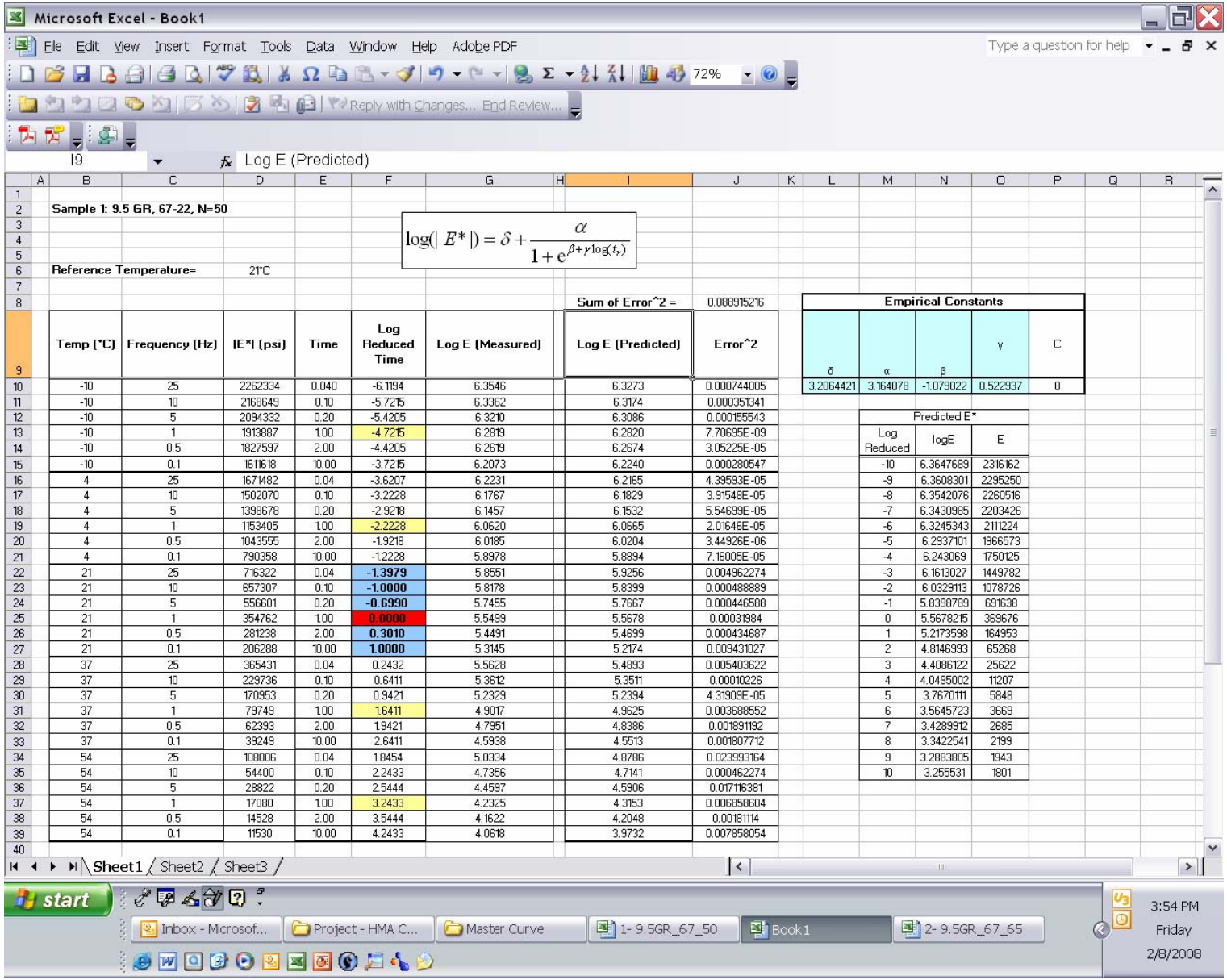

Figure 4.2 Master Curve Spreadsheet

Table 4.1 Shift Factor

Temperature, ° C	Log[α (T)]
-10	4.7215
4	2.2228
21	0.0000
37	-1.6411
54	-3.2433

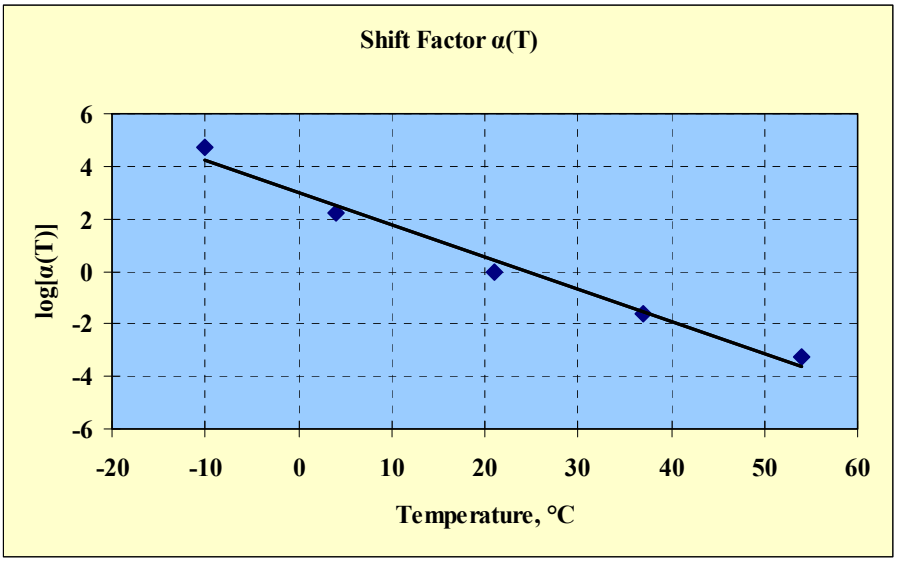

Figure 4.3 Shift Factors for Mix 1

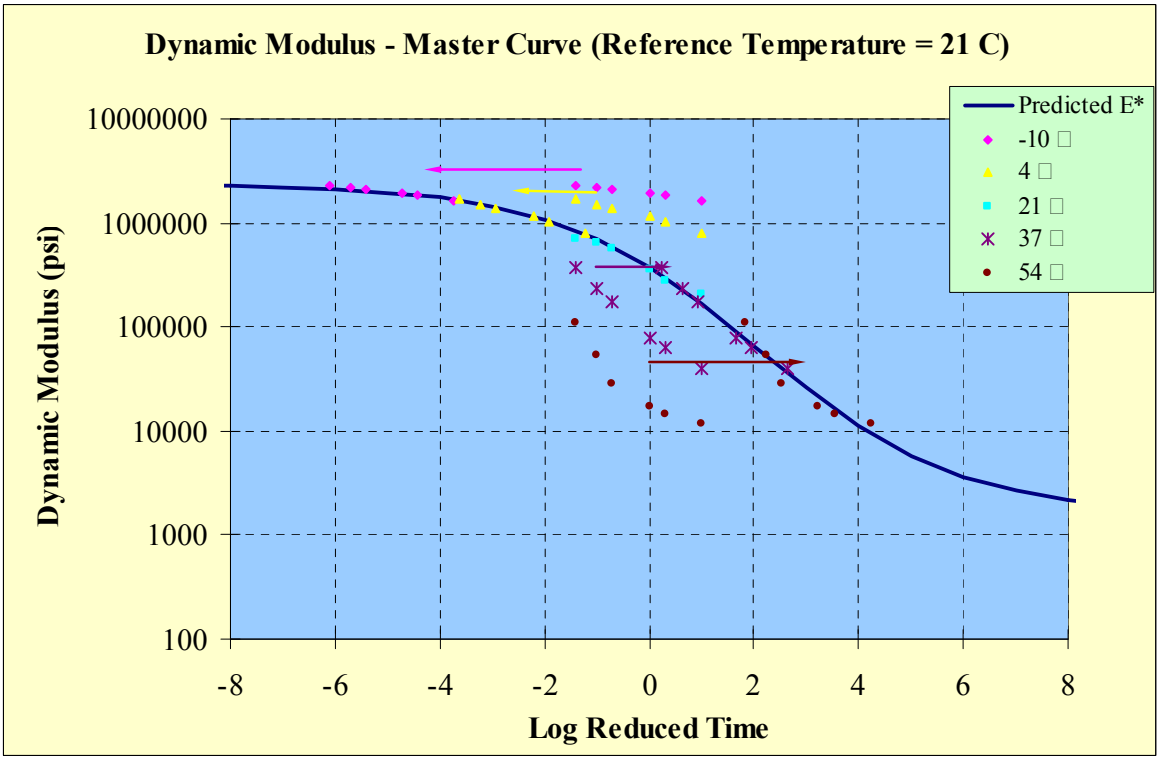

Figure 4.4 Master Curve for Mix 1

Table 4.2 Coefficients for Prediction Equation and Shift Factors

Mix	Coefficients				Shift Factors				
	δ	α	β	γ	-10°C	4°C	21°C	37°C	54°C
1	3.2064	3.1641	-1.0790	0.5229	4.7215	2.2228	0.0000	-1.6411	-3.2433
2	3.4203	3.0148	-1.1554	0.5659	4.5998	2.2532	0.0000	-1.6217	-3.2070
3	3.8108	2.5865	-0.8166	0.5950	4.4009	2.0596	0.0000	-1.6552	-2.9341
4	3.7831	2.6176	-1.1739	0.5588	5.1276	2.0294	0.0000	-1.7690	-3.0459
5	3.1748	3.2177	-1.4625	0.5457	5.4290	2.0296	0.0000	-2.3027	-3.7863
6	3.3403	3.0456	-1.4103	0.5733	5.4504	1.9846	0.0000	-2.2565	-3.6225
7	3.9670	2.3493	-0.7667	0.6473	4.0693	2.2224	0.0000	-1.2958	-2.6153
8	3.9021	2.4262	-0.7133	0.6287	4.1866	2.1743	0.0000	-1.3455	-2.4989
9	3.4578	2.8671	-0.9708	0.6108	4.2245	2.1440	0.0000	-1.1636	-2.8369
10	3.3989	2.9266	-0.9988	0.6035	4.2504	2.1543	0.0000	-1.3557	-2.8817
11	3.4769	2.8466	-0.9636	0.6174	4.2078	2.1323	0.0000	-1.1839	-2.6857
12	3.7515	2.6699	-0.8859	0.5494	4.6854	1.8690	0.0000	-1.2823	-2.6040
13	3.8861	2.5259	-0.9606	0.6583	4.5444	2.1347	0.0000	-1.5539	-2.9432
14	3.9811	2.4390	-0.9423	0.6759	4.3838	2.0895	0.0000	-1.4922	-2.9390
15	3.9821	2.5136	-0.7239	0.5659	4.5858	2.2007	0.0000	-1.4388	-2.7401
16	3.9823	2.3224	-0.9016	0.6504	3.6740	1.9551	0.0000	-1.7082	-2.9477
17	3.9796	2.5228	-1.0170	0.6421	4.6568	2.1130	0.0000	-1.5561	-3.0730
18	3.9904	2.5210	-0.8502	0.6040	5.2092	2.3326	0.0000	-1.6478	-3.0384
19	4.1267	2.2556	-0.8004	0.6494	4.3684	1.9557	0.0000	-1.2949	-2.7197
20	4.0392	2.4633	-0.8347	0.6260	5.3152	2.3092	0.0000	-2.1596	-3.3747
21	3.9349	2.5797	-0.8776	0.5941	5.1852	2.3405	0.0000	-1.0927	-2.6627
22	3.8774	2.6395	-0.9064	0.5830	5.2087	2.3575	0.0000	-1.0736	-2.5952
23	3.6548	2.8599	-1.1335	0.5364	5.8499	2.1906	0.0000	-1.3778	-2.9443
24	4.0129	2.4887	-0.7730	0.5578	5.4879	2.2106	0.0000	-1.6209	-2.8250
25*	2.4967	3.9736	-1.3659	0.4443	4.6798	2.3757	0.0000	-1.7377	-2.9990

*For Mix 25, at a temperature of 54°C, dynamic modulus results for testing at frequencies of 0.5-Hz and 0.1-Hz were not obtained. The test failed at these frequencies due to deformation of the core tested at the lowest specified loading.

4.3 APA Results

Asphalt Pavement Analyzer criteria for laboratory prepared and compacted specimens was developed by Buchanan, et al. The criteria are given in Table 4.3.

Table 4.3 MDOT APA Laboratory Rutting Criteria

Mixture Type	ESALs	Maximum Allowable APA Lab Rutting, mm
LT	$<1x10^6$	12
MT	1 to $3x10^6$	
HT	$>3x10^6$	6

Table 4.4 shows mixtures meeting the HT criteria (6mm) and Table 4.5 shows mixtures meeting MT and LT criteria.

Table 4.4 Mixtures Meeting HT Criteria (Shaded)

Gradation	Aggregate Type	Binder PG	NMAS Gradation	N_{design}	Rut Depth @64°C, mm
Coarse	Gravel	67-22	9.5	50	14.585
				65	13.559
			12.5	50	14.279
				65	13.494
			19.0	50	7.380
				50*	9.105
				65	9.320
				85	8.340
		76-22	9.5	85	3.383
			12.5	85	4.058
			19.0	85	3.859
		82-22	9.5	85	3.740
			12.5	85	3.262
	Limestone / Gravel	67-22	9.5	50	11.655
				65	8.389
			12.5	50	9.202
				65	8.404
			19.0	50	6.048
				65	7.040
				85	7.096
		76-22	9.5	85	3.974
			12.5	85	1.688
			19.0	85	3.252
		82-22	9.5	85	3.159
			12.5	85	3.405

* Mix Designed 3% Air Voids

Table 4.5 Mixtures Meeting MT and LT Criteria (Shaded)

Gradation	Aggregate Type	Binder PG	NMAS Gradation	N_{design}	Rut Depth @64°C, mm
Coarse	Gravel	67-22	9.5	50	14.585
				65	13.559
			12.5	50	14.279
				65	13.494
			19.0	50	7.380
				50*	9.105
				65	9.320
				85	8.340
		76-22	9.5	85	3.383
			12.5	85	4.058
			19.0	85	3.859
		82-22	9.5	85	3.740
			12.5	85	3.262
	Limestone / Gravel	67-22	9.5	50	11.655
				65	8.389
			12.5	50	9.202
				65	8.404
			19.0	50	6.048
				65	7.040
				85	7.096
		76-22	9.5	85	3.974
			12.5	85	1.688
			19.0	85	3.252
		82-22	9.5	85	3.159
			12.5	85	3.405

* Mix Designed at 3% Air Voids

CHAPTER 5 CONCLUSIONS

5.1 INTRODUCTION

The primary objective of this study was to conduct dynamic modulus characterization of selected Mississippi HMA mixtures. Results of the study produced necessary parameters to define functions for estimating dynamic modulus for twenty-five HMA mixtures. As part of a data base, MDOT will have functions to estimate HMA dynamic moduli input for calibrating the 2002 pavement design guide. Also, experience was gained in preparing, testing and analyzing the results. The secondary study objective was to conduct APA rutting tests on the twenty-five mixtures.

5.2 Test Specimen Preparation

Compacting specimens for dynamic modulus testing is significantly more complicated than compacting specimens for volumetric mix design. For mix design, mix is compacted to a standard N_{design} level. Dynamic modulus samples have to be compacted to a target air void content. The results (air voids) can vary with gradation, aggregate type, asphalt content and mass of mix compacted. Another problem is the Superpave gyratory compacted cylindrical samples have a density gradient. Developers of the test method minimized the density gradient by cutting a 100mm core from the larger, original 150mm sample. To achieve the target air void content of 7.0±0.5 percent for cored dynamic modulus test specimens,, the 150mm samples were compacted to an air void level of approximately 8.0±0.5 percent. Because of uncertainty in the air void level that would be produced, four to five 150mm samples of a mixture were compacted with a goal of producing three with the target air void level. Then the cored 100 mm diameter test specimens were checked that they met the target air void level of 7.0±0.5 percent. In some cases, new samples and cored specimens had to be prepared with an adjusted air void level.

5.3 Coring and Sawing

As noted, new or modified jigs were made to hold specimens during coring and sawing. With a new core barrel no other problems were encountered during coring. An

existing but relatively new concrete saw was not capable of sawing the specimen ends parallel. As a result, a new, replacement saw was purchased that was capable of sawing the ends parallel. However, there was some end spalling which was largely stopped by wrapping duct tape around the specimen's ends prior to sawing.

5.4 Dynamic Modulus Testing

The dynamic modulus testing protocol was not difficult to follow. Five graduate and undergraduate students were trained to run the test. There were some software and equipment control problems. As a follow up to the testing experience, steps will be taken to clarify why some of the data labels are set as they are. On some occasions the dynamic modulus equipment was shut down. This seemed to have the effect of turning off or resetting the software or equipment controls. As a consequence, extensive checks had to be run, often requiring software changes by the equipment supplier. These problems delayed the testing program. The other issue is the large amount of data that has to be managed to produce a result.

5.5 APA Tests

There were no problems in running the APA tests once specimens with target air voids were prepared. To a degree, the same problem exists in preparing the APA test specimens as for the dynamic modulus specimens. However, since only 150mm diameter specimens were utilized for APA tests preparation was not as difficult.

5.6 Results

Study results are categorized as primary and secondary. Primary results are the dynamic modulus results consisting of the parameters of the fitted sigmoid function of the master curve for each mixture. Associated are the shift factor values for each test temperature. The dynamic modulus testing was successful in producing usable results. Asphalt Pavement Analyzer rutting tests are secondary results. Relative values of rutting potential between the mixtures are in agreement with experience for the aggregate type, NMAS, binder stiffness and compaction level.

CHAPTER 6 REFERENCES

AASHTO Road Test, HRB Special Reports 61-A to 61G, Washington D.C.

AASHO Interim Guide for Design of Pavement Structures, AASHTO, Washington, DC, 1972.

2002 Guide for Design of New and Rehabilitated Pavements, NCHRP 1-37A, National Cooperative Highway Research Program, National Research Council, Washington D.C.

AASHTO TP 62-03, Standard Method of Test for Determining Dynamic Modulus of Hot-Mix Asphalt Concrete Mixtures, *Standard Specifications for Transportation Materials and Methods of Sampling and Testing*, AASHTO, Washington, DC, 2005.

AASHTO T 27, Sieve Analysis of Fine and Coarse Aggregate, *Standard Specifications for Transportation Materials and Methods of Sampling and Testing*, AASHTO, Washington, DC, 2005.

AASHTO T 84, Specific Gravity and Absorption of Fine Aggregate, *Standard Specifications for Transportation Materials and Methods of Sampling and Testing*, AASHTO, Washington, DC, 2005.

AASHTO T 85, Specific Gravity and Absorption of Coarse Aggregate, *Standard Specifications for Transportation Materials and Methods of Sampling and Testing*, AASHTO, Washington, DC, 2005.

AASHTO T-166, Bulk Specific Gravity of Compacted Bituminous Mixtures Using Saturated Surface-Dry Specimens, *Standard Specifications for Transportation Materials and Methods of Sampling and Testing*, AASHTO, Washington, DC, 2005.

AASHTO T-209, Theoretical Maximum Specific Gravity and Density of Hot-Mix Asphalt Paving Mixtures, *Standard Specifications for Transportation Materials and Methods of Sampling and Testing*, AASHTO, Washington, DC, 2005..

AASHTO T 269, Percent Air Voids in Compacted Dense and Open Asphalt Mixtures, *Standard Specifications for Transportation Materials and Methods of Sampling and Testing*, AASHTO, Washington, DC, 2005..

AASHTO T-304, Uncompacted Void Content of Fine Aggregate, *Standard Specifications for Transportation Materials and Methods of Sampling and Testing*, AASHTO, Washington, DC, 2005.

AASHTO T 312, Preparing and Determining the Density of Hot-Mix (HMA) Specimens by Means of the Superpave Gyratory Compactor, *Standard Specifications for Transportation Materials and Methods of Sampling and Testing*, AASHTO, Washington, DC, 2005.

.

ASTM D5801-01, Standard Method for Determining the Percentage of Fractured Particles in Coarse Aggregate, ASTM, Philidelphia, PA, 2001.

Buchanan, M. Shane and Thomas D. White, MDOT Study 155, Use of the Asphalt Pavement Analyzer to Study In-Service Asphalt Mixture Performance, August 2004.

Mississippi Department of Transportation Standard Operating Procedure No. TMD-11-78-00-000: *Volumetric Mix Design of Hot Mix Asphalt Mixtures Using the Superpave Gyratory Compactor*, November 2000.

Witczak, M. W. and Andres Sotil, Simple Performance Test for Superpave Mix Design NCHRP 9-10: A Recommended Methodology for Developing Dynamic Modulus E* Master Curves from Non-Linear Optimization, Arizona State University, Department of Civil and Environmental Engineering, Tempe, AZ, 2004.

APPENDIX A

DESIGN ASPHALT CONTENT

Table A1 9.5GR67-22, N50

G_{binder}	AC%	Sample ID	Dry Weight, grams	Pyc,Asphalt, Water, grams	Pyc,Water, grams	Gmm	Average Gmm	Gse
1.0250	5.5	1	1599.5	8478.5	7572.5	2.3064	2.3054	2.4862
		2	1582.9	8343.0	7447.0	2.3044		

Gmm Values		Sample ID	Dry Weight, grams	Submerged Weight, grams	SSD Weight, grams	Gmb	Average Gmb	Percent Air Voids
AC Content	Gmm							
4.5	2.3363	1	4268.3	2301.7	4326.3	2.108	2.107	9.82
		2	4270.9	2309.8	4338.3	2.105		
5.5	2.3054	1	4328.6	2334.3	4361.4	2.135	2.126	7.77
		2	4332.8	2334.3	4380.8	2.117		
6.5	2.2753	1	4367.0	2359.1	4377.1	2.164	2.147	5.65
		2	4369.5	2343.9	4395.8	2.129		

Asphalt Content @ 4% Air Voids: 7.30

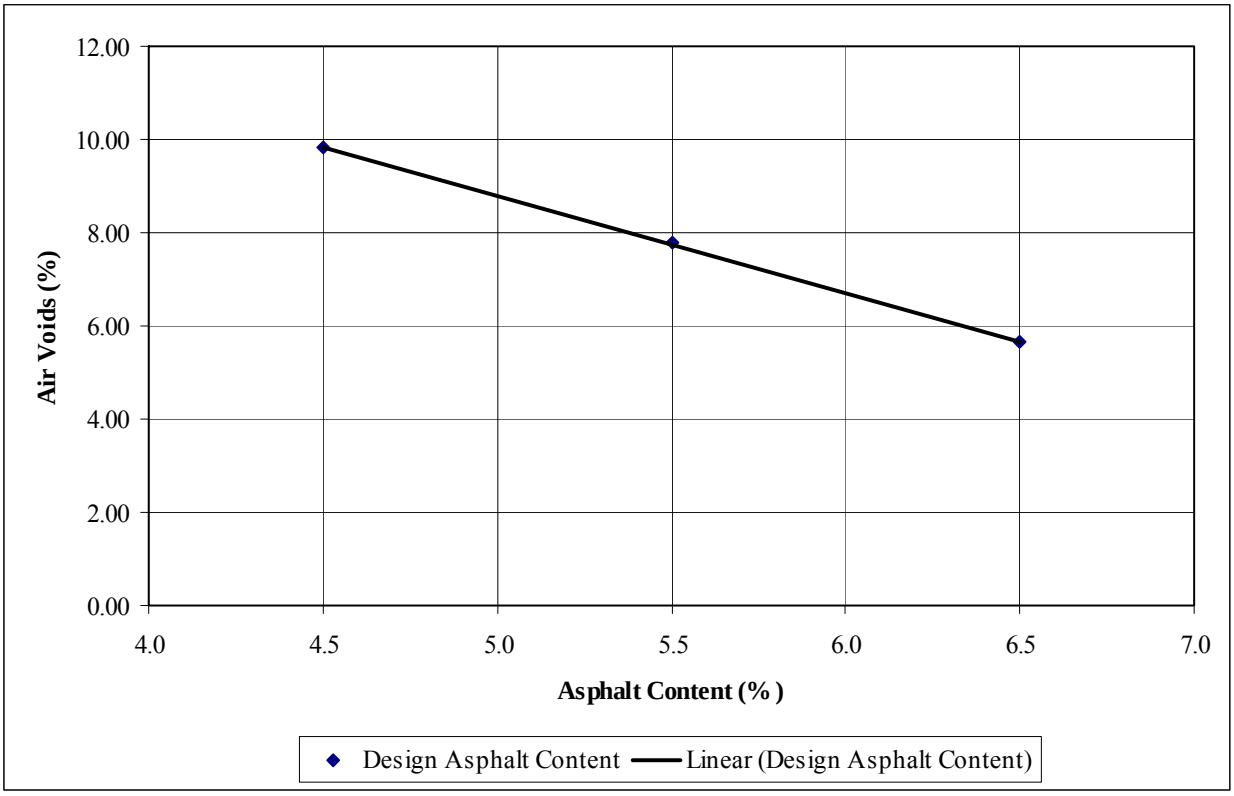

Figure A1 9.5GR67-22, N50

Table A2 9.5GR67-22, N65

G_{binder}	AC%	Sample ID	Dry Weight, grams	Pyc,Asphalt, Water, grams	Pyc,Water, grams	Gmm	Average Gmm	Gse
1.0250	5.5	1	1599.5	8478.5	7572.5	2.3064	2.3054	2.4862
		2	1582.9	8343.0	7447.0	2.3044		

Gmm Values		Sample ID	Dry Weight, grams	Submerged Weight, grams	SSD Weight, grams	Gmb	Average Gmb	Percent Air Voids
AC Content	Gmm							
4.5	2.3363	1	4461.1	2403.5	4532.7	2.095	2.106	9.85
		2	4280.2	2322.8	4344.5	2.117		
5.5	2.3054	1	4512.1	2444.3	4555.3	2.137	2.141	7.12
		2	4307.8	2334.7	4342.7	2.145		
6.5	2.2753	1	4341.4	2363.1	4351.2	2.184	2.171	4.57
		2	4391.8	2365.9	4400.1	2.159		

Asphalt Content @ 4% Air Voids: 6.70

Figure A2 9.5GR67-22, N65

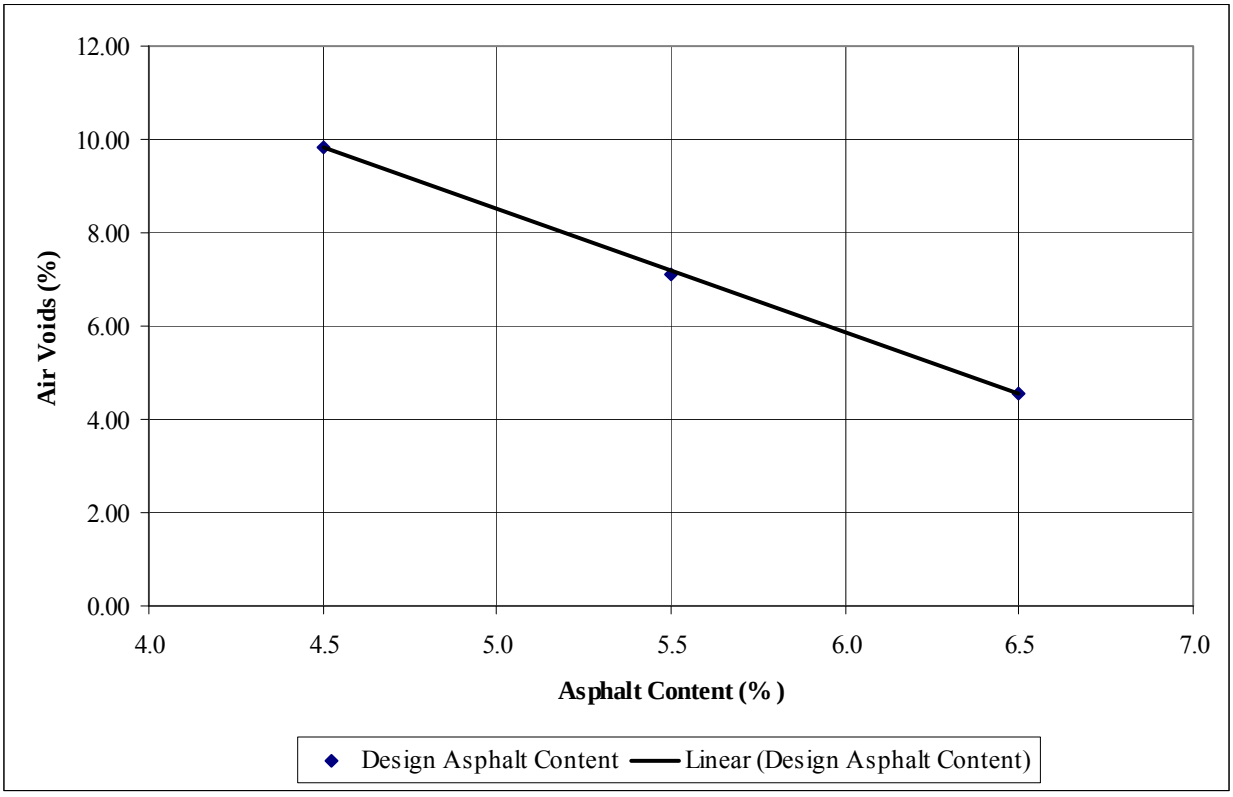

Figure A2 9.5GR67-22, N65

Table A3 9.5GR76-22, N85

G_{binder}	AC%	Sample ID	Dry Weight, grams	Pyc,Asphalt, Water, grams	Pyc,Water, grams	Gmm	Average Gmm	Gse
1.0250	5.5	1	1567.0	8469.2	7571.4	2.3416	2.3312	2.5179
		2	1558.4	8333.9	7447.0	2.3208		

Gmm Values		Sample ID	Dry Weight, grams	Submerged Weight, grams	SSD Weight, grams	Gmb	Average Gmb	Percent Air Voids
AC Content	Gmm							
4.5	2.3631	1	4276.3	2304.8	4322.7	2.119	2.120	10.27
		2	4265.5	2300.2	4310.7	2.122		
5.5	2.3312	1	4310.5	2341.1	4350.0	2.146	2.154	7.58
		2	4317.7	2351.0	4347.0	2.163		
6.5	2.3002	1	4350.3	2369.2	4365.1	2.180	2.177	5.37
		2	4351.0	2363.0	4364.6	2.174		

Asphalt Content @ 4% Air Voids: 7.02

Figure A3 9.5GR76-22, N85

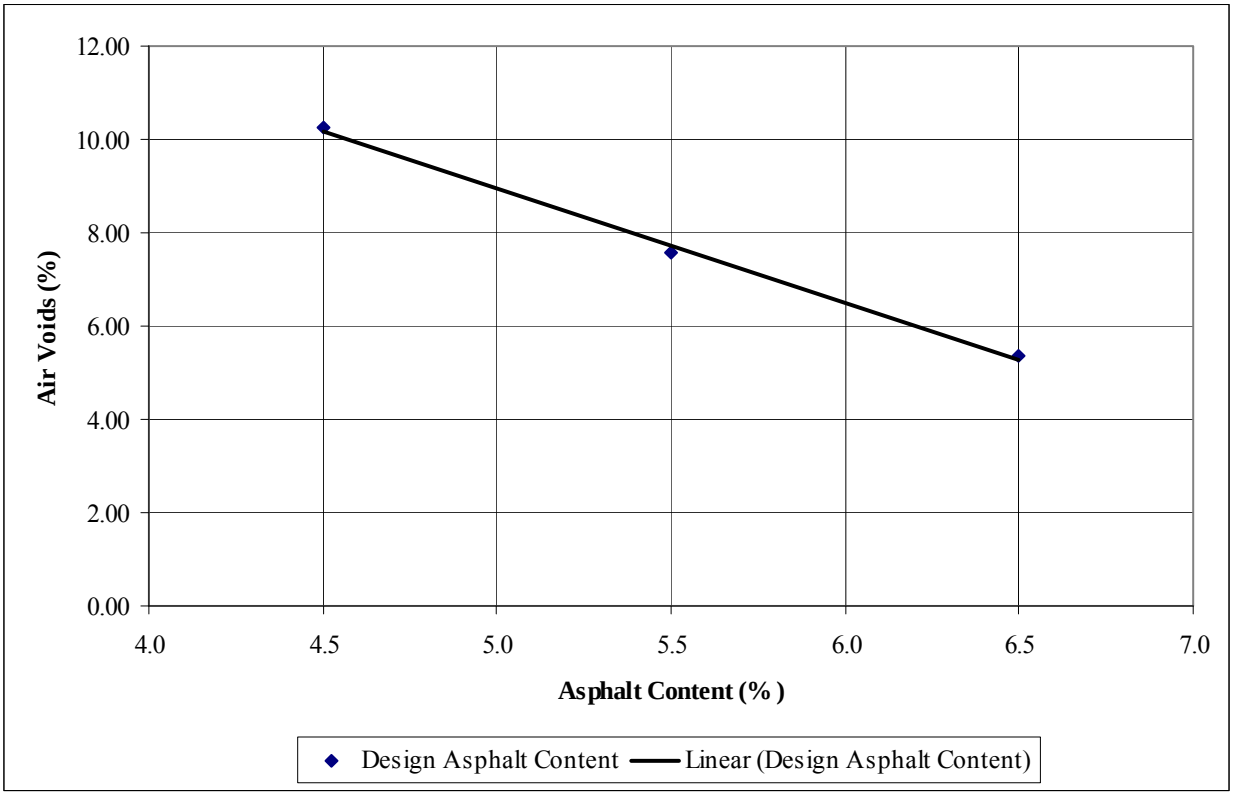

Figure A3 9.5GR76-22, N85

Table A4 9.5GR82-22, N85

G_{binder}	AC%	Sample ID	Dry Weight, grams	Pyc,Asphalt, Water, grams	Pyc,Water, grams	Gmm	Average Gmm	Gse
1.0250	5.5	1	1571.0	8472.5	7572.5	2.3413	2.3438	2.5335
		2	1587.5	8357.9	7447.0	2.3463		

Gmm Values		Sample ID	Dry Weight, grams	Submerged Weight, grams	SSD Weight, grams	Gmb	Average Gmb	Percent Air Voids
AC Content	Gmm							
4.5	2.3761	1	4262.4	2330.6	4300.5	2.164	2.173	8.56
		2	4268.3	2346.9	4303.5	2.181		
5.5	2.3438	1	4312.6	2370.8	4337.2	2.193	2.197	6.26
		2	4311.4	2378.3	4337.3	2.201		
6.5	2.3123	1	4348.3	2396.4	4365.2	2.209	2.204	4.66
		2	4358.2	2398.7	4379.4	2.200		

Asphalt Content @ 4% Air Voids: 6.77

Figure A4 9.5GR82-22, N85

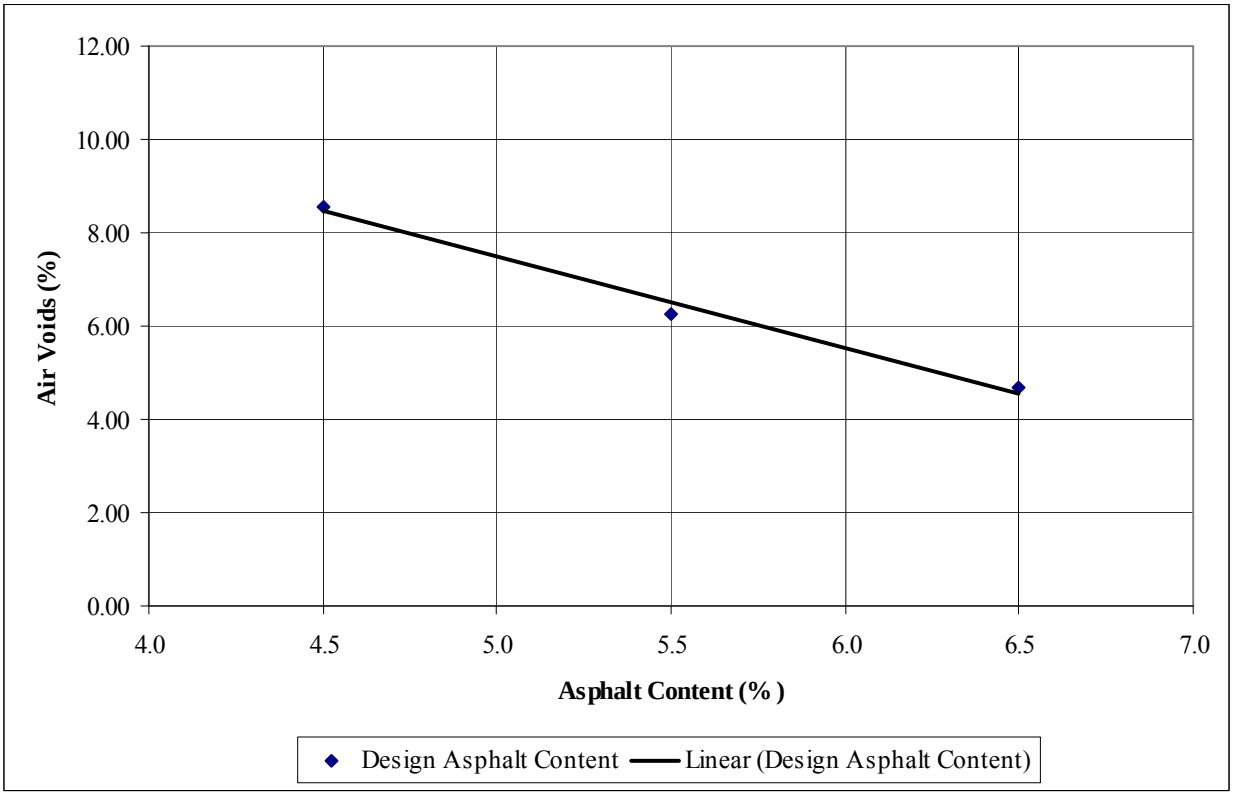

Figure A4 9.5GR82-22, N85

Table A5 12.5GR67-22, N50

G_{binder}	AC%	Sample ID	Dry Weight, grams	Pyc,Asphalt, Water, grams	Pyc,Water, grams	Gmm	Average Gmm	Gse
1.0250	5.5	1	1586.3	8465.2	7572.5	2.2871	2.3019	2.4819
		2	1580.5	8345.3	7447.0	2.3168		

Gmm Values		Sample ID	Dry Weight, grams	Submerged Weight, grams	SSD Weight, grams	Gmb	Average Gmb	Percent Air Voids
AC Content	Gmm							
4.5	2.3327	1	4270.0	2329.2	4377.2	2.085	2.096	10.16
		2	4287.9	2332.0	4367.9	2.106		
5.5	2.3019	1	4328.2	2326.5	4374.1	2.114	2.114	8.17
		2	4326.5	2330.6	4377.2	2.114		
6.5	2.2720	1	4370.6	2343.6	4380.2	2.146	2.142	5.71
		2	4365.4	2336.9	4378.5	2.138		

Asphalt Content @ 4% Air Voids: 7.30

Figure A5 12.5GR67-22, N50

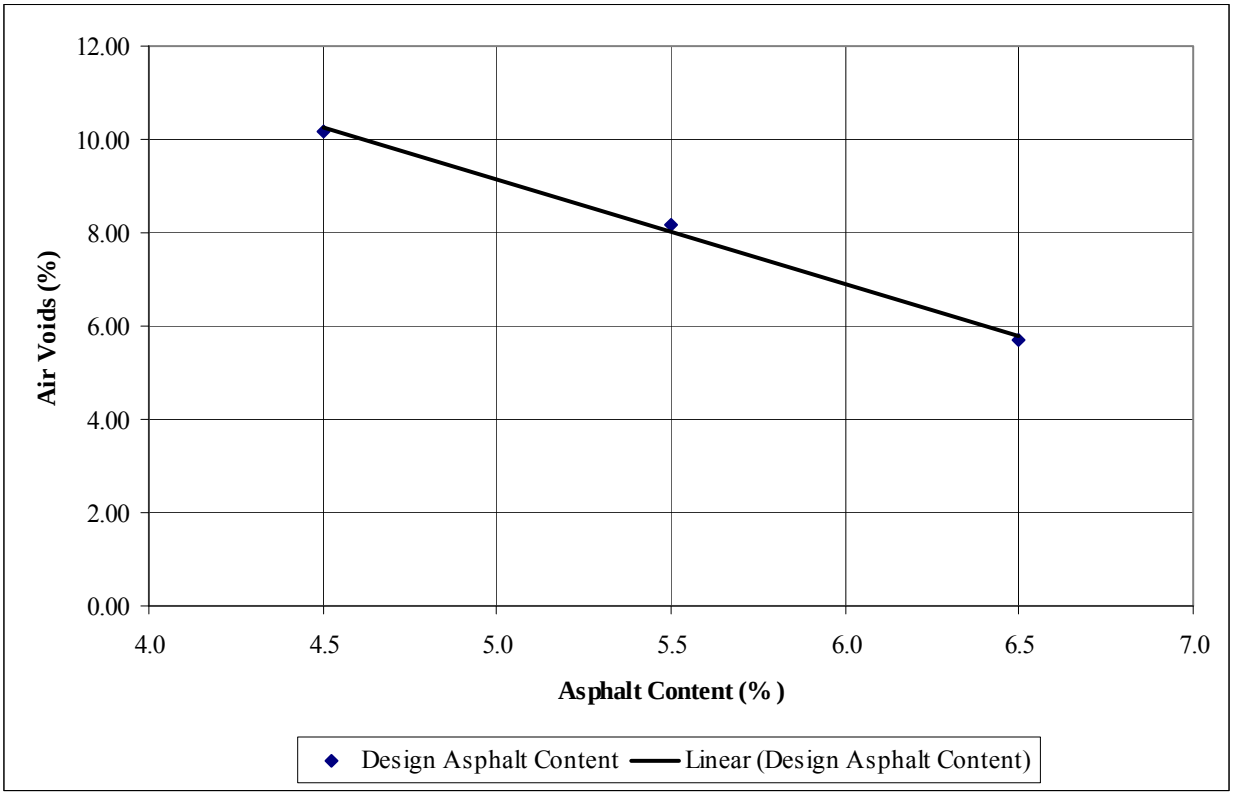

Figure A5 12.5GR67-22, N50

Table A6 12.5GR67-22, N65

G_{binder}	AC%	Sample ID	Dry Weight, grams	Pyc,Asphalt, Water, grams	Pyc,Water, grams	Gmm	Average Gmm	Gse
1.0250	5.5	1	1586.3	8465.2	7572.5	2.2871	2.3019	2.4819
		2	1580.5	8345.3	7447.0	2.3168		

Gmm Values		Sample ID	Dry Weight, grams	Submerged Weight, grams	SSD Weight, grams	Gmb	Average Gmb	Percent Air Voids
AC Content	Gmm							
4.5	2.3327	1	4284.3	2334.5	4378.0	2.097	2.095	10.19
		2	4274.7	2334.4	4376.2	2.094		
5.5	2.3019	1	4324.5	2330.5	4364.1	2.127	2.132	7.36
		2	4337.8	2342.1	4370.6	2.138		
6.5	2.2720	1	4361.5	2335.7	4376.4	2.137	2.149	5.41
		2	4344.8	2342.8	4353.3	2.161		

Asphalt Content @ 4% Air Voids: 7.01

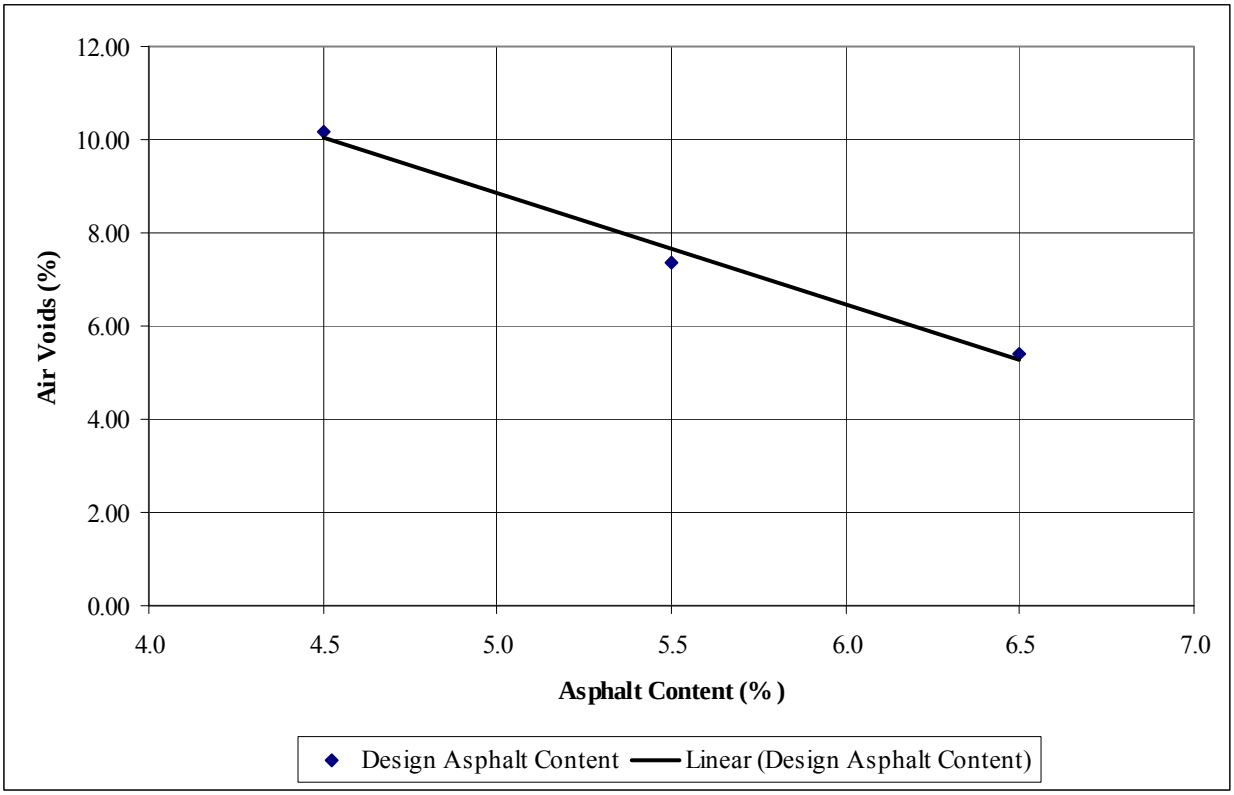

Figure A6 12.5GR67-22, N65

Table A7 12.5GR76-22, N85

G_{binder}	AC%	Sample ID	Dry Weight, grams	Pyc,Asphalt, Water, grams	Pyc,Water, grams	Gmm	Average Gmm	Gse
1.0250	5.5	1	1573.6	8462.1	7567.3	2.3182	2.2983	2.4774
		2	1592.4	8339.9	7446.4	2.2784		

Gmm Values		Sample ID	Dry Weight, grams	Submerged Weight, grams	SSD Weight, grams	Gmb	Average Gmb	Percent Air Voids
AC Content	Gmm							
4.5	2.3289	1	4262.5	2313.8	4338.8	2.105	2.117	9.10
		2	4262.5	2333.0	4334.9	2.129		
5.5	2.2983	1	4318.2	2336.5	4354.2	2.140	2.141	6.82
		2	4322.2	2344.5	4361.6	2.143		
6.5	2.2685	1	4350.3	2350.5	4361.9	2.163	2.166	4.51
		2	4347.9	2355.1	4359.3	2.169		

Asphalt Content @ 4% Air Voids: 6.73

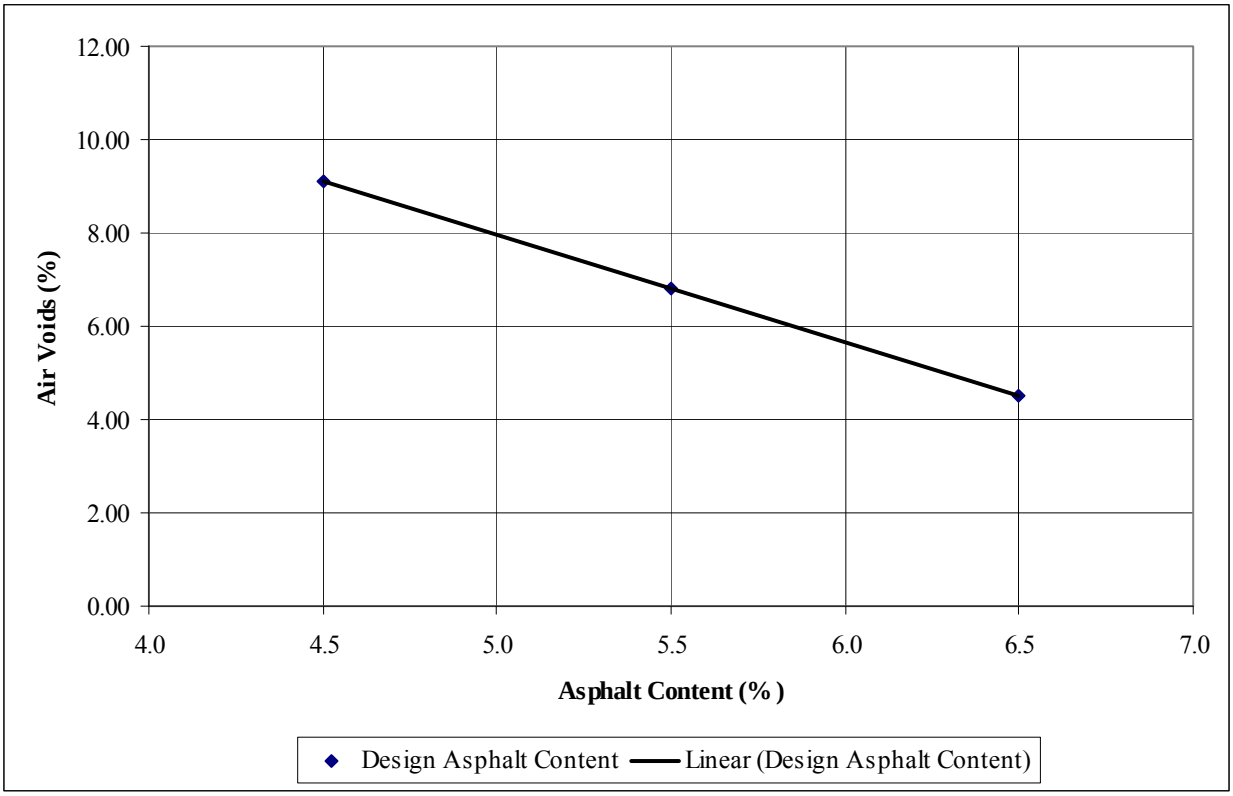

Figure A7 12.5GR76-22, N85

Table A8 12.5GR82-22, N85

G_{binder}	AC%	Sample ID	Dry Weight, grams	Pyc,Asphalt, Water, grams	Pyc,Water, grams	Gmm	Average Gmm	Gse
1.0250	5.5	1	1575.0	8468.8	7572.5	2.3206	2.3159	2.4991
		2	1582.9	8345.0	7447.0	2.3111		

Gmm Values		Sample ID	Dry Weight, grams	Submerged Weight, grams	SSD Weight, grams	Gmb	Average Gmb	Percent Air Voids
AC Content	Gmm							
4.5	2.3472	1	4255.8	2334.2	4332.6	2.130	2.130	9.26
		2	4263.8	2331.0	4332.8	2.130		
5.5	2.3159	1	4307.4	2347.7	4347.8	2.154	2.151	7.11
		2	4311.9	2351.7	4358.1	2.149		
6.5	2.2854	1	4340.3	2366.7	4360.5	2.177	2.168	5.14
		2	4349.4	2365.0	4379.5	2.159		

Asphalt Content @ 4% Air Voids: 7.04

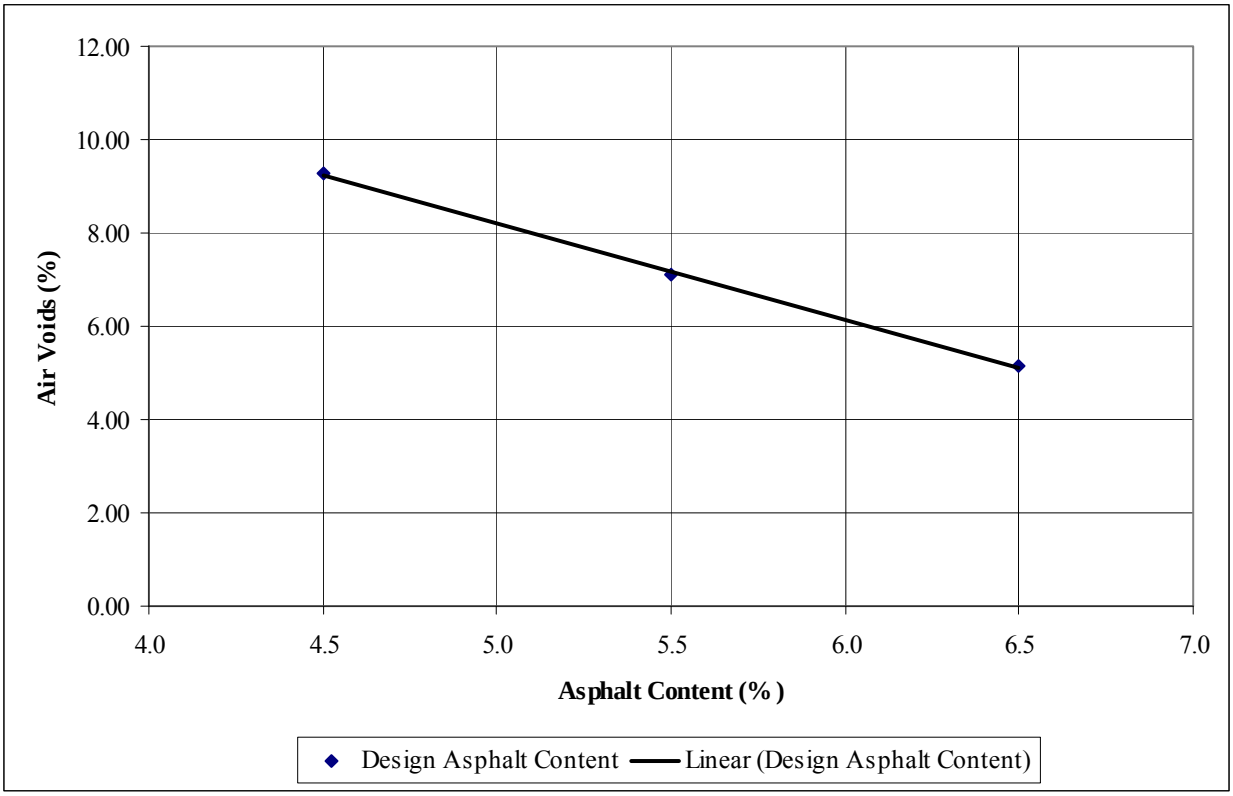

Figure A8 12.5GR82-22, N85

Table A9 19.0GR67-22, N50

G_{binder}	AC%	Sample ID	Dry Weight, grams	Pyc,Asphalt, Water, grams	Pyc,Water, grams	Gmm	Average Gmm	Gse
1.0250	5.5	1	1576.5	8461.8	7572.5	2.2941	2.3035	2.4838
		2	1569.1	8337.7	7447.0	2.3129		

Gmm Values		Sample ID	Dry Weight, grams	Submerged Weight, grams	SSD Weight, grams	Gmb	Average Gmb	Percent Air Voids
AC Content	Gmm							
4.5	2.3343	1	4259.2	2336.0	4342.6	2.123	2.131	8.72
		2	4273.4	2350.9	4348.9	2.139		
5.5	2.3035	1	4317.8	2344.5	4339.5	2.164	2.165	6.03
		2	4308.7	2339.4	4329.8	2.165		
6.5	2.2735	1	4344.6	2359.8	4350.9	2.182	2.189	3.72
		2	4350.4	2376.7	4357.8	2.196		

Asphalt Content @ 4% Air Voids: 6.36

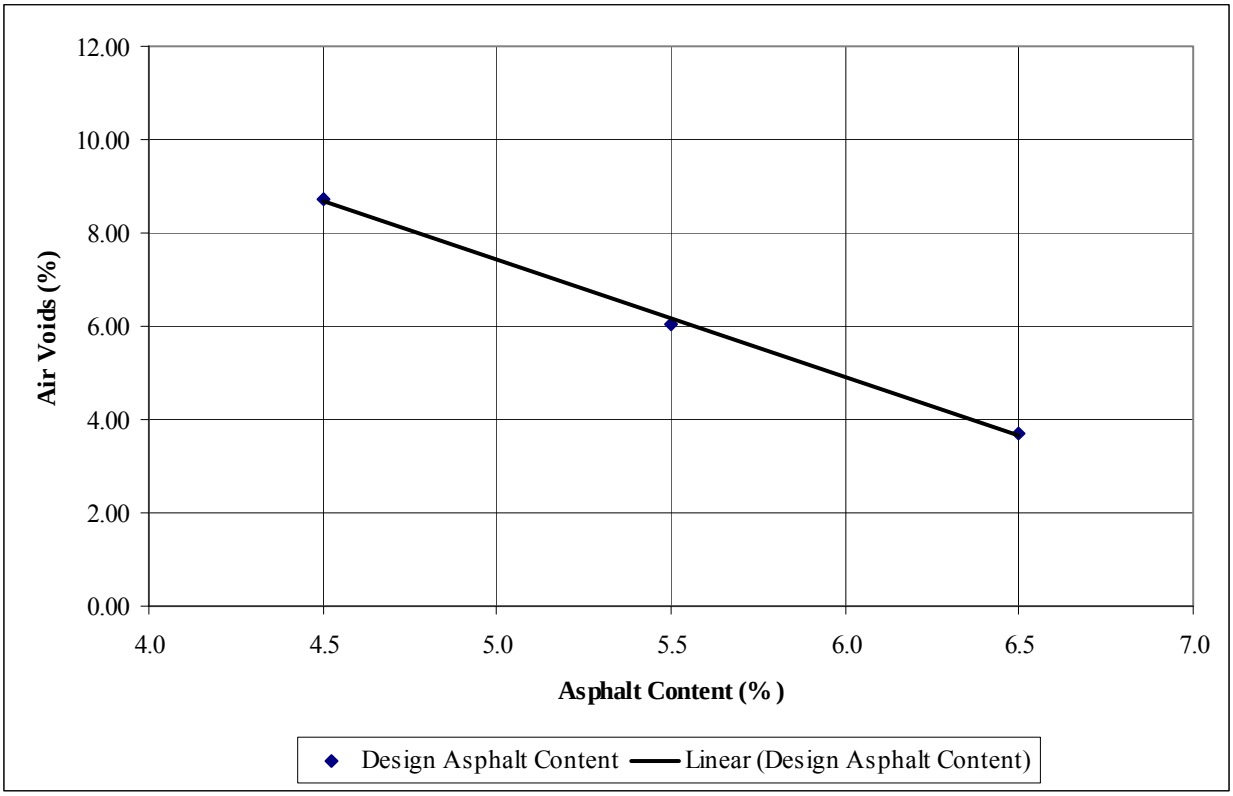

Figure A9 19.0GR67-22, N50

Table A10 19.0GR67-22, N65

G_{binder}	AC%	Sample ID	Dry Weight, grams	Pyc,Asphalt, Water, grams	Pyc,Water, grams	Gmm	Average Gmm	Gse
1.0250	5.5	1	1576.5	8461.8	7572.5	2.2941	2.3035	2.4838
		2	1569.1	8337.7	7447.0	2.3129		

Gmm Values		Sample ID	Dry Weight, grams	Submerged Weight, grams	SSD Weight, grams	Gmb	Average Gmb	Percent Air Voids
AC Content	Gmm							
4.5	2.3343	1	4268.1	2340.0	4330.6	2.144	2.145	8.11
		2	4263.6	2342.1	4328.9	2.146		
5.5	2.3035	1	4322.0	2348.0	4336.5	2.173	2.170	5.81
		2	4314.6	2339.6	4331.9	2.166		
6.5	2.2735	1	4332.4	2359.8	4337.2	2.191	2.195	3.45
		2	4350.0	2376.7	4354.8	2.199		

Asphalt Content @ 4% Air Voids: 6.27

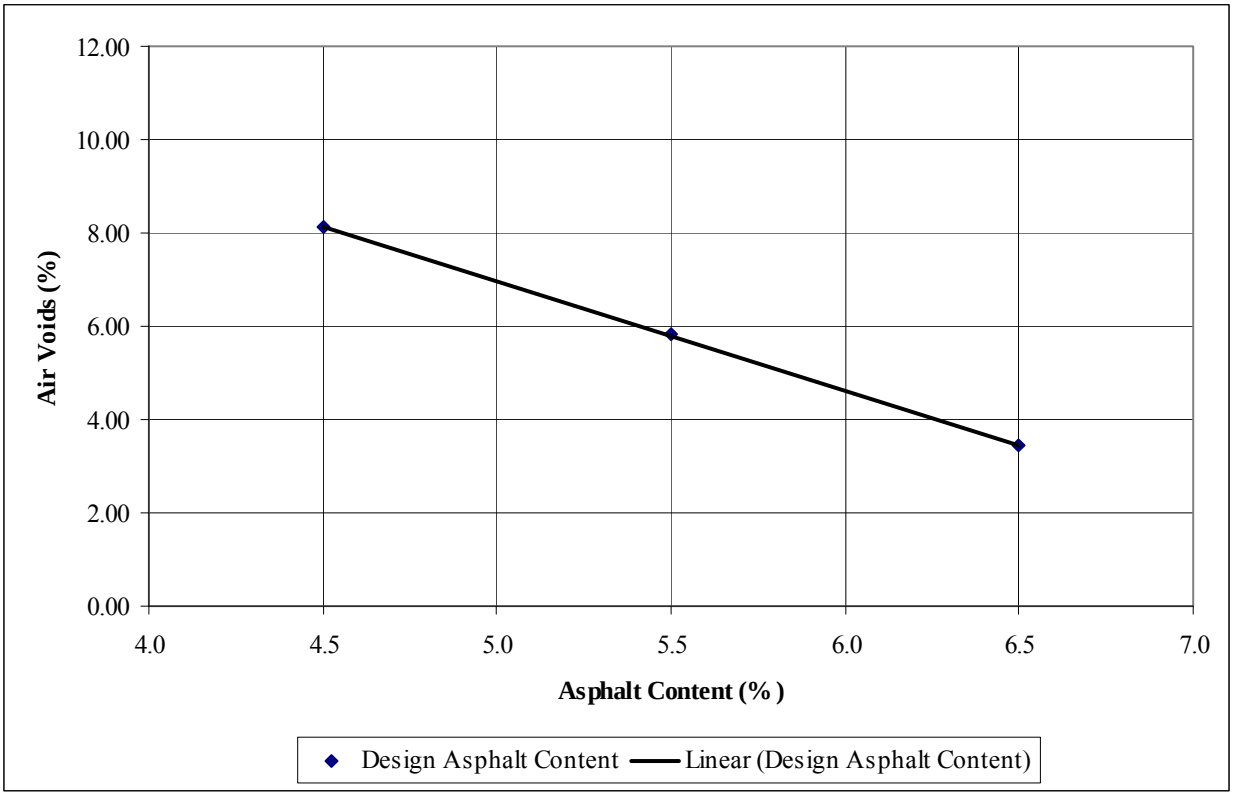

Figure A10 19.0GR67-22, N65

Table A11 19.0GR67-22, N85

G_{binder}	AC%	Sample ID	Dry Weight, grams	Pyc,Asphalt, Water, grams	Pyc,Water, grams	Gmm	Average Gmm	Gse
1.0250	5.5	1	1576.5	8461.8	7572.5	2.2941	2.3035	2.4838
		2	1569.1	8337.7	7447.0	2.3129		

Gmm Values		Sample ID	Dry Weight, grams	Submerged Weight, grams	SSD Weight, grams	Gmb	Average Gmb	Percent Air Voids
AC Content	Gmm							
4.5	2.3343	1	4269.8	2342.3	4319.5	2.160	2.157	7.61
		2	4274.8	2343.1	4327.7	2.154		
5.5	2.3053	1	4313.2	2349.1	4329.1	2.178	2.180	5.36
		2	4315.5	2351.5	4329.7	2.182		
6.5	2.2735	1	4352.7	2387.6	4357.4	2.210	2.212	2.70
		2	4355.5	2393.4	4360.1	2.215		

Asphalt Content @ 4% Air Voids: 6.00

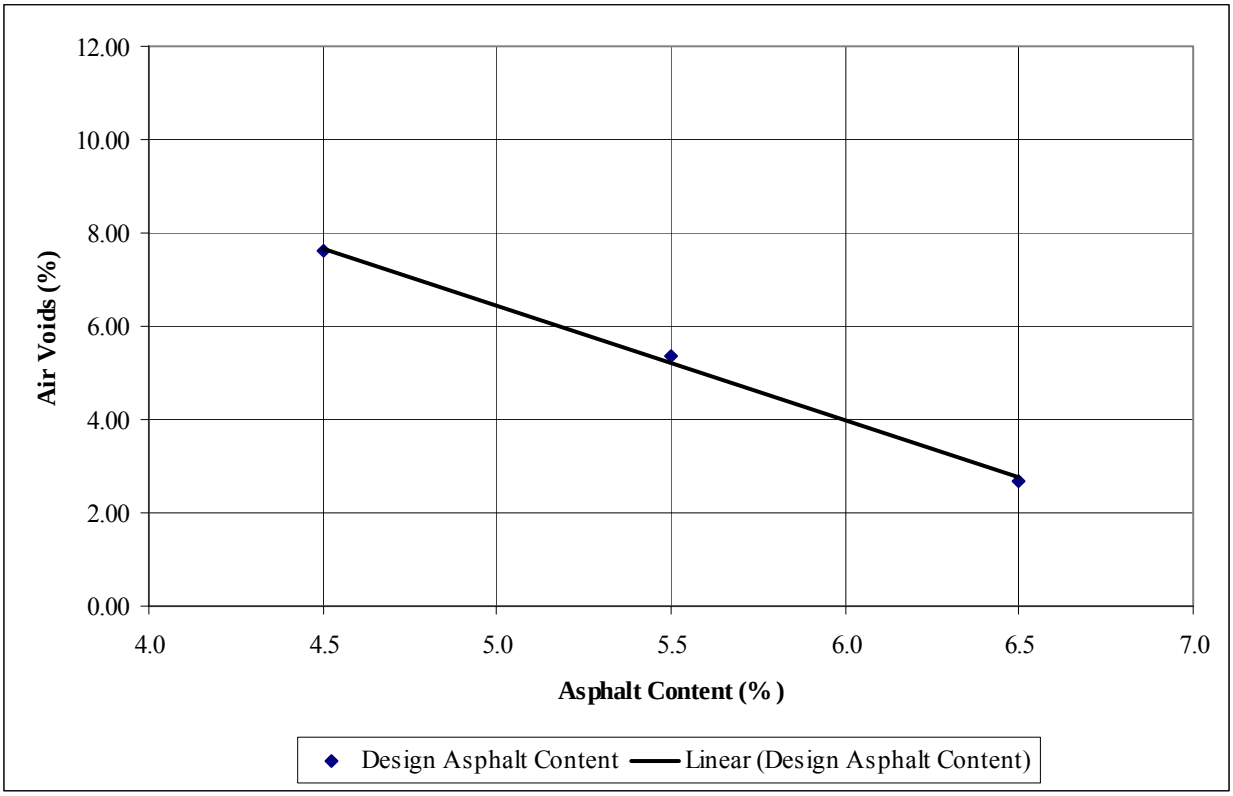

Figure A11 19.0GR67-22, N85

Table A12 19.0GR76-22, N85

G_{binder}	AC%	Sample ID	Dry Weight, grams	Pyc,Asphalt, Water, grams	Pyc,Water, grams	Gmm	Average Gmm	Gse
1.0250	5.5	1	1574.3	8451.4	7571.6	2.2668	2.2874	2.4640
		2	1571.5	8333.2	7442.6	2.3080		

Gmm Values		Sample ID	Dry Weight, grams	Submerged Weight, grams	SSD Weight, grams	Gmb	Average Gmb	Percent Air Voids
AC Content	Gmm							
4.5	2.3176	1	4247.2	2331.0	4336.7	2.118	2.130	8.11
		2	4262.2	2348.3	4338.4	2.142		
5.5	2.2874	1	4297.5	2343.8	4331.0	2.163	2.164	5.38
		2	4317.5	2348.2	4341.4	2.166		
6.5	2.2580	1	4331.1	2372.8	4340.6	2.201	2.199	2.60
		2	4352.5	2381.9	4362.6	2.197		

Asphalt Content @ 4% Air Voids: 6.00

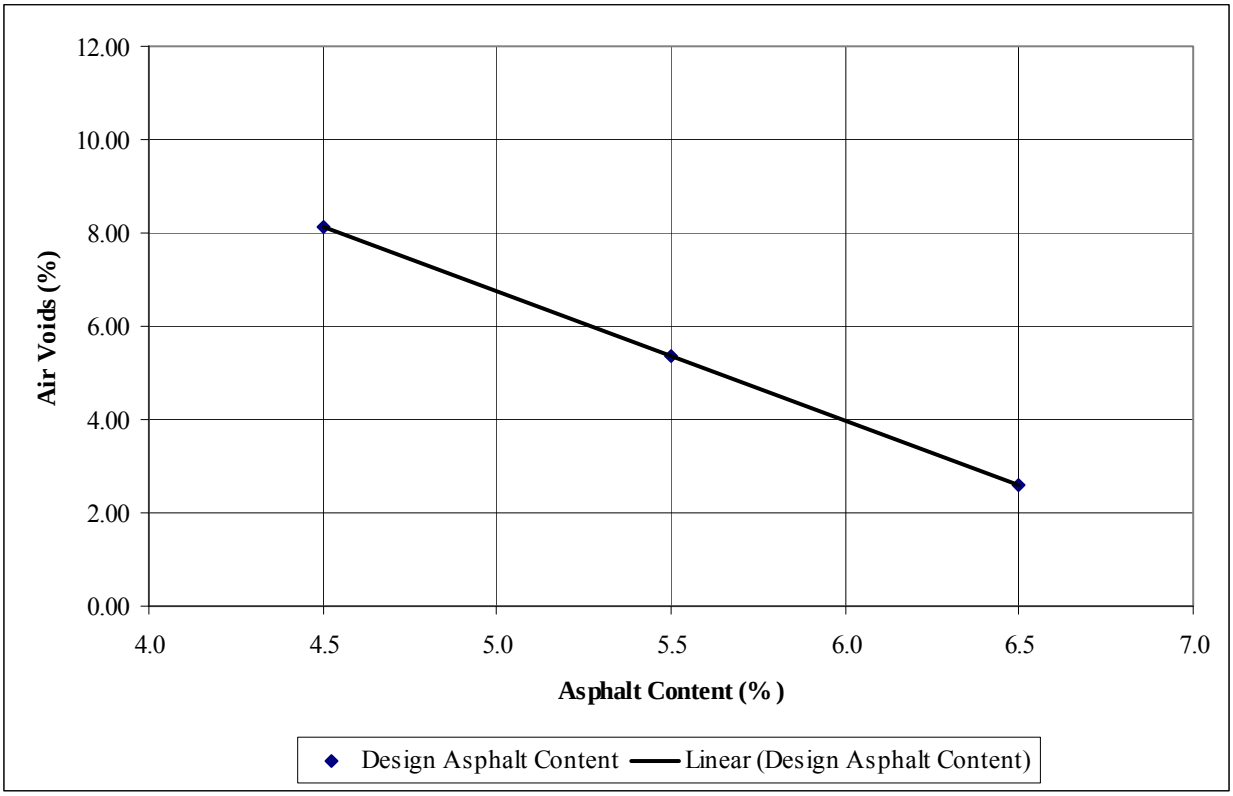

Figure A12 19.0GR76-22, N85

Table A13 9.5L/G67-22, N50

G_{binder}	AC%	Sample ID	Dry Weight, grams	Pyc,Asphalt, Water, grams	Pyc,Water, grams	Gmm	Average Gmm	Gse
1.0250	5.5	1	1586.7	8496.7	7572.5	2.3950	2.3991	2.6022
		2	1590.7	8375.8	7447.0	2.4032		

Gmm Values		Sample ID	Dry Weight, grams	Submerged Weight, grams	SSD Weight, grams	Gmb	Average Gmb	Percent Air Voids
AC Content	Gmm							
4.5	2.4337	1	4476.9	2517.8	4527.6	2.228	2.242	7.87
		2	4485.2	2526.8	4514.3	2.257		
5.5	2.3991	1	4531.8	2541.9	4537.7	2.271	2.277	5.81
		2	4526.1	2547.5	4530.5	2.282		
6.5	2.3656	1	4567.8	2597.0	4568.9	2.316	2.318	2.02
		2	4577.1	2604.9	4578.7	2.319		

Asphalt Content @ 4% Air Voids: 5.84

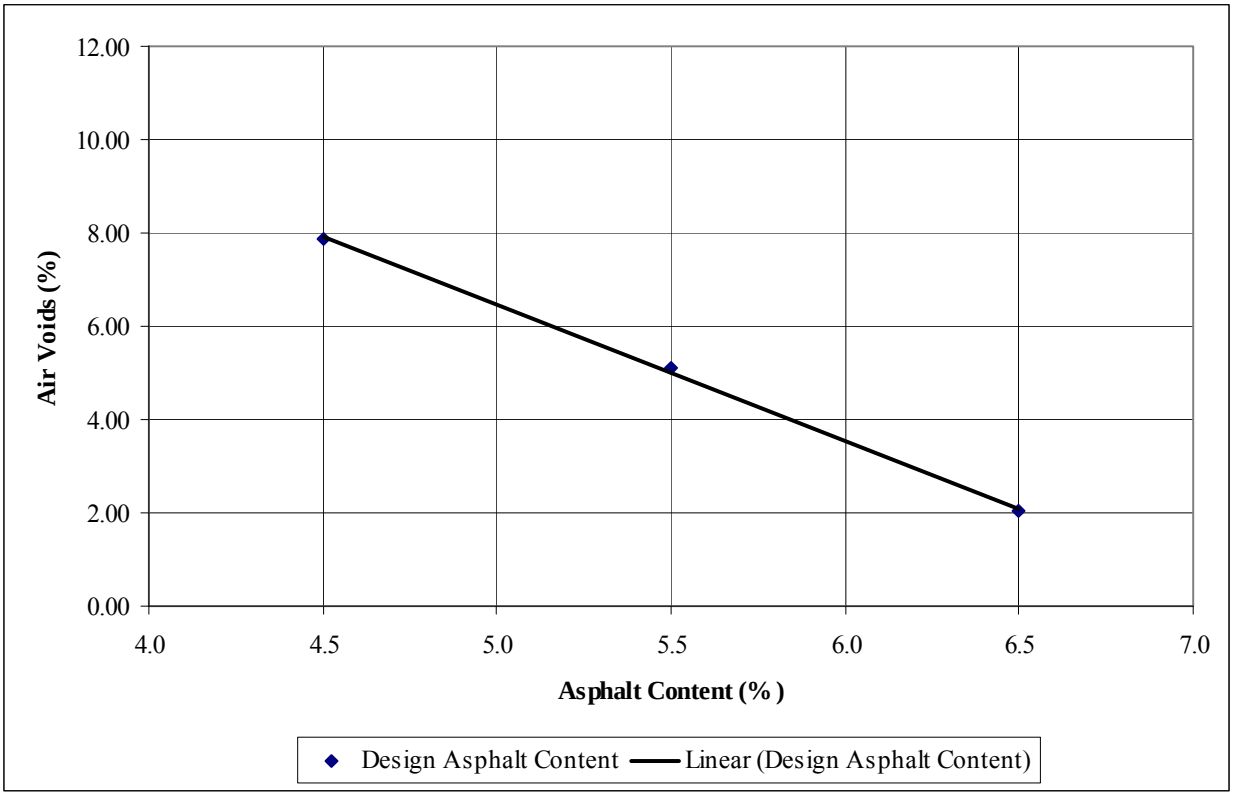

Figure A13 9.5L/G67-22, N50

Table A14 9.5L/G67-22, N65

G_{binder}	AC%	Sample ID	Dry Weight, grams	Pyc,Asphalt, Water, grams	Pyc,Water, grams	Gmm	Average Gmm	Gse
1.0250	5.5	1	1586.7	8496.7	7572.5	2.3950	2.3991	2.6022
		2	1590.7	8375.8	7447.0	2.4032		

Gmm Values		Sample ID	Dry Weight, grams	Submerged Weight, grams	SSD Weight, grams	Gmb	Average Gmb	Percent Air Voids
AC Content	Gmm							
4.5	2.4337	1	4478.8	2526.5	4513.0	2.255	2.255	7.34
		2	4491.0	2532.0	4523.2	2.255		
5.5	2.3991	1	4534.2	2571.5	4540.0	2.303	2.301	4.11
		2	4536.0	2568.5	4542.6	2.298		
6.5	2.3656	1	4579.3	2610.0	4582.4	2.322	2.325	1.70
		2	4573.4	2612.1	4575.8	2.329		
		Asphalt Content @ 4% Air Voids:			5.63			

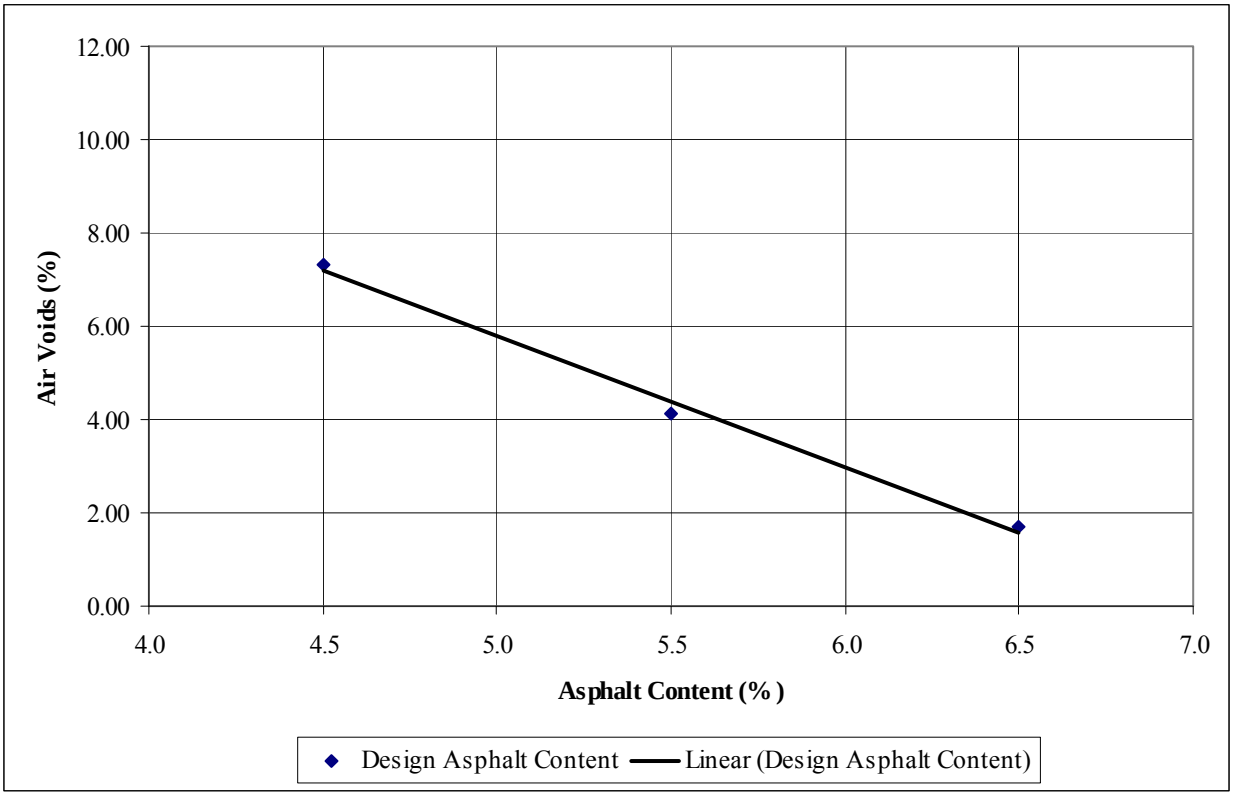

Figure A14 9.5L/G67-22, N65

Table A15 9.5L/G76-22, N85

G_{binder}	AC%	Sample ID	Dry Weight, grams	Pyc,Asphalt, Water, grams	Pyc,Water, grams	Gmm	Average Gmm	Gse
1.0250	5.5	1	1573.0	8484.4	7572.5	2.3794	2.3890	2.5896
		2	1584.3	8370.8	7447.0	2.3986		

Gmm Values		Sample ID	Dry Weight, grams	Submerged Weight, grams	SSD Weight, grams	Gmb	Average Gmb	Percent Air Voids
AC Content	Gmm							
4.5	2.4231	1	4480.7	2525.3	4507.1	2.261	2.259	6.76
		2	4480.4	2526.1	4510.5	2.258		
5.5	2.3890	1	4523.6	2562.2	4529.4	2.300	2.296	3.91
		2	4523.6	2555.1	4529.1	2.292		
6.5	2.3558	1	4551.1	2591.3	4555.8	2.317	2.317	1.66
		2	4561.9	2597.5	4566.6	2.317		

Asphalt Content @ 4% Air Voids: 5.54

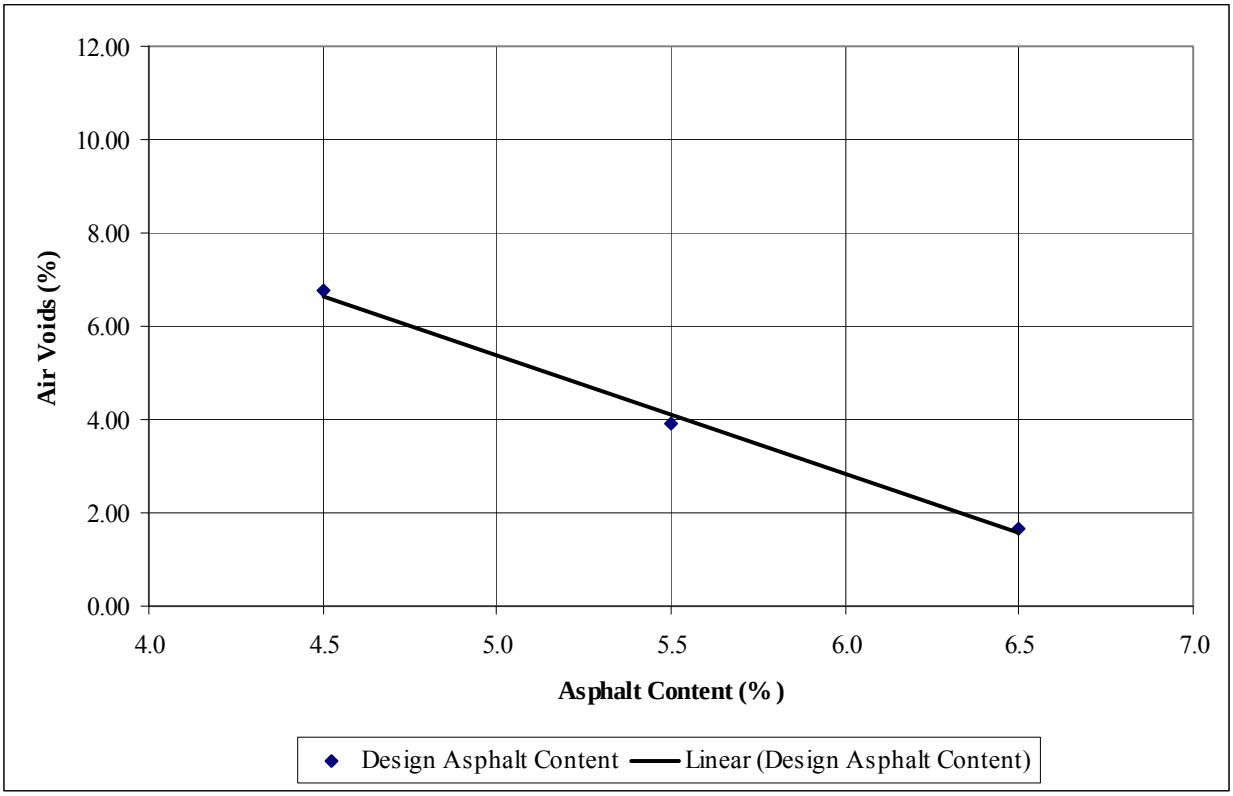

Figure A15 9.5L/G76-22, N85

Table A16 9.5L/G82-22, N85

G_{binder}	AC%	Sample ID	Dry Weight, grams	Pyc,Asphalt, Water, grams	Pyc,Water, grams	Gmm	Average Gmm	Gse
1.0250	5.5	1	1583.9	8489.0	7572.5	2.3732	2.3898	2.5906
		2	1580.3	8370.6	7447.0	2.4064		

Gmm Values		Sample ID	Dry Weight, grams	Submerged Weight, grams	SSD Weight, grams	Gmb	Average Gmb	Percent Air Voids
AC Content	Gmm							
4.5	2.4240	1	4477.2	2520.6	4526.7	2.232	2.230	8.02
		2	4471.6	2519.2	4526.6	2.228		
5.5	2.3898	1	4514.2	2538.9	4530.2	2.267	2.239	6.3
		2	4517.6	2527.3	4570.2	2.211		
6.5	2.3566	1	4572.9	2572.5	4584.9	2.272	2.272	3.58
		2	4572.9	2572.5	4584.9	2.272		

Asphalt Content @ 4% Air Voids: 6.37

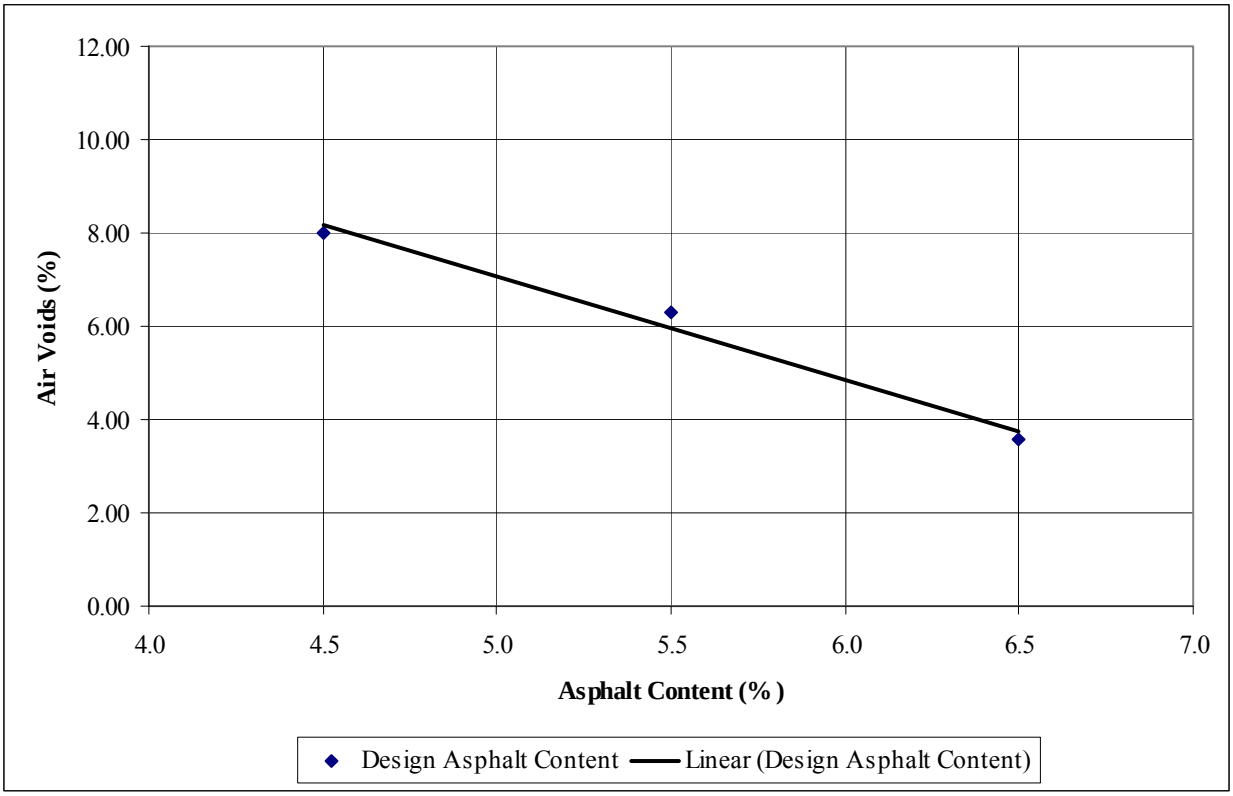

Figure A16 9.5L/G82-22, N85

Table A17 12.5L/G67-22, N50

G_{binder}	AC%	Sample ID	Dry Weight, grams	Pyc,Asphalt, Water, grams	Pyc,Water, grams	Gmm	Average Gmm	Gse
1.0250	5.5	1	1580.0	8488.3	7572.5	2.3788	2.3745	2.5715
		2	1576.4	8358.3	7447.0	2.3702		

Gmm Values		Sample ID	Dry Weight, grams	Submerged Weight, grams	SSD Weight, grams	Gmb	Average Gmb	Percent Air Voids
AC Content	Gmm							
4.5	2.4080	1	4273.9	2414.5	4300.0	2.267	2.265	5.94
		2	4271.4	2411.4	4298.8	2.263		
5.5	2.3745	1	4317.9	2445.8	4321.8	2.302	2.308	2.81
		2	4311.3	2451.9	4315.2	2.314		
6.5	2.3419	1	4343.8	2484.2	4344.8	2.335	2.335	0.28
		2	4349.8	2489.2	4351.2	2.336		

Asphalt Content @ 4% Air Voids: 5.15

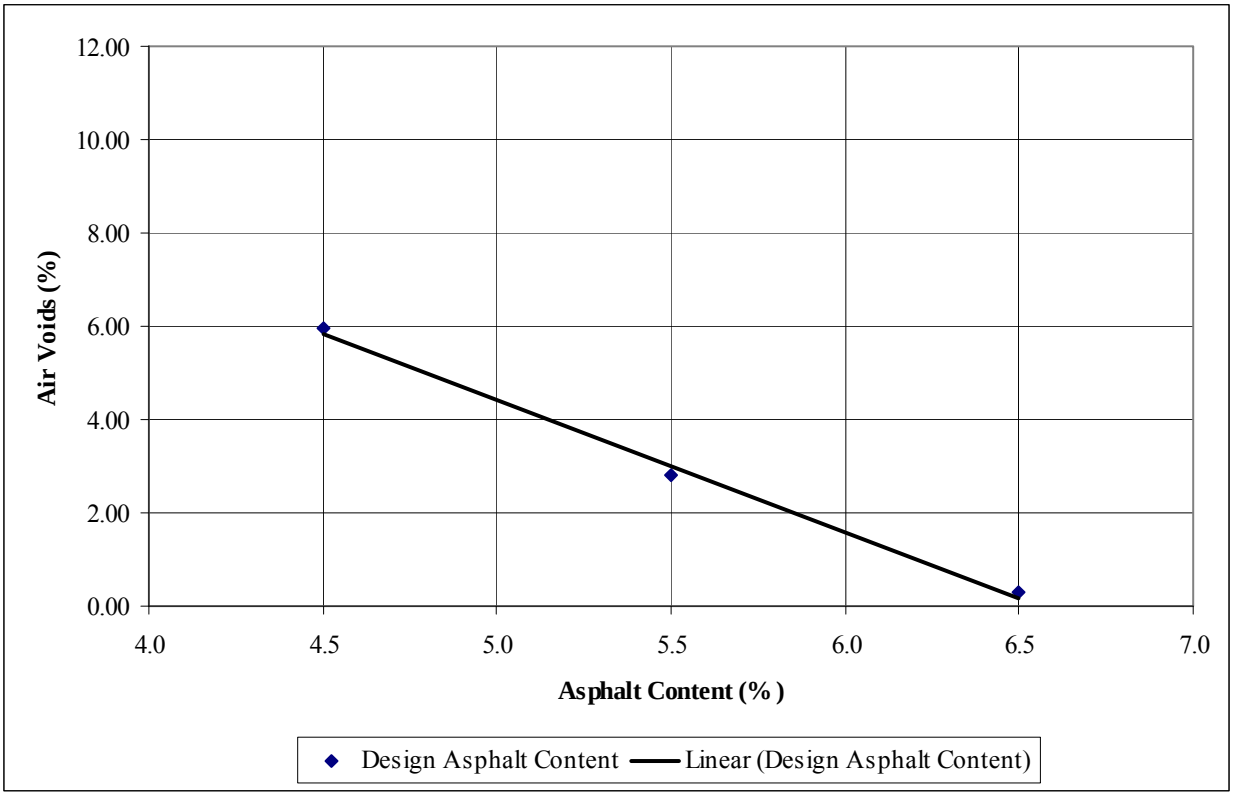

Figure A17 12.5L/G67-22, N50

Table A18 12.5L/G67-22, N65

G_{binder}	AC%	Sample ID	Dry Weight, grams	Pyc,Asphalt, Water, grams	Pyc,Water, grams	Gmm	Average Gmm	Gse
1.0250	5.5	1	1580.0	8488.3	7572.5	2.3788	2.3745	2.5715
		2	1576.4	8358.3	7447.0	2.3702		

Gmm Values		Sample ID	Dry Weight, grams	Submerged Weight, grams	SSD Weight, grams	Gmb	Average Gmb	Percent Air Voids
AC Content	Gmm							
4.5	2.4080	1	4484.5	2536.6	4505.2	2.278	2.279	5.37
		2	4474.5	2532.6	4495.5	2.280		
5.5	2.3754	1	4530.0	2583.6	4534.5	2.322	2.326	2.05
		2	4523.5	2586.5	4528.3	2.330		
6.5	2.3419	1	4563.5	2613.7	4564.7	2.339	2.336	0.25
		2	4552.9	2603.2	4554.7	2.333		
		Asphalt Content @ 4% Air Voids:			4.95			

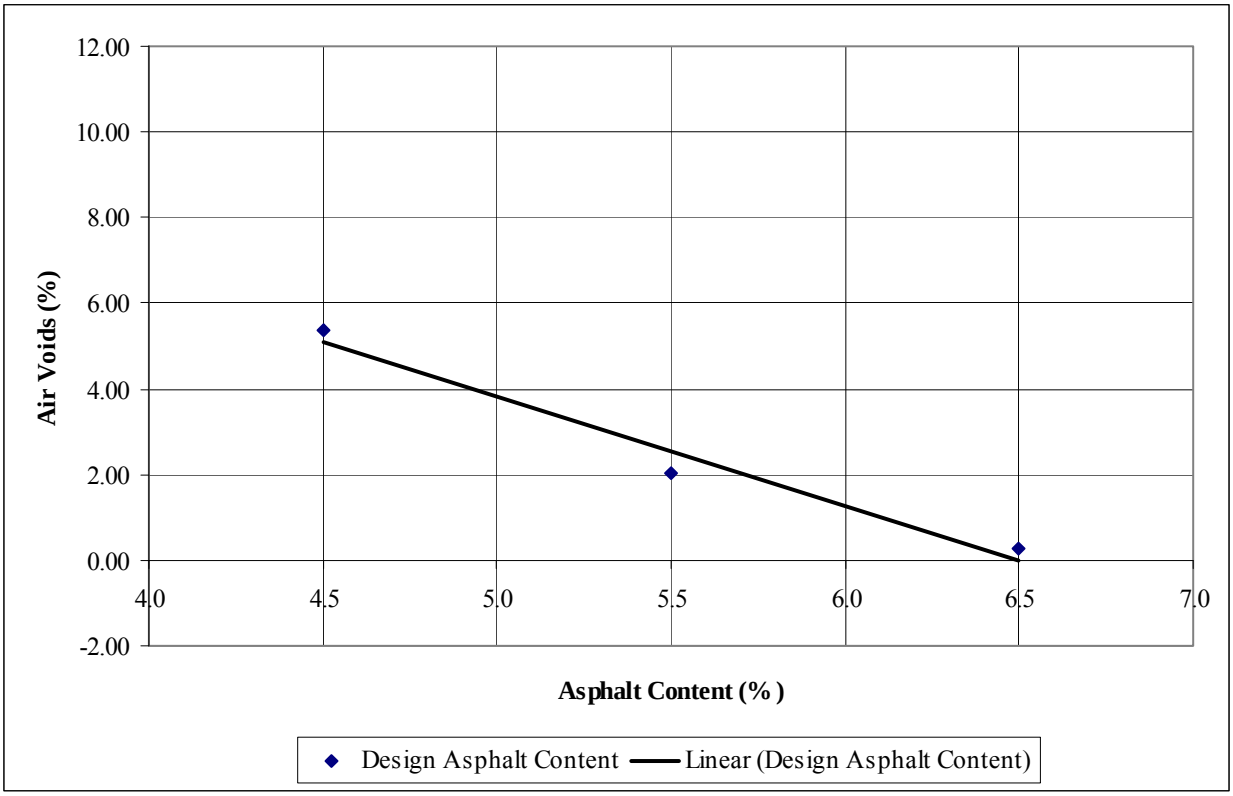

Figure A18 12.5L/G67-22, N65

Table A19 12.5L/G76-22, N85

G_{binder}	AC%	Sample ID	Dry Weight, grams	Pyc,Asphalt, Water, grams	Pyc,Water, grams	Gmm	Average Gmm	Gse
1.0250	5.5	1	1589.6	8492.6	7572.5	2.3743	2.3748	2.5720
		2	1573.2	8357.9	7447.0	2.3754		

Gmm Values		Sample ID	Dry Weight, grams	Submerged Weight, grams	SSD Weight, grams	Gmb	Average Gmb	Percent Air Voids
AC Content	Gmm							
4.5	2.4084	1	4481.1	2536.2	4506.5	2.274	2.279	5.38
		2	4468.7	2535.6	4492.7	2.283		
5.5	2.3748	1	4518.0	2567.7	4523.4	2.310	2.317	2.43
		2	4511.2	2575.0	4516.1	2.324		
6.5	2.3422	1	4543.9	2597.1	4546.2	2.331	2.333	0.39
		2	4556.1	2607.3	4558.5	2.335		

Asphalt Content @ 4% Air Voids: 5.00

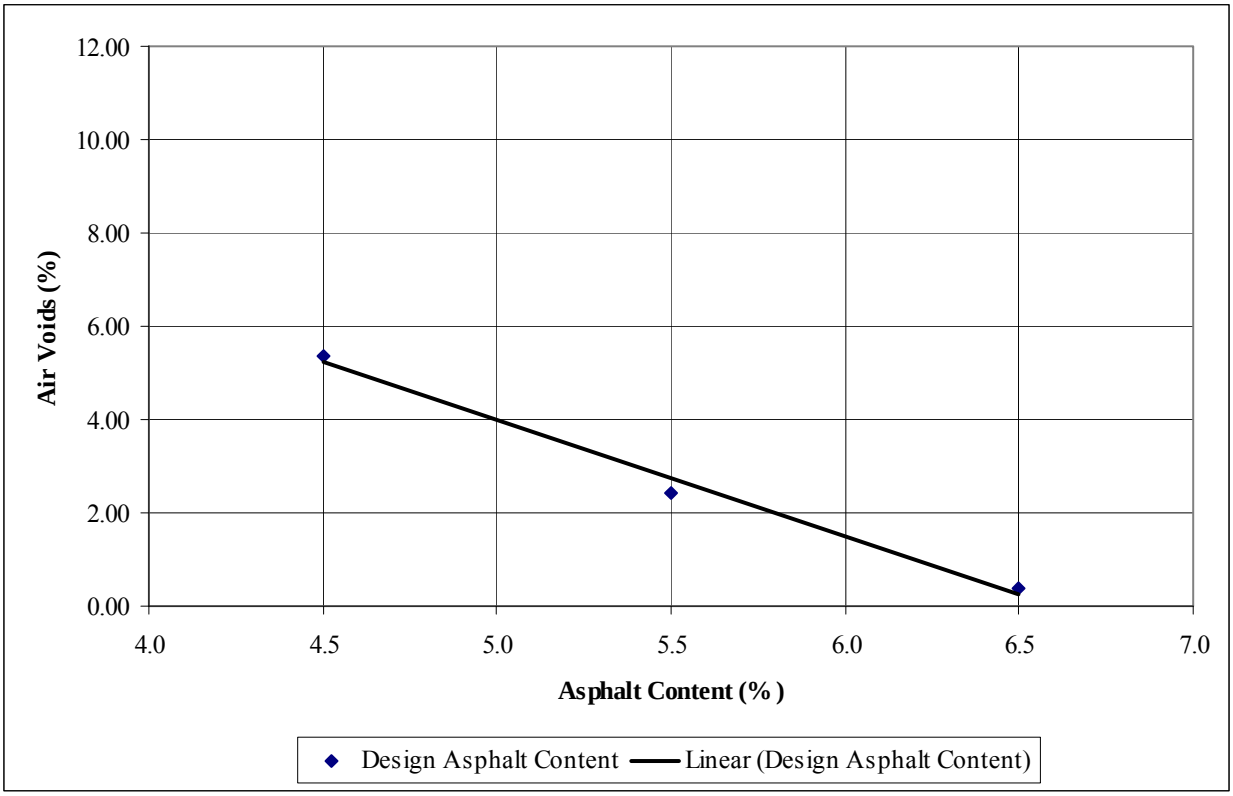

FigureA19 12.5L/G76-22, N85

Table A20 12.5L/G82-22, N85

G_{binder}	AC%	Sample ID	Dry Weight, grams	Pyc,Asphalt, Water, grams	Pyc,Water, grams	Gmm	Average Gmm	Gse
1.0250	5.5	1	1585.7	8496.9	7572.5	2.3979	2.3897	2.5905
		2	1572.6	8359.3	7447.0	2.3816		

Gmm Values		Sample ID	Dry Weight, grams	Submerged Weight, grams	SSD Weight, grams	Gmb	Average Gmb	Percent Air Voids
AC Content	Gmm							
4.5	2.4239	1	4468.6	2520.8	4540.0	2.213	2.227	8.11
		2	4471.6	2522.6	4517.5	2.242		
5.5	2.3897	1	4517.8	2539.6	4536.7	2.262	2.245	6.04
		2	4504.3	2511.0	4532.1	2.229		
6.5	2.3565	1	4552.9	2546.8	4566.1	2.255	2.253	4.37
		2	4560.3	2550.1	4574.9	2.252		

Asphalt Content @ 4% Air Voids: 6.66

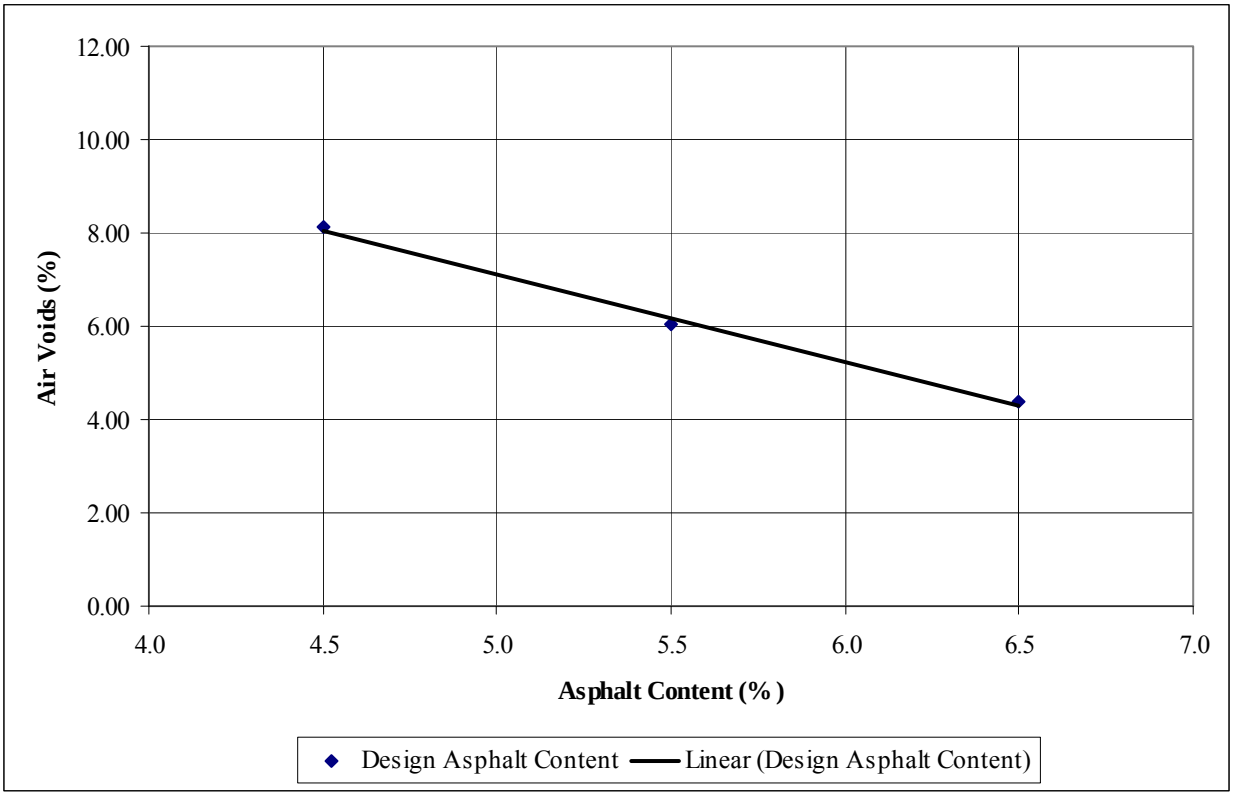

Figure A20 12.5L/G82-22, N85

Table A21 19.0L/G67-22, N50

G_{binder}	AC%	Sample ID	Dry Weight, grams	Pyc,Asphalt, Water, grams	Pyc,Water, grams	Gmm	Average Gmm	Gse
1.0250	5.5	1	1593.5	8496.7	7572.5	2.3808	2.3846	2.5841
		2	1516.1	8328.3	7447.0	2.3883		

Gmm Values		Sample ID	Dry Weight, grams	Submerged Weight, grams	SSD Weight, grams	Gmb	Average Gmb	Percent Air Voids
AC Content	Gmm							
4.5	2.4185	1	4483.4	2566.5	4492.8	2.327	2.330	3.67
		2	4483.1	2572.8	4495.2	2.332		
5.5	2.3846	1	4520.0	2600.6	4522.8	2.351	2.354	1.28
		2	4524.4	2608.4	4528.2	2.357		
6.5	2.3516	1	4545.5	2613.4	4546.6	2.351	2.353	-0.05
		2	4555.8	2622.1	4557.3	2.354		

Asphalt Content @ 4% Air Voids: 4.26

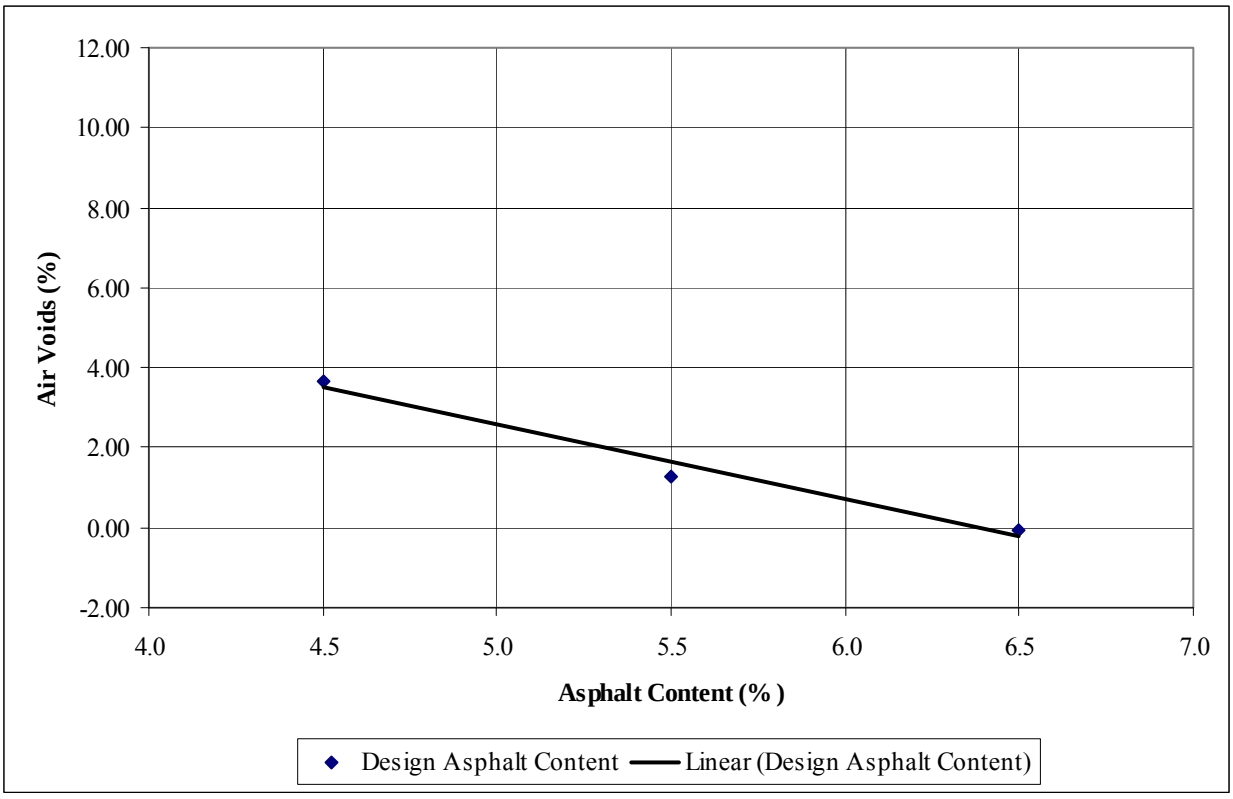

Figure A21 19.0L/G67-22, N50

Table A22 19.0L/G67-22, N65

G_{binder}	AC%	Sample ID	Dry Weight, grams	Pyc,Asphalt, Water, grams	Pyc,Water, grams	Gmm	Average Gmm	Gse
1.0250	5.5	1	1593.5	8496.7	7572.5	2.3808	2.3846	2.5841
		2	1516.1	8328.3	7447	2.3883		

Gmm Values		Sample ID	Dry Weight, grams	Submerged Weight, grams	SSD Weight, grams	Gmb	Average Gmb	Percent Air Voids
AC Content	Gmm							
4.5	2.4185	1	4479.6	2568.0	4489.4	2.331	2.338	3.33
		2	4483.1	2579.9	4492.0	2.345		
5.5	2.3846	1	4522.2	2618.1	4524.2	2.372	2.367	0.73
		2	4518.1	2608.1	4521.1	2.362		
6.5	2.3516	1	4556.7	2621.8	4557.3	2.354	2.354	-0.11
		2	4558.2	2623.0	4559.4	2.354		

Asphalt Content @ 4% Air Voids: 4.06

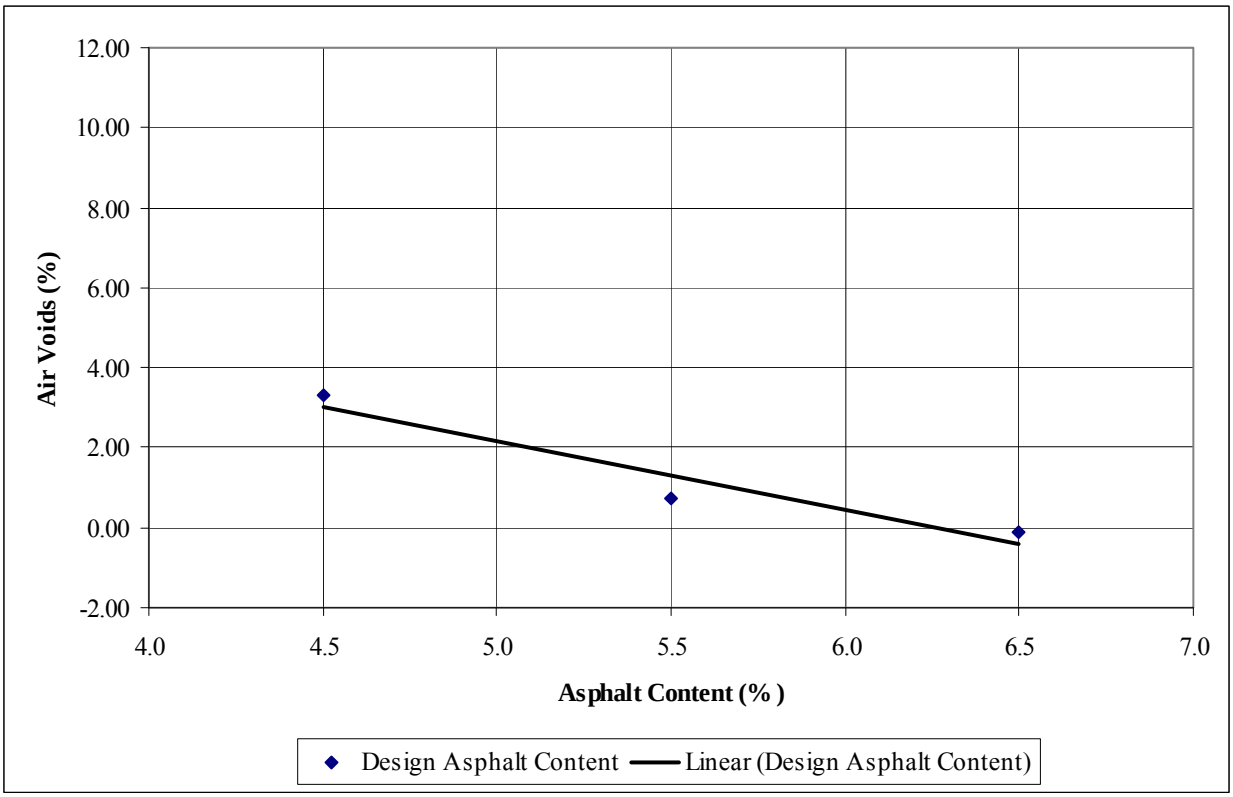

Figure A22 19.0L/G67-22, N65

Table A23 19.0L/G76722, N85

G_{binder}	AC%	Sample ID	Dry Weight, grams	Pyc,Asphalt, Water, grams	Pyc,Water, grams	Gmm	Average Gmm	Gse
1.0250	5.5	1	1593.5	8496.7	7572.5	2.3808	2.3846	2.5841
		2	1516.1	8328.3	7447	2.3883		

Gmm Values		Sample ID	Dry Weight, grams	Submerged Weight, grams	SSD Weight, grams	Gmb	Average Gmb	Percent Air Voids
AC Content	Gmm							
4.5	2.4535	1	4442.7	2539.2	4473.9	2.296	2.295	6.47
		2	4440.8	2543.9	4480.3	2.293		
5.5	2.4185	1	4482.9	2572.4	4493.2	2.334	2.329	3.71
		2	4481.2	2564.4	4492.7	2.324		
6.5	2.3846	1	4511.9	2608.7	4514.4	2.368	2.367	0.74
		2	4522.6	2614.1	4525.3	2.366		
		Asphalt Content @ 4% Air Voids:			4.37			

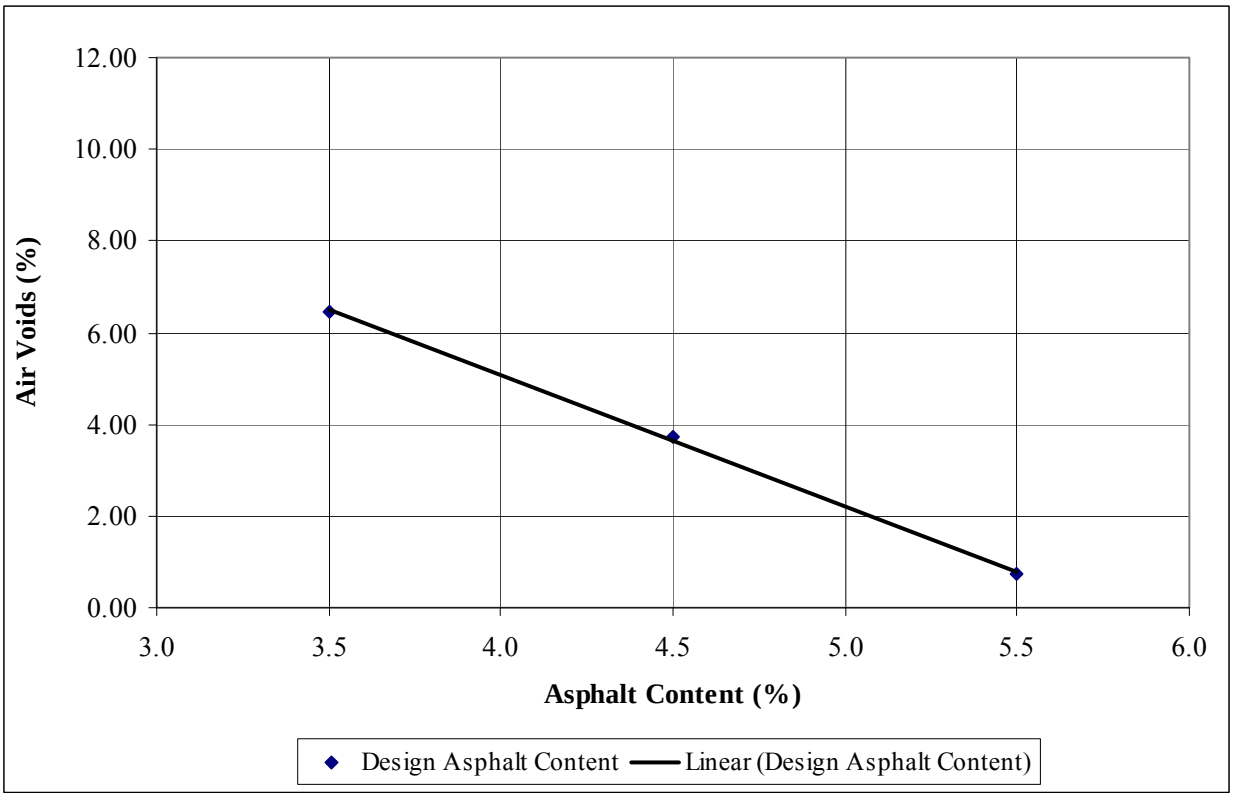

Figure A23 19.0L/G67-22, N85

Table A24 19.0L/G76-22, N85

G_{binder}	AC%	Sample ID	Dry Weight, grams	Pyc,Asphalt, Water, grams	Pyc,Water, grams	Gmm	Average Gmm	Gse
1.0250	5.5	1	1579.5	8488.2	7572.5	2.3795	2.3796	2.5779
		2	1552.8	8347.3	7447.0	2.3798		

Gmm Values		Sample ID	Dry Weight, grams	Submerged Weight, grams	SSD Weight, grams	Gmb	Average Gmb	Percent Air Voids
AC Content	Gmm							
4.5	2.4134	1	4473.4	2561.8	4483.5	2.328	2.334	3.27
		2	4462.8	2564.2	4470.5	2.341		
5.5	2.3796	1	4500.6	2598.8	4505.9	2.360	2.358	0.91
		2	4511.9	2602.3	4517.3	2.356		
6.5	2.3468	1	4544.4	2620.3	4546.9	2.359	2.359	-0.5
		2	4554.6	2626.2	4557.5	2.358		

Asphalt Content @ 4% Air Voids: 4.06

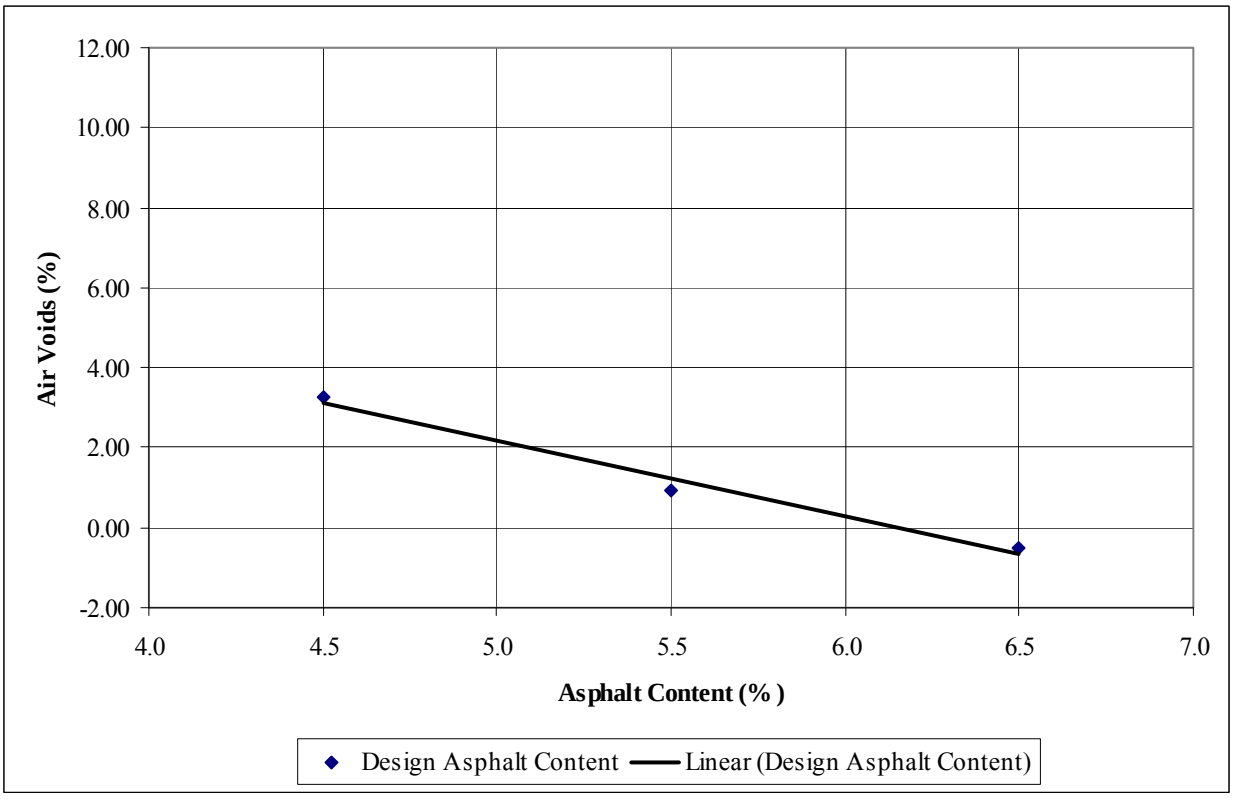

Figure A24 19.0L/G76-22, N85

Table A25 19.0GR67-22, N50 (3% AV Design)

G_{binder}	AC%	Sample ID	Dry Weight, grams	Pyc,Asphalt, Water, grams	Pyc,Water, grams	Gmm	Average Gmm	Gse
1.0250	5.5	1	1579.5	8488.2	7572.5	2.3795	2.3796	2.5779
		2	1552.8	8347.3	7447.0	2.3798		

Gmm Values		Sample ID	Dry Weight, grams	Submerged Weight, grams	SSD Weight, grams	Gmb	Average Gmb	Percent Air Voids
AC Content	Gmm							
4.5	2.4134	1	4473.4	2561.8	4483.5	2.328	2.334	3.27
		2	4462.8	2564.2	4470.5	2.341		
5.5	2.3796	1	4500.6	2598.8	4505.9	2.360	2.358	0.91
		2	4511.9	2602.3	4517.3	2.356		
6.5	2.3468	1	4544.4	2620.3	4546.9	2.359	2.359	-0.5
		2	4554.6	2626.2	4557.5	2.358		

Asphalt Content @ 3% Air Voids: 4.58

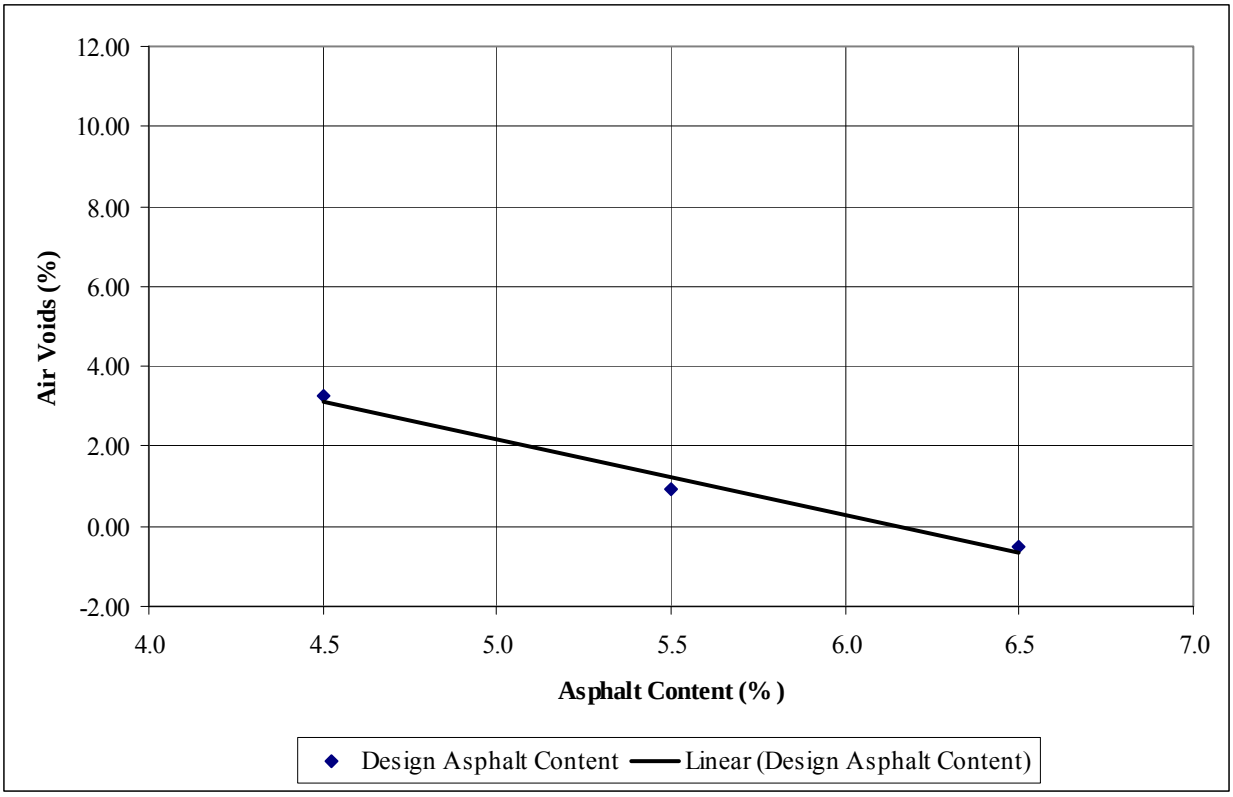

Figure A25 19.0GR67-22, N50 (3% AV Design)

APPENDIX B

DYNAMIC MODULI DATA

Table B1 9.5GR67-22, N50

Temperature, °C	Frequency, Hz	Dynamic Modulus, psi			
		A	B	C	Average
-10	25	2637304	1761973	2387725	2262334
	10	2529084	1670636	2306228	2168649
	5	2438805	1614603	2229588	2094332
	1	2240194	1464418	2037050	1913887
	0.5	2141993	1396979	1943819	1827597
	0.1	1891148	1241528	1702177	1611618
4	25	1825279	1447866	1741300	1671482
	10	1657567	1279496	1569146	1502070
	5	1546643	1189964	1459427	1398678
	1	1272673	991296	1196245	1153405
	0.5	1152306	907609	1070749	1043555
	0.1	876746	705849	788478	790358
21	25	838131	802233	508602	716322
	10	685207	643618	643095	657307
	5	569005	545852	554946	556601
	1	359648	345229	359410	354762
	0.5	281586	278091	284038	281238
	0.1	294560	162568	161735	206288
37	25	406667	385005	304619	365431
	10	276736	240085	172388	229736
	5	205601	174511	132748	170953
	1	100004	79635	59608	79749
	0.5	76283	64253	46644	62393
	0.1	47587	39774	30387	39249
54	25	127529	115039	81451	108006
	10	62529	54685	45985	54400
	5	34171	28451	23846	28822
	1	20496	16884	13860	17080
	0.5	16903	14273	12407	14528
	0.1	13265	11306	10018	11530

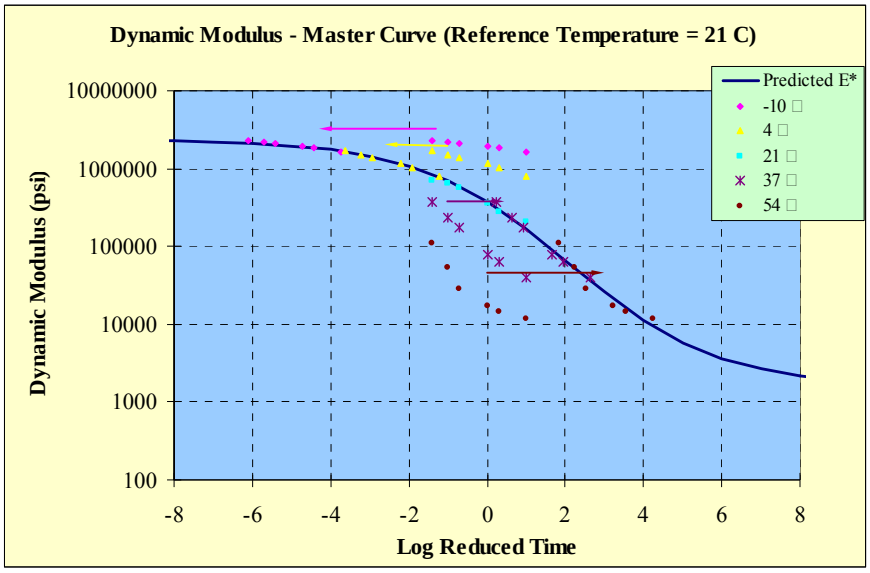

Figure B1 9.5GR67-22, N50

Table B2 9.5GR67-22, N65

Temperature, °C	Frequency, Hz	Dynamic Modulus, psi			
		A	B	C	Average
-10	25	1543523	2886312	3499598	2643144
	10	1521930	2827788	3261238	2536985
	5	1471132	2768035	3160150	2466439
	1	1350957	2567141	2856438	2258179
	0.5	1288724	2483762	2738496	2170327
	0.1	1137673	2267806	2419108	1941529
4	25	1031875	2116659	2230451	1792995
	10	951226	1999431	2027614	1659424
	5	892869	1908007	1882464	1561113
	1	743658	1588765	1558503	1296975
	0.5	671405	1433794	1412410	1172536
	0.1	516089	1098421	1083066	899192
21	25	936901	989042	1028195	984713
	10	659377	805633	890048	785019
	5	585891	683643	772487	680674
	1	369974	440166	577059	462400
	0.5	318656	354118	483087	385287
	0.1	202237	209079	284458	231925
37	25	481481	432790	444596	452956
	10	330086	304501	299519	311369
	5	250715	229137	219148	233000
	1	120133	111178	119954	117088
	0.5	99397	87868	92845	93370
	0.1	63760	50518	52840	55706
54	25	160658	148774	140766	150066
	10	85083	67955	65257	72765
	5	45176	39615	40587	41793
	1	25827	22392	23920	24047
	0.5	21543	19109	20021	20224
	0.1	15392	13772	14179	14448

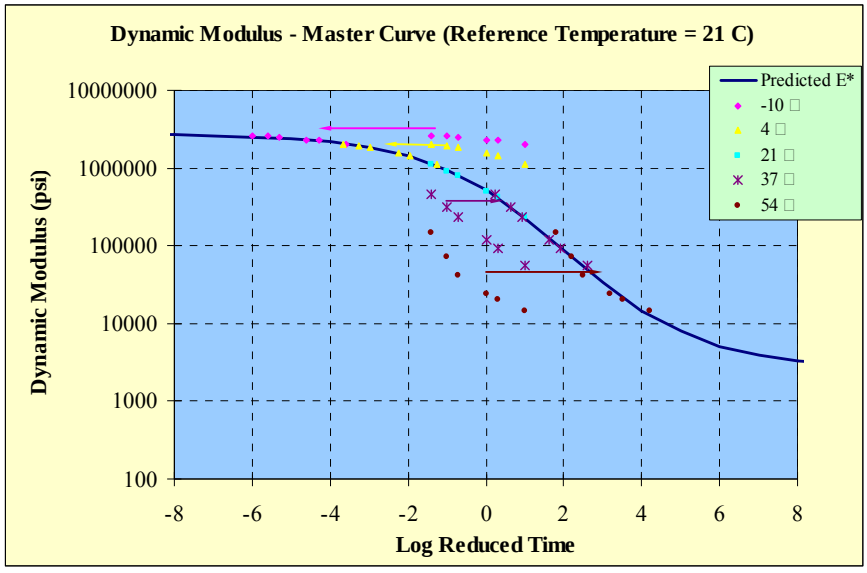

Figure B2 9.5GR67-22, N65

Table B3 9.5GR76-22, N85

Temperature, °C	Frequency, Hz	Dynamic Modulus, psi			
		A	B	C	Average
-10	25	2562490	2517532	2277809	2452610
	10	2450255	2434667	2154857	2346593
	5	2325048	2362043	2086654	2257915
	1	2114564	2174021	1911429	2066671
	0.5	2010162	2077083	1834608	1973951
	0.1	1755920	1842411	1638973	1745768
4	25	1849556	1808765	1750790	1803037
	10	1653907	1637880	1607216	1633001
	5	1529526	1519171	1480470	1509722
	1	1243861	1261920	1196758	1234180
	0.5	1118485	1151467	1070574	1113509
	0.1	841053	891815	793224	842030
21	25	898101	965652	860729	908161
	10	715006	791907	677968	728294
	5	598028	683859	560292	614060
	1	379237	454081	350338	394552
	0.5	316980	376182	285292	326152
	0.1	189041	228887	169859	195929
37	25	357062	422515	363651	381076
	10	233096	261323	215778	236732
	5	155403	180942	145582	160642
	1	84999	109911	85722	93544
	0.5	69762	86665	67085	74504
	0.1	45536	54022	41991	47183
54	25	149309	151520	135125	145318
	10	80532	89632	73398	81187
	5	52359	58551	45616	52175
	1	25385	28476	23048	25636
	0.5	26068	28331	23496	25965
	0.1	23216	25131	21571	23306

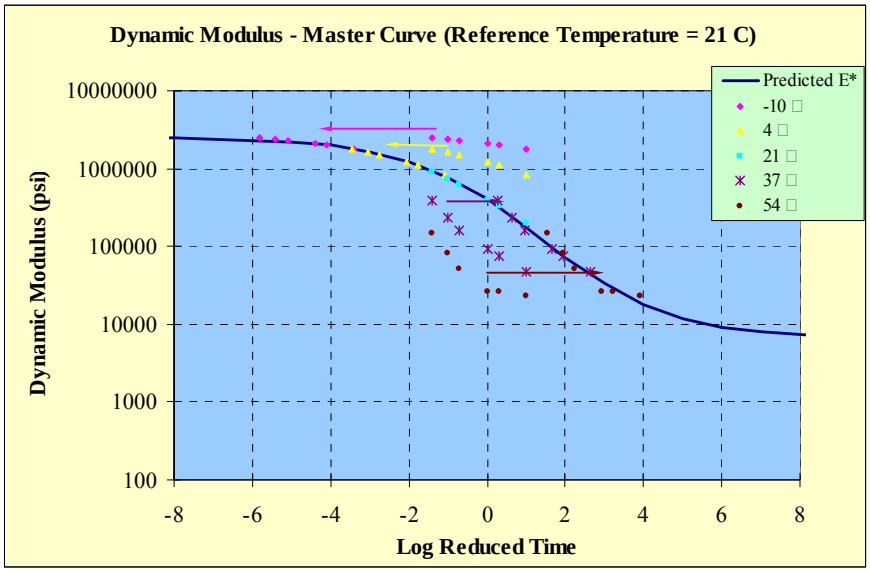

Figure B3 9.5GR76-22, N85

Table B4 9.5GR82-22, N85

Temperature, °C	Frequency, Hz	Dynamic Modulus, psi			
		A	B	C	Average
-10	25	2227577	2786160	2557425	2523721
	10	2132169	2739214	2473986	2448456
	5	2077387	2682263	2619951	2459867
	1	1943519	2502746	2430111	2292125
	0.5	1867370	2420640	2343879	2210630
	0.1	1694870	2197363	2122030	2004754
4	25	1837565	2189923	1639089	1888859
	10	1685473	2053681	1513486	1750880
	5	1608955	1942469	1455113	1668846
	1	1384111	1653718	1262143	1433324
	0.5	1276969	1527817	1218627	1341138
	0.1	1020243	1232504	978149	1076965
21	25	1033867	1261415	1202300	1165861
	10	860755	1041264	908899	936973
	5	752512	920879	816836	830076
	1	548544	654555	604040	602379
	0.5	460915	557177	517622	511905
	0.1	296189	359382	334573	330048
37	25	535338	561451	595448	564079
	10	337322	361987	374845	358051
	5	237729	228624	274345	246899
	1	147469	140589	167713	151924
	0.5	119807	123977	133616	125800
	0.1	74246	78636	81609	78164
54	25	240512	244388	233593	239498
	10	128729	135173	139623	134508
	5	76721	82002	86131	81618
	1	47455	49355	48466	48425
	0.5	42395	42508	42414	42439
	0.1	31439	30718	31879	31345

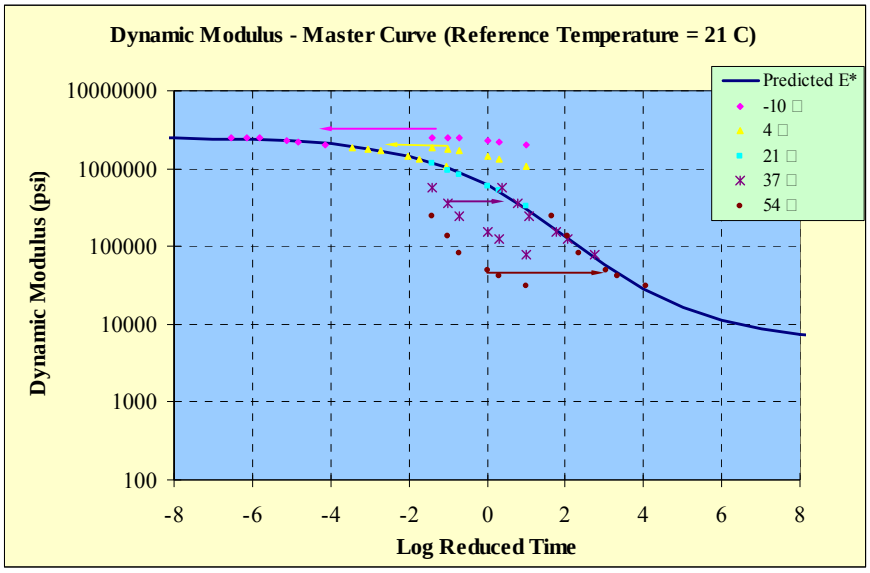

Figure B4 9.5GR82-22, N85

Table B5 12.5GR67-22, N50

Temperature, °C	Frequency, Hz	Dynamic Modulus, psi			
		A	B	C	Average
-10	25	2379602	2314931	2373096	2355876
	10	2241301	2078574	2251130	2190335
	5	2163412	1999872	2171920	2111735
	1	1965776	1844215	1971356	1927116
	0.5	1862891	1790750	1873949	1842530
	0.1	1614892	1606184	1644606	1621894
4	25	1640535	1764633	1667952	1691040
	10	1459645	1603536	1533100	1532094
	5	1342064	1499342	1434886	1425431
	1	1084823	1243847	1188075	1172248
	0.5	974641	1129936	1084034	1062870
	0.1	731604	863630	837381	810872
21	25	802454	854406	848917	835259
	10	649239	700719	681705	677221
	5	543281	596242	581148	573557
	1	332683	377905	361290	357293
	0.5	265950	308893	292751	289198
	0.1	150561	181286	171310	167719
37	25	360500	342239	382288	361676
	10	218835	211691	230715	220413
	5	153883	147280	160651	153938
	1	86479	79502	89160	85047
	0.5	65461	59045	66952	63819
	0.1	39035	33897	39007	37313
54	25	118155	124739	111783	118226
	10	49259	66207	46573	54013
	5	32588	41968	32352	35636
	1	14158	18811	14123	15697
	0.5	11474	15304	11827	12869
	0.1	11292	11164	11623	11360

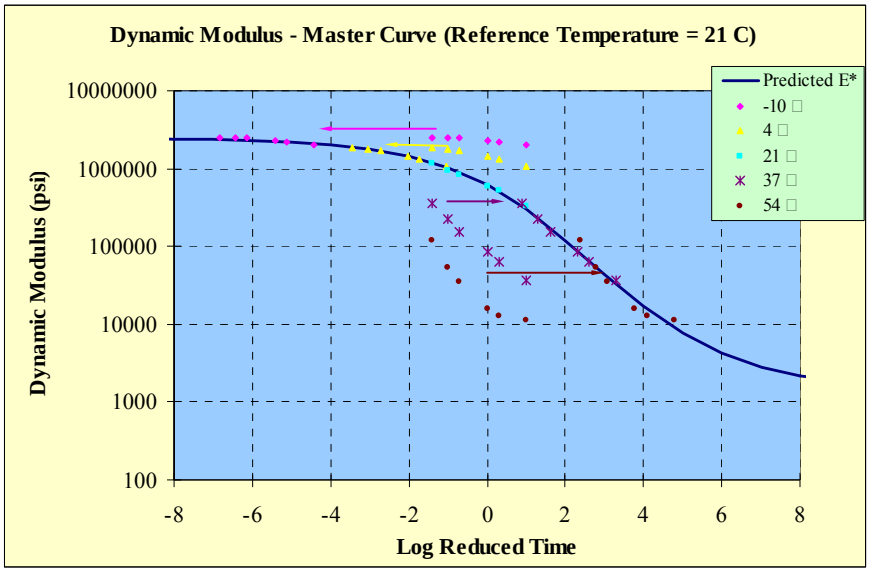

Figure B5 12.5GR67-22, N50

Table B6 12.5GR67-22, N65

Temperature, °C	Frequency, Hz	Dynamic Modulus, psi			
		A	B	C	Average
-10	25	3247427	2149028	1505146	2300534
	10	3166864	1833077	1466523	2155488
	5	3043298	1775758	1396609	2071888
	1	2770611	1641851	1319360	1910607
	0.5	2642129	1613332	1298847	1851436
	0.1	2337619	1441483	1211746	1663616
4	25	2290449	2005068	1637919	1977812
	10	2075110	1853955	1398558	1775874
	5	1891141	1712292	1321432	1641622
	1	1566685	1393159	1087459	1349101
	0.5	1405585	1264181	986939	1218902
	0.1	1045908	966753	737393	916685
21	25	924062	958967	900396	927808
	10	726008	779180	722415	742534
	5	601355	659542	623638	628178
	1	356703	410999	385535	384412
	0.5	280353	324558	308160	304357
	0.1	154325	179815	310829	214990
37	25	356344	421706	343262	373771
	10	234463	283807	218745	245672
	5	105703	206760	155687	156050
	1	81820	88543	69481	79948
	0.5	62565	70260	51038	61287
	0.1	38599	42803	36203	39201
54	25	124307	170251	91525	128694
	10	60026	87190	51411	66209
	5	32734	46945	25729	35136
	1	19150	24845	14324	19440
	0.5	15929	21214	12741	16628
	0.1	12475	14552	10428	12485

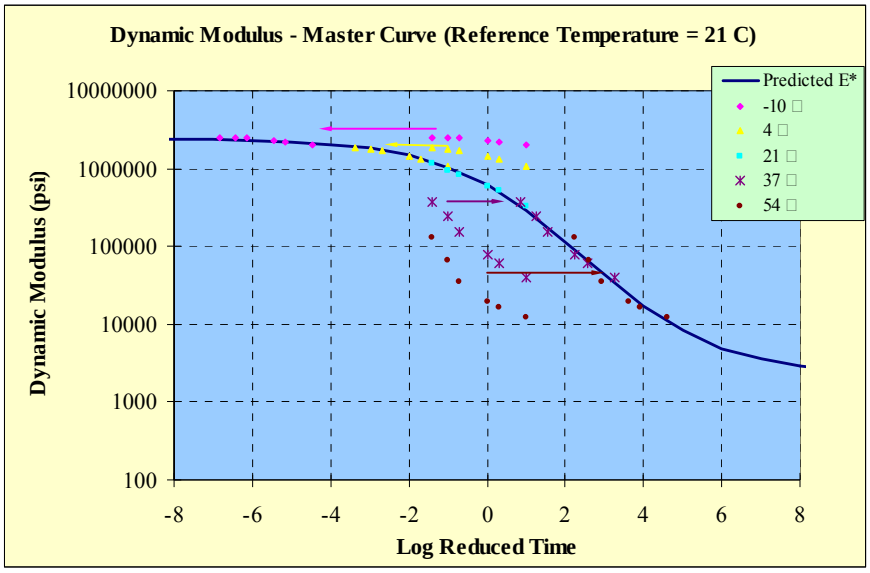

Figure B6 12.5GR67-22, N65

Table B7 12.5GR76-22, N85

Temperature, °C	Frequency, Hz	Dynamic Modulus, psi			
		A	B	C	Average
-10	25	1916321	2363933	1815373	2031876
	10	1825697	2278821	1712284	1938934
	5	1760424	2196942	1686797	1881388
	1	1593116	1993899	1569998	1719004
	0.5	1527273	1910299	1548915	1662162
	0.1	1357318	1693905	1386734	1479319
4	25	1468264	1755348	1746830	1656814
	10	1333425	1626322	1602475	1520741
	5	1264889	1527991	1502977	1431952
	1	1047994	1269123	1237990	1185036
	0.5	960596	1158141	1125180	1081306
	0.1	744559	891989	865247	833932
21	25	798185	900130	831887	843401
	10	626236	717446	671735	671806
	5	531256	607167	558036	565486
	1	353257	398176	355570	369001
	0.5	288326	320717	287207	298750
	0.1	177091	191955	173902	180983
37	25	416285	446512	445450	436082
	10	272734	323915	316985	304544
	5	213207	232265	241084	228852
	1	87387	117812	117041	107413
	0.5	81114	97679	99067	92620
	0.1	61970	60946	62428	61781
54	25	166760	180374	172155	173096
	10	92444	95023	91523	92997
	5	61934	59054	82646	67878
	1	35183	35266	33625	34691
	0.5	31665	32267	33401	32444
	0.1	26668	27091	27863	27207

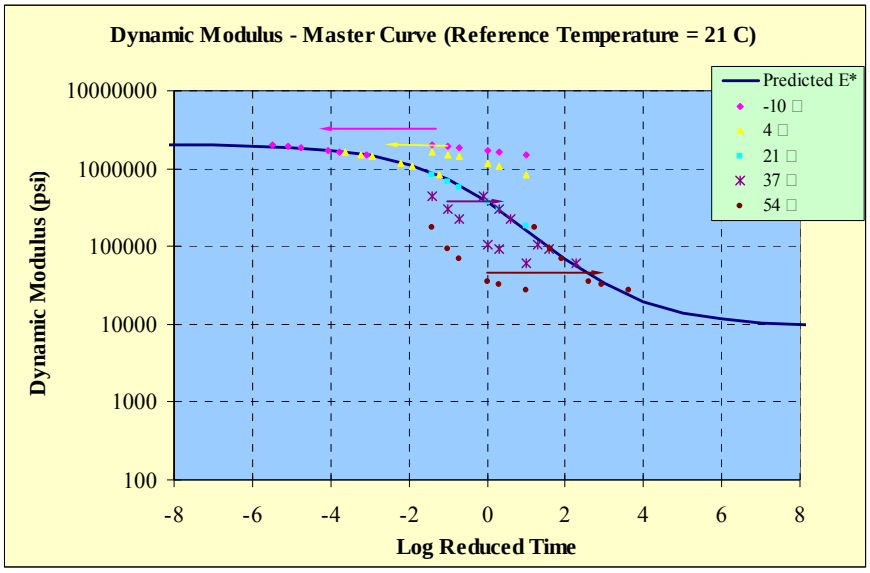

Figure B7 12.5GR76-22, N85

Table B8 12.5GR82-22, N85

Temperature, °C	Frequency, Hz	Dynamic Modulus, psi			
		A	B	C	Average
-10	25	1998082	1946225	2388849	2111052
	10	1897602	1811269	2291371	2000081
	5	1829384	1724657	2211781	1921941
	1	1686771	1590656	2019571	1765666
	0.5	1615243	1491562	1920126	1675644
	0.1	1437344	1247601	1692519	1459155
4	25	1533877	1406782	1798809	1579823
	10	1397217	1263824	1638799	1433280
	5	1319014	1222260	1534630	1358635
	1	1113725	1010152	1256946	1126941
	0.5	1018187	921062	1127826	1022358
	0.1	792863	695004	842427	776764
21	25	836193	769234	831719	812382
	10	656556	583494	643731	627927
	5	548588	483881	531510	521326
	1	365873	299685	336774	334111
	0.5	298905	241303	268649	269619
	0.1	184148	143764	160777	162896
37	25	434637	373802	383936	397458
	10	264720	248682	259086	257496
	5	193818	188798	171106	184574
	1	112087	85999	97803	98630
	0.5	90089	73677	79556	81107
	0.1	58503	47858	51459	52607
54	25	183272	156106	164724	168034
	10	109187	88328	99661	99058
	5	60683	69821	75949	68818
	1	36471	27424	30087	31327
	0.5	34296	27809	31747	31284
	0.1	27661	24921	27514	26699

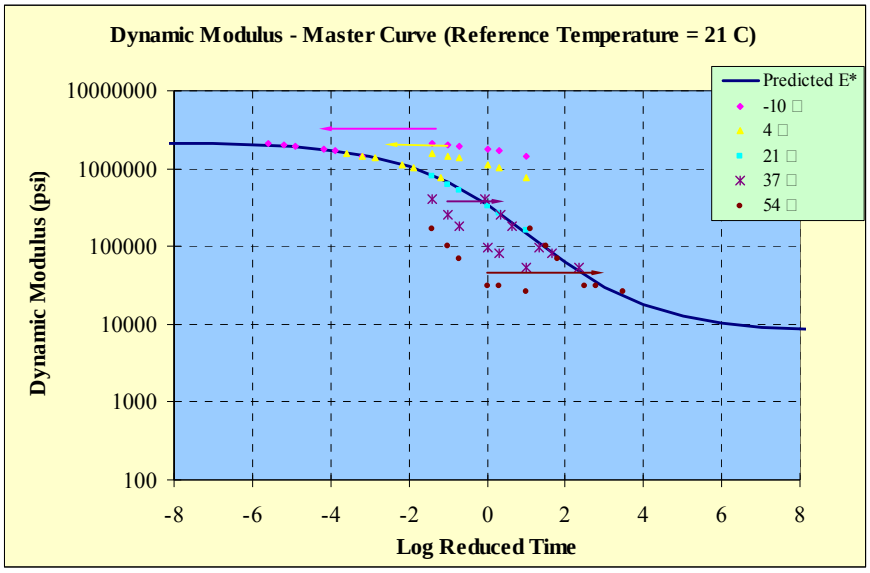

Figure B8 12.5GR82-22, N85

Table B9 19.0GR67-22, N50

Temperature, °C	Frequency, Hz	Dynamic Modulus, psi			
		A	B	C	Average
-10	25	2857665	2300001	2372923	2510196
	10	2756453	2194506	2291951	2414303
	5	2670699	2128283	2227817	2342266
	1	2450877	1947014	2047968	2148620
	0.5	2342858	1862697	1964418	2056658
	0.1	2091729	1661567	1781667	1844988
4	25	2145500	1894703	1827294	1955832
	10	1980452	1729922	1698662	1803012
	5	1862181	1620096	1602469	1694915
	1	1544974	1354785	1341087	1413615
	0.5	1398558	1230336	1219497	1282797
	0.1	1075177	945020	940339	986845
21	25	1161989	1072178	1088220	1107462
	10	932946	845870	878604	885806
	5	790006	712833	744807	749216
	1	497376	438480	467331	467729
	0.5	390683	353195	373365	372414
	0.1	211821	192530	202074	202142
37	25	588490	477805	385227	483841
	10	363856	291418	227767	294347
	5	266434	213682	159831	213316
	1	137327	114713	87713	113251
	0.5	105653	86969	66834	86485
	0.1	52533	45812	40146	46164
54	25	136768	123740	126355	128954
	10	67212	60436	63010	63553
	5	35480	32201	33072	33584
	1	20670	18157	19568	19465
	0.5	17123	15952	16573	16549
	0.1	13605	12649	13454	13236

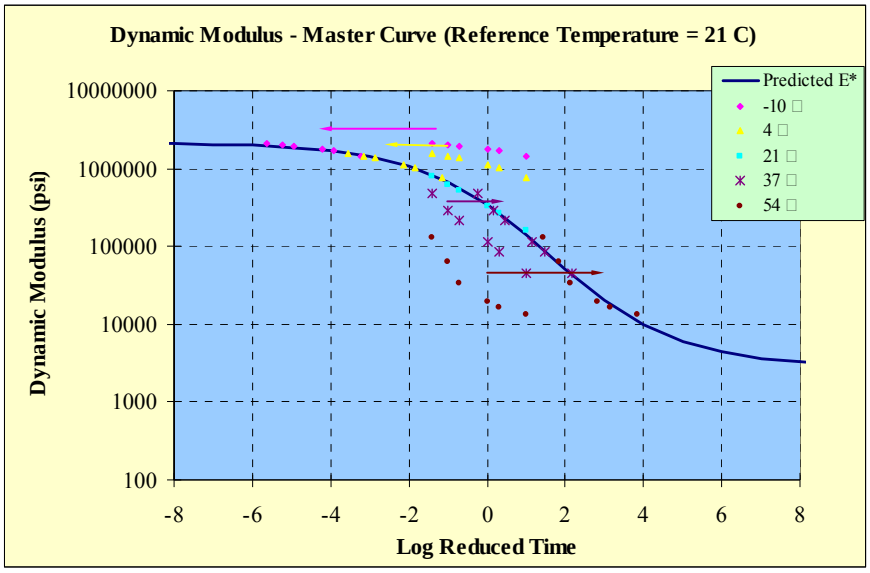

Figure B9 19.0GR67-22, N50

Table B10 19.0GR67-22, N65

Temperature, °C	Frequency, Hz	Dynamic Modulus, psi			
		A	B	C	Average
-10	25	4076065	2852158	2806858	3245027
	10	3838666	2668390	2775649	3094235
	5	3698581	2556100	2688920	2981200
	1	3332749	2423048	2443047	2732948
	0.5	3191511	2335609	2326718	2617946
	0.1	2801716	2083356	2040350	2308474
4	25	2964887	1651698	2076875	2231153
	10	2686806	1454781	1917229	2019605
	5	2484849	1332479	1788990	1868773
	1	2038890	1101969	1472837	1537899
	0.5	1833471	1036174	1335950	1401865
	0.1	1380117	814918	1034262	1076432
21	25	1211591	1087599	1054452	1117881
	10	969918	856952	858869	895246
	5	811159	713053	731977	752063
	1	496856	428196	456706	460586
	0.5	387902	331950	361343	360399
	0.1	204676	176771	200983	194144
37	25	398138	419825	438648	418870
	10	236491	244259	258544	246431
	5	168047	173407	183312	174922
	1	89906	91318	98201	93142
	0.5	63973	67703	72453	68043
	0.1	42332	39680	42058	41357
54	25	121492	123527	130732	125250
	10	58667	54350	69367	60794
	5	30732	35468	39998	35399
	1	17231	14601	17681	16504
	0.5	15386	12521	14997	14301
	0.1	13254	11855	13893	13000

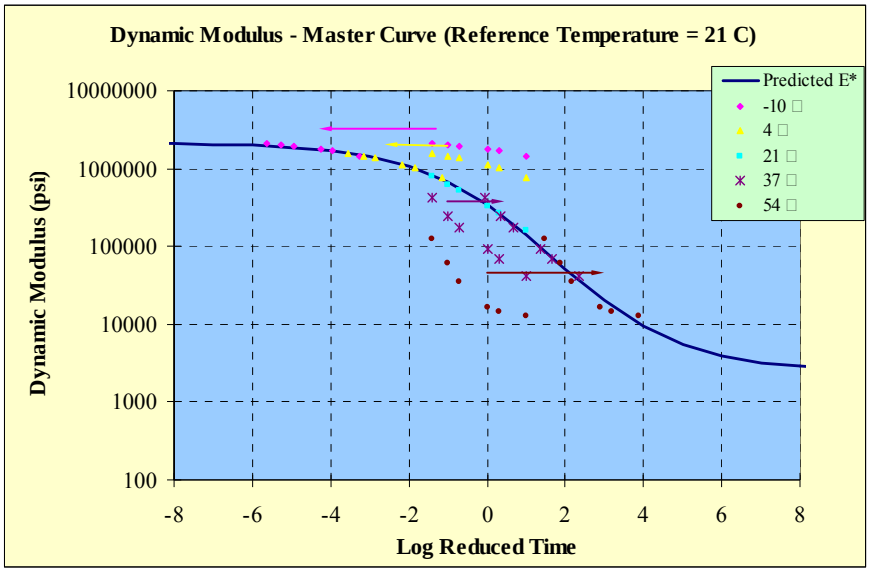

Figure B10 19.0GR67-22, N65

Table B11 19.0GR67-22, N85

Temperature, °C	Frequency, Hz	Dynamic Modulus, psi			
		A	B	C	Average
-10	25	3233151	2685985	2665207	2861448
	10	3013983	2608817	2607806	2743535
	5	2879232	2550388	2593596	2674405
	1	2652868	2376504	2408930	2479434
	0.5	2558197	2299821	2355854	2404624
	0.1	2285325	2099579	2144655	2176520
4	25	2506052	2098003	2266147	2290067
	10	2334062	1968691	2077673	2126809
	5	2187930	1856432	1942243	1995535
	1	1809201	1549483	1587531	1648738
	0.5	1648846	1422936	1439182	1503655
	0.1	1265287	1098566	1078944	1147599
21	25	1318866	1223215	1200183	1247421
	10	1094759	1005992	1019816	1040189
	5	934216	871540	877835	894530
	1	611047	580108	574856	588670
	0.5	490814	470014	461131	473986
	0.1	272320	264786	253639	263582
37	25	456564	471675	471625	466621
	10	309535	316397	290089	305340
	5	213917	217284	206713	212638
	1	90693	104888	110210	101930
	0.5	72991	78699	85477	79056
	0.1	49442	51618	47116	49392
54	25	160249	151133	151272	154218
	10	75754	71303	71996	73017
	5	41552	37917	38341	39270
	1	21472	21167	21449	21363
	0.5	18992	18224	18456	18557
	0.1	14985	14190	14214	14463

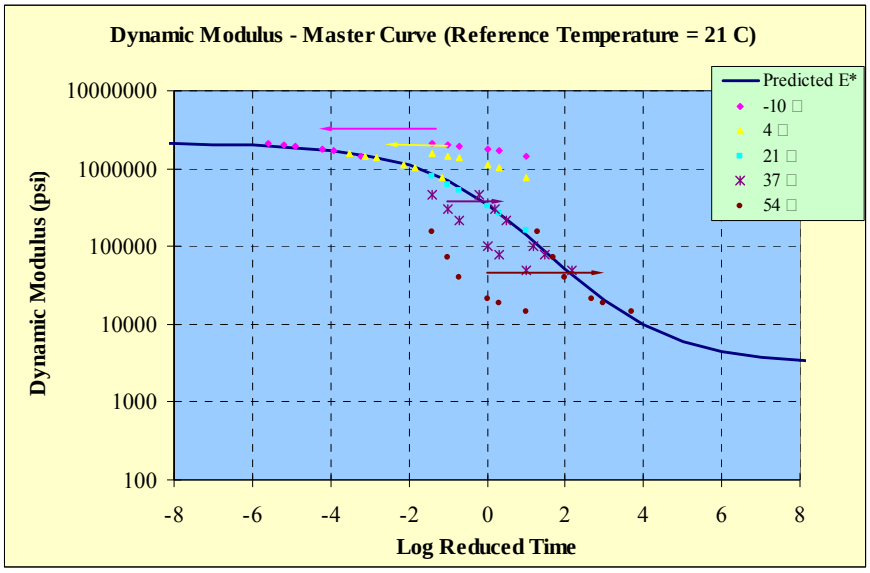

Figure B11 19.0GR67-22, N85

Table B12 19.0GR76-22, N85

Temperature, °C	Frequency, Hz	Dynamic Modulus, psi			
		A	B	C	Average
-10	25	2803166	2709223	2410840	2641076
	10	2629214	2471932	2308306	2469817
	5	2516642	2378741	2236369	2377251
	1	2277078	2185106	2061066	2174417
	0.5	2167920	2099378	1979640	2082313
	0.1	1901964	1882209	1774125	1852766
4	25	1713852	1919206	1785962	1806340
	10	1545203	1769787	1170009	1495000
	5	1415664	1667845	1069101	1384203
	1	1147892	1415267	928393	1163851
	0.5	1028906	1300164	857129	1062066
	0.1	776699	1021839	682122	826886
21	25	854402	1040939	944889	946743
	10	654593	843962	763731	754096
	5	550679	728212	657007	645299
	1	370073	501861	449818	440584
	0.5	300484	416872	366444	361267
	0.1	182256	257432	224028	221239
37	25	467158	575992	574427	539192
	10	293170	419586	406998	373251
	5	209822	302540	286658	266340
	1	117893	163501	152939	144778
	0.5	94662	137228	127882	119924
	0.1	59089	86531	79263	74961
54	25	190856	227649	222074	213526
	10	108767	128038	135086	123964
	5	83727	98660	103330	95239
	1	36642	40579	40842	39355
	0.5	33630	44532	39926	39363
	0.1	27917	35783	32165	31955

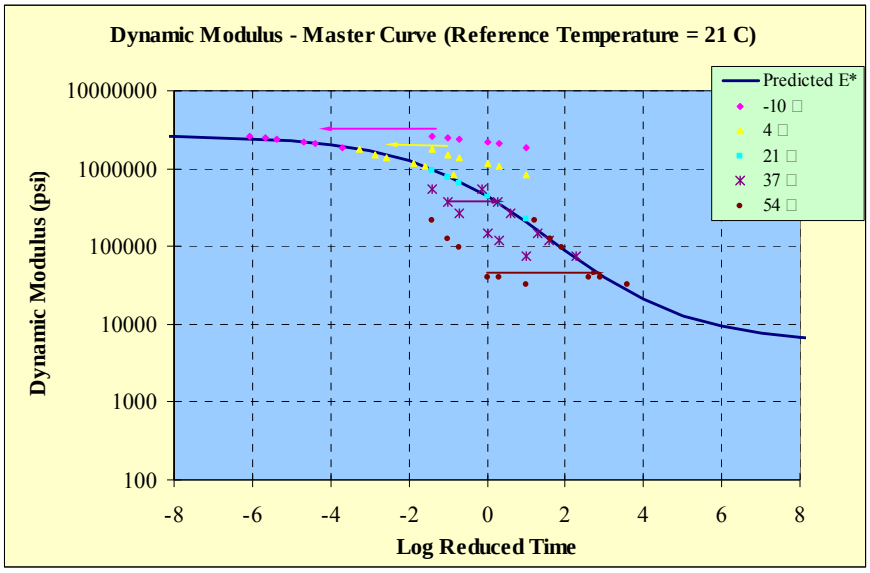

Figure B12 19.0GR76-22, N85

Table B13 9.5L/G67-22, N50

Temperature, °C	Frequency, Hz	Dynamic Modulus, psi			
		A	B	C	Average
-10	25	2264704	2976439	2669092	2636745
	10	2206261	2905678	2608500	2573480
	5	2150457	2820387	2524510	2498451
	1	1993313	2626513	2363402	2327743
	0.5	1925400	2527621	2275374	2242798
	0.1	1738866	2263323	2043558	2015249
4	25	1830206	2157326	2175660	2054397
	10	1745990	1961356	2007735	1905027
	5	1682518	1871965	1885043	1813175
	1	1442826	1580559	1593323	1538903
	0.5	1334512	1455251	1463422	1417728
	0.1	1041778	1126233	1139344	1102452
21	25	1067684	1180861	1122396	1123647
	10	866124	963855	921430	917137
	5	748466	822830	796375	789223
	1	480772	528853	521154	510260
	0.5	395381	427429	426040	416284
	0.1	230498	239798	247525	239273
37	25	499381	476248	520533	498721
	10	343686	327348	367779	346271
	5	230588	215136	257066	234263
	1	120356	112748	120826	117977
	0.5	94670	88119	98034	93608
	0.1	55150	52682	56825	54886
54	25	165628	160283	163342	163084
	10	85206	87172	85965	86114
	5	68070	48949	68947	61989
	1	32613	31716	31997	32109
	0.5	26795	26271	27945	27004
	0.1	24072	23788	23398	23753

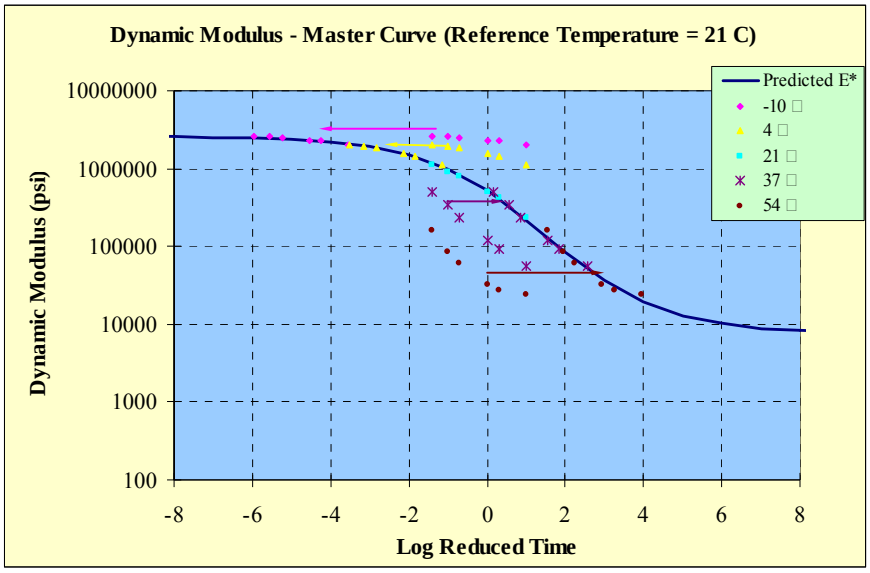

Figure B13 9.5L/G67-22, N50

Table B14 9.5L/G67-22, N65

Temperature, °C	Frequency, Hz	Dynamic Modulus, psi			
		A	B	C	Average
-10	25	3210071	2670750	2280123	2720315
	10	3083510	2568892	2201130	2617844
	5	2974653	2516115	2137212	2542660
	1	2772203	2351512	1981420	2368378
	0.5	2658030	2269562	1900742	2276111
	0.1	2375515	2044839	1709065	2043140
4	25	2456121	2153769	1813257	2141049
	10	2278385	2011372	1674493	1988083
	5	2135446	1901216	1576889	1871184
	1	1792805	1597626	1331607	1574013
	0.5	1642342	1465630	1232075	1446682
	0.1	1286223	1146494	979528	1137415
21	25	1219354	1171109	1071487	1153983
	10	1002964	961312	864596	942957
	5	866795	829699	754493	816996
	1	570227	553317	492176	538573
	0.5	472665	452227	411268	445387
	0.1	271993	262108	240138	258080
37	25	563648	566220	555164	561677
	10	381979	363533	391601	379037
	5	267063	294003	247487	269517
	1	136667	129939	124986	130531
	0.5	108079	107319	99584	104994
	0.1	63159	62866	59493	61839
54	25	199675	195865	183287	192942
	10	95208	93696	89628	92844
	5	56986	55809	51114	54636
	1	37032	36635	34018	35895
	0.5	33304	33132	31086	32507
	0.1	27203	26489	25475	26389

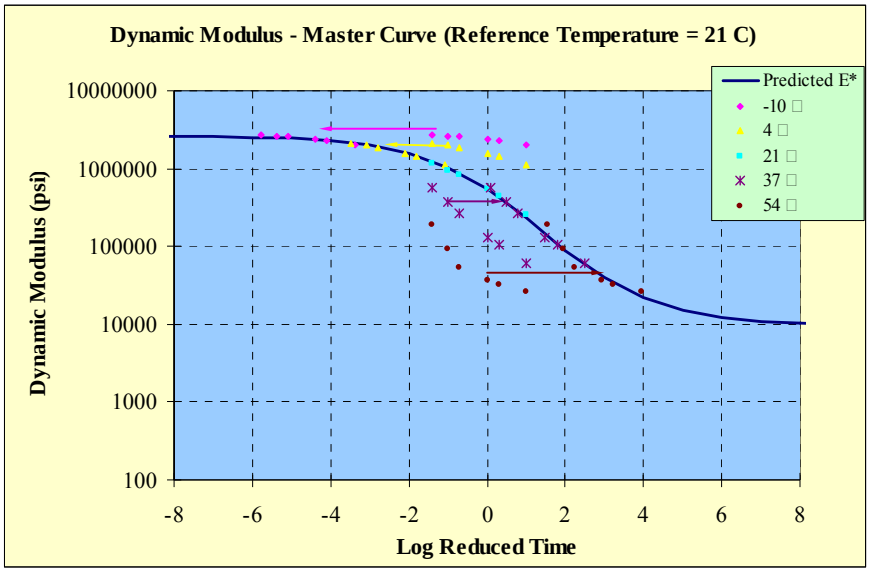

Figure B14 9.5L/G67-22, N65

Table B15 9.5L/G76-22, N85

Temperature, °C	Frequency, Hz	Dynamic Modulus, psi			
		A	B	C	Average
-10	25	2606841	3414968	3102703	3041504
	10	2337526	3255884	3136826	2910079
	5	2142889	3118185	3043354	2768143
	1	1968064	2849587	2809694	2542448
	0.5	1929776	2713896	2703952	2449208
	0.1	1659691	2387175	2402546	2149804
4	25	1847770	2233161	2440582	2173838
	10	1733496	2054855	2166073	1984808
	5	1623204	1902250	2008605	1844686
	1	1333675	1555000	1660785	1516487
	0.5	1210056	1411458	1500641	1374052
	0.1	931556	1076480	1145533	1051190
21	25	969333	1080345	1136393	1062024
	10	725974	870000	911579	835851
	5	589348	742048	779487	703627
	1	388240	486704	517545	464163
	0.5	357952	400826	426523	395100
	0.1	222362	239871	258296	240176
37	25	516094	520666	510205	515655
	10	378834	372528	319210	356857
	5	273401	229552	230916	244623
	1	142011	141745	142320	142025
	0.5	113345	115169	113286	113933
	0.1	74916	74125	72328	73790
54	25	204325	215887	210673	210295
	10	138902	126111	110109	125040
	5	101834	68352	67108	79098
	1	39313	48060	46478	44617
	0.5	45913	41162	40541	42539
	0.1	37503	36330	35227	36353

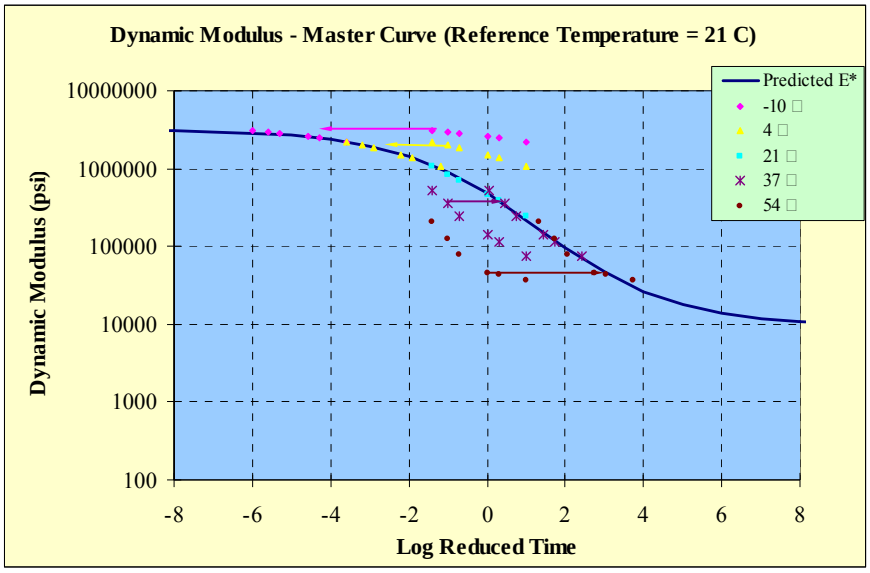

Figure B15 9.5L/G76-22, N85

Table B16 9.5L/G82-22, N85

Temperature, °C	Frequency, Hz	Dynamic Modulus, psi			
		A	B	C	Average
-10	25	2181610	1747452	1904197	1944420
	10	2126893	1678244	1731284	1845474
	5	1976890	1620987	1797570	1798482
	1	1802299	1475459	1719071	1665610
	0.5	1716277	1414886	1671791	1600985
	0.1	1483131	1255980	1425821	1388311
4	25	1799183	1455336	1665459	1639993
	10	1609429	1313549	1537492	1486823
	5	1509133	1241312	1421222	1390556
	1	1262440	1018497	1137273	1139403
	0.5	1153917	924603	1045993	1041504
	0.1	902120	701584	770856	791520
21	25	1079055	823320	908497	936957
	10	865783	664879	673054	734572
	5	753534	566580	556787	625634
	1	511317	373223	386320	423620
	0.5	424117	307105	321018	350747
	0.1	260514	189682	193468	214555
37	25	446876	369934	375334	397381
	10	276176	216900	221117	238064
	5	193985	149010	150506	164500
	1	120702	92399	91719	101607
	0.5	97526	74703	73615	81948
	0.1	61706	48783	47847	52779
54	25	153959	159263	151582	154935
	10	111773	92227	81665	95222
	5	67160	53302	48172	56211
	1	29420	30066	27312	28933
	0.5	34704	30027	29501	31411
	0.1	28652	25630	25855	26712

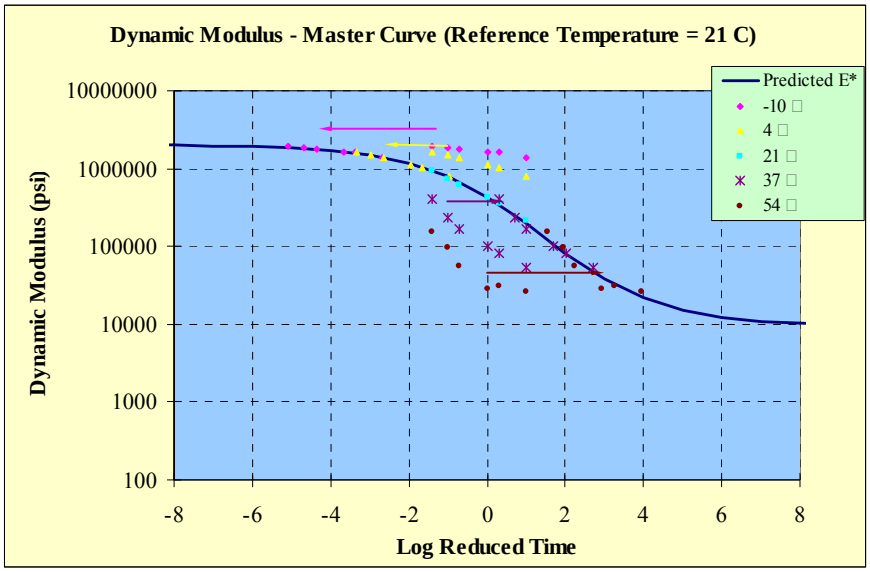

Figure B16 9.5L/G82-22, N85

Table B17 12.5L/G67-22, N50

Temperature, °C	Frequency, Hz	Dynamic Modulus, psi			
		A	B	C	Average
-10	25	3425536	3111881	3335854	3291090
	10	3172356	3069974	3256404	3166245
	5	3063921	3011057	3182311	3085763
	1	2812228	2823723	2975970	2870640
	0.5	2750457	2734619	2871921	2785666
	0.1	2424431	2501324	2613694	2513150
4	25	2696047	2335422	2497394	2509621
	10	2563497	2200371	2332580	2365483
	5	2431127	2079721	2226895	2245914
	1	2052719	1762739	1899932	1905130
	0.5	1880056	1621992	1757981	1753343
	0.1	1466377	1274692	1399519	1380196
21	25	1443260	1308484	1435765	1395836
	10	1169791	1085765	1212199	1155918
	5	1001027	938326	1056589	998647
	1	666265	635570	726825	676220
	0.5	543710	526843	601680	557411
	0.1	315333	314189	362673	330732
37	25	661429	639697	670817	657314
	10	427954	456679	486244	456959
	5	327611	326858	343403	332624
	1	158346	166384	172059	165596
	0.5	123487	130561	135880	129976
	0.1	71210	76017	76907	74711
54	25	217726	206902	225341	216656
	10	117067	99561	106406	107678
	5	64397	63047	66787	64744
	1	43336	42902	43632	43290
	0.5	37581	37187	37855	37541
	0.1	29612	28833	29001	29149

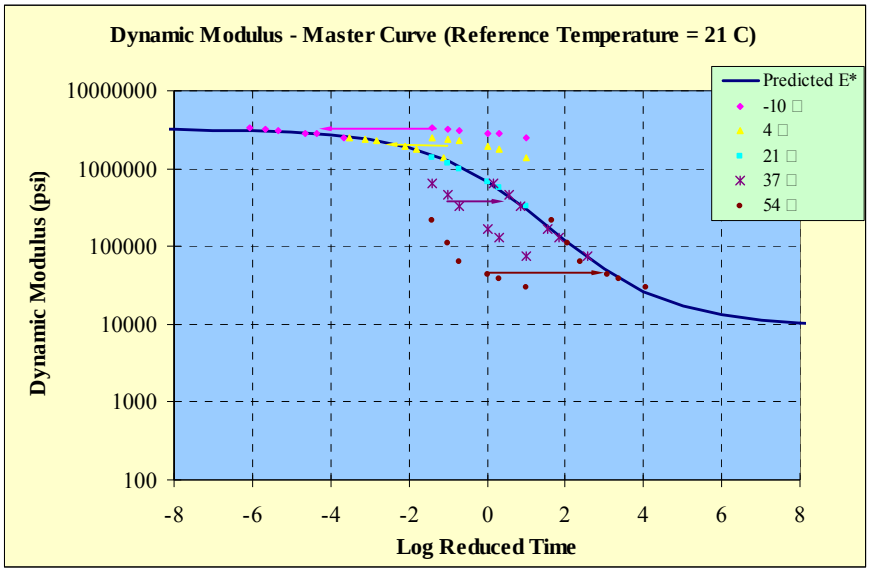

Figure B17 12.5L/G67-22, N50

Table B18 12.5L/G67-22, N65

Temperature, °C	Frequency, Hz	Dynamic Modulus, psi			
		A	B	C	Average
-10	25	3580866	2930145	3442356	3317789
	10	3493684	2844022	3346496	3228067
	5	3413561	2769644	3254954	3146053
	1	3180548	2576786	3051971	2936435
	0.5	3071841	2489510	2942839	2834730
	0.1	2785392	2268522	2676854	2576923
4	25	2578949	2225593	2499428	2434657
	10	2412441	2085255	2354930	2284209
	5	2265461	1957235	2243010	2155235
	1	1916371	1684075	1917171	1839206
	0.5	1751238	1564956	1775513	1697236
	0.1	1378754	1261497	1424238	1354830
21	25	1295659	1318478	1350097	1321411
	10	762046	1082319	1119618	987994
	5	564553	944105	968843	825834
	1	374729	655540	655022	561763
	0.5	322393	539473	538799	466888
	0.1	211314	322314	320241	284623
37	25	643814	695932	653533	664426
	10	460514	443908	428112	444178
	5	318265	347592	327161	331006
	1	164436	172919	162829	166728
	0.5	129021	138124	129801	132315
	0.1	71702	78618	75058	75126
54	25	197220	232396	215644	215086
	10	95621	112120	106293	104678
	5	61663	70863	83968	72165
	1	40881	45743	36137	40921
	0.5	33603	36639	36982	35741
	0.1	27350	30793	31090	29744

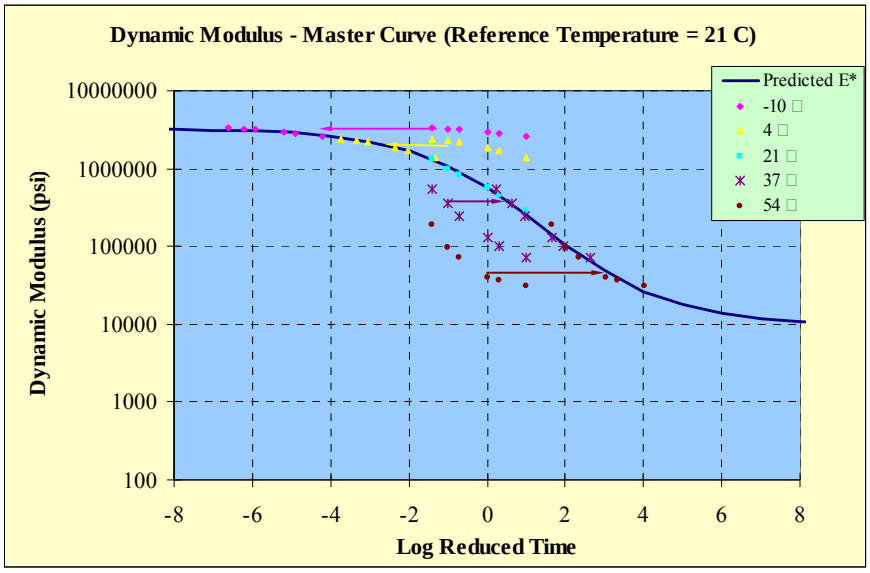

Figure B18 12.5L/G67-22, N65

Table B19 12.5L/G76-22, N85

Temperature, °C	Frequency, Hz	Dynamic Modulus, psi			
		A	B	C	Average
-10	25	3042500	2582971	1774466	2466646
	10	2900955	2496372	1699831	2365719
	5	2845888	2416386	1629779	2297351
	1	2591734	2221343	1520112	2111063
	0.5	2480450	2127605	1473911	2027322
	0.1	2204172	1899660	1327967	1810600
4	25	2081808	1782107	1565292	1809736
	10	1909067	1714074	1406898	1676680
	5	1775882	1581737	1330602	1562740
	1	1482934	1343549	1095657	1307380
	0.5	1359291	1224512	1035316	1206373
	0.1	1051972	945827	823518	940439
21	25	1109585	1009953	1079893	1066477
	10	882594	773964	845146	833901
	5	753697	658998	697440	703378
	1	514357	432261	489710	478776
	0.5	426774	351580	405113	394489
	0.1	258001	211774	251536	240437
37	25	619827	536505	583522	579951
	10	436072	367698	415085	406285
	5	298291	255212	301089	284864
	1	162404	138512	163752	154889
	0.5	136478	115723	133523	128575
	0.1	84399	73912	83357	80556
54	25	228555	217482	237552	227863
	10	117400	108741	121023	115721
	5	76396	66888	73355	72213
	1	52145	49150	52141	51146
	0.5	45377	40564	45603	43848
	0.1	37621	36011	35111	36248

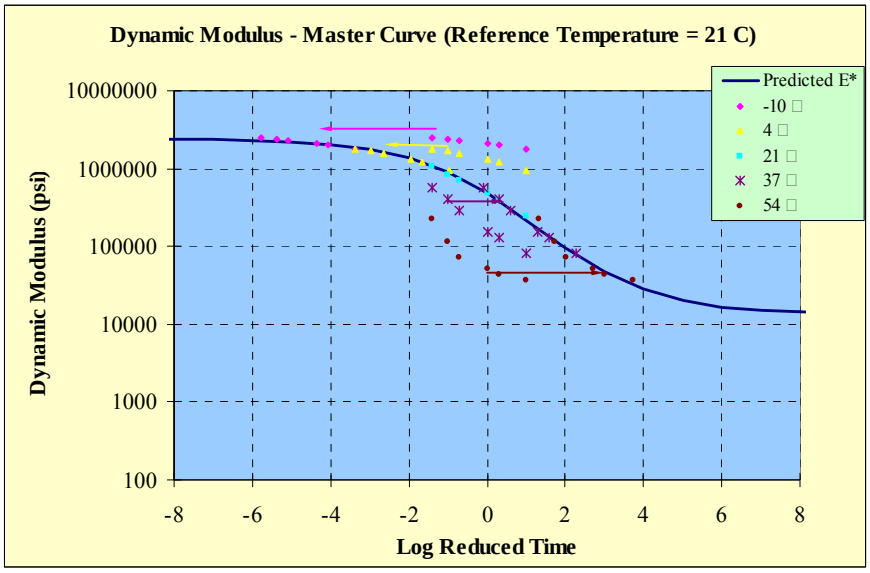

Figure B19 12.5L/G76-22, N85

Table B20 12.5L/G82-22, N85

Temperature, °C	Frequency, Hz	Dynamic Modulus, psi			
		A	B	C	Average
-10	25	2443927	2459005	2501492	2468141
	10	2333763	2373073	2419322	2375386
	5	2240015	2317827	2357657	2305166
	1	2007927	2125058	2175455	2102813
	0.5	1899459	2037616	2086484	2007853
	0.1	1631937	1768878	1830219	1743678
4	25	1669292	1725240	1763587	1719373
	10	1517296	1559849	1562605	1546583
	5	1401256	1439073	1413768	1418032
	1	1104238	1142303	1100115	1115552
	0.5	974388	1010453	962469	982437
	0.1	690079	717862	671222	693054
21	25	755844	791956	721851	756550
	10	556956	597925	525942	560274
	5	451757	493171	427996	457641
	1	270692	302545	261935	278391
	0.5	212600	237671	206056	218775
	0.1	125462	137765	215437	159555
37	25	332064	362438	353437	349313
	10	212403	244876	234996	230758
	5	162225	183118	134494	159946
	1	78325	83096	75150	78857
	0.5	65535	71002	65476	67338
	0.1	45169	47299	45690	46052
54	25	141522	156405	148772	148900
	10	70648	76360	72378	73129
	5	40736	44363	42355	42485
	1	33335	34374	34782	34164
	0.5	31267	31470	32738	31825
	0.1	27158	26019	28126	27101

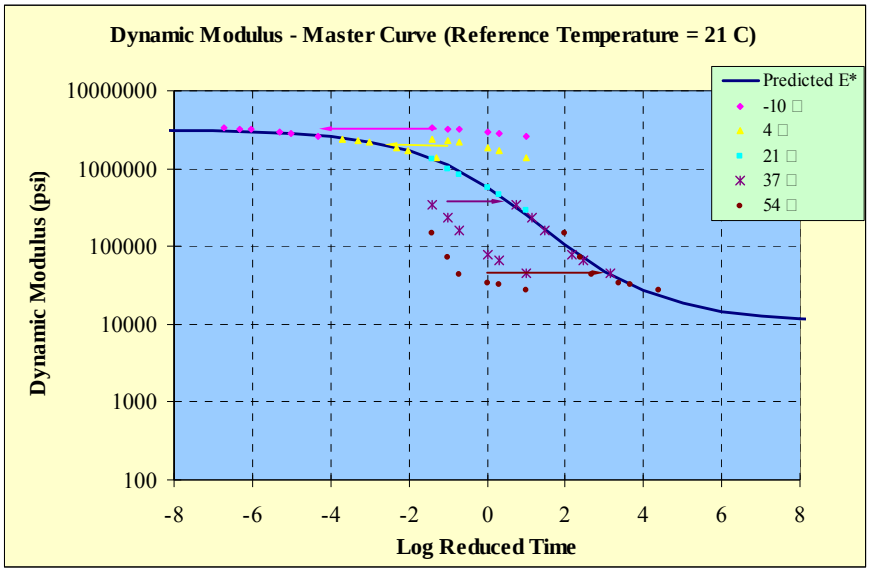

Figure B20 12.5L/G82-22, N85

Table B21 19.0L/G67-22, N50

Temperature, °C	Frequency, Hz	Dynamic Modulus, psi			
		A	B	C	Average
-10	25	2206421	3511103	3333381	3016968
	10	1883416	3464295	3210639	2852783
	5	1718303	3420124	3115310	2751246
	1	1589194	3227496	2965505	2594065
	0.5	1580135	3135439	2878556	2531377
	0.1	1479688	2888739	2654944	2341124
4	25	1613364	2499709	2587479	2233517
	10	1427078	2341396	2395730	2054735
	5	1377716	2211176	2264864	1951252
	1	1239009	1892377	1949510	1693632
	0.5	1136807	1755689	1808594	1567030
	0.1	897373	1423722	1474655	1265250
21	25	1086941	1414783	1400354	1300693
	10	880192	1184443	1181695	1082110
	5	789293	1051780	1047160	962744
	1	553484	738218	737119	676274
	0.5	482707	624430	623896	577011
	0.1	298270	390938	394911	361373
37	25	722834	780453	802372	768553
	10	466849	572847	591358	543685
	5	361379	438572	437558	412503
	1	197230	241304	236984	225172
	0.5	149925	189996	189553	176491
	0.1	84073	105249	108037	99120
54	25	238340	288418	308298	278352
	10	126039	151698	144607	140781
	5	68370	90603	92543	83838
	1	45879	57975	60882	54912
	0.5	39111	49550	52016	46892
	0.1	29907	37026	38773	35235

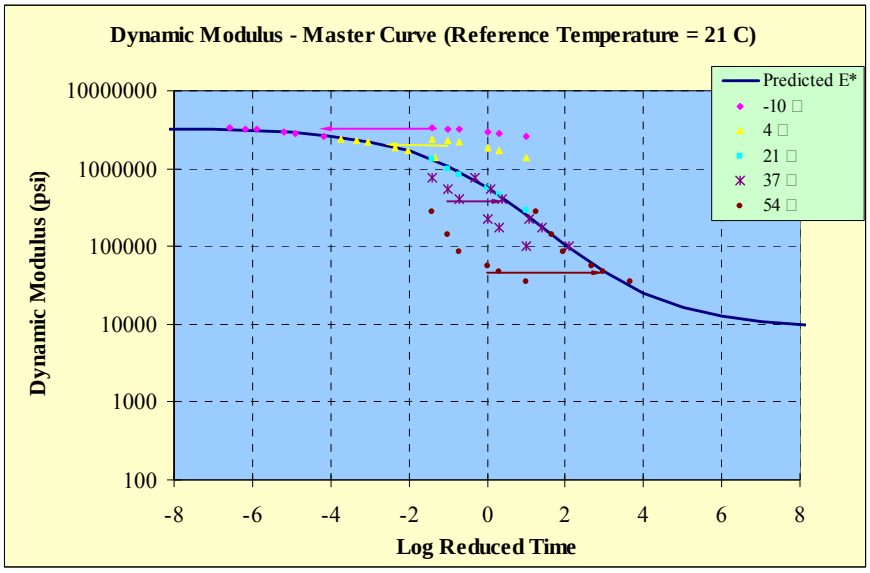

Figure B21 19.0L/G67-22, N50

Table B22 19.0L/G67-22, N65

Temperature, °C	Frequency, Hz	Dynamic Modulus, psi			
		A	B	C	Average
-10	25	3134571	3175055	2959952	3089859
	10	3056929	3115594	2868836	3013786
	5	2978308	3042892	2789158	2936786
	1	2779774	2843716	2588796	2737429
	0.5	2679848	2750208	2501054	2643703
	0.1	2450874	2519861	2277167	2415967
4	25	2316290	2470794	2213156	2333413
	10	2167567	2293593	2042508	2167889
	5	2048476	2169467	1946620	2054854
	1	1757084	1864235	1649781	1757033
	0.5	1628816	1733926	1539577	1634106
	0.1	1323464	1419091	1253923	1332159
21	25	1300624	1572599	1362128	1411784
	10	1103927	1328695	1131755	1188126
	5	982622	1166705	1001431	1050253
	1	695467	818843	693997	736102
	0.5	592717	679057	582701	618158
	0.1	379633	413918	356492	383348
37	25	762464	814125	746968	774519
	10	559020	591247	494324	548197
	5	437190	430363	399262	422272
	1	248844	226499	206521	227288
	0.5	199848	177028	168028	181635
	0.1	113643	97217	95152	102004
54	25	302360	289590	253293	281748
	10	173395	166284	125331	155003
	5	119680	87685	83035	96800
	1	61326	53492	51206	55341
	0.5	50014	45363	44872	46750
	0.1	38843	35854	34069	36256

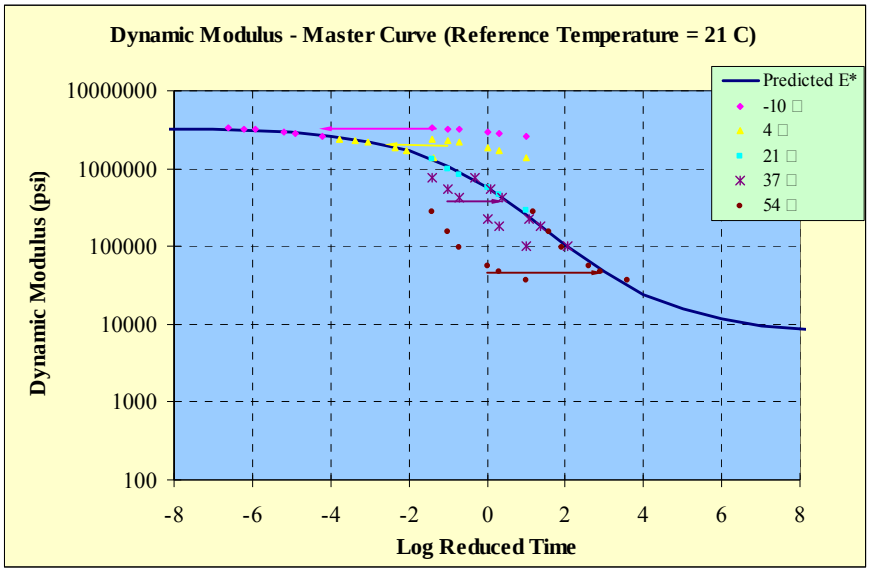

Figure B22 19.0L/G67-22, N65

Table B23 19.0L/G67-22, N85

Temperature, °C	Frequency, Hz	Dynamic Modulus, psi			
		A	B	C	Average
-10	25	3439059	3664403	2879614	3327692
	10	3384540	3619954	2840667	3281720
	5	3326361	3526351	2798875	3217196
	1	3113879	3277093	2671848	3020940
	0.5	3013342	3151228	2575016	2913195
	0.1	2739194	2858644	2359032	2652290
4	25	2332350	2601093	2264513	2399319
	10	2151498	2424596	2071354	2215816
	5	2020185	2275967	1939982	2078711
	1	1725267	1927194	1660544	1771002
	0.5	1585757	1775719	1546351	1635942
	0.1	1275355	1405221	1271377	1317318
21	25	1197080	1313840	1294657	1268526
	10	828967	1083487	1083910	998788
	5	851439	952173	960216	921276
	1	632980	652127	683126	656078
	0.5	559002	547447	589784	565411
	0.1	369664	336760	369293	358572
37	25	768146	680897	782560	743868
	10	522427	483319	564216	523320
	5	421271	351263	408392	393642
	1	230394	192636	231020	218017
	0.5	180883	151576	194486	175648
	0.1	96664	83720	105940	95441
54	25	298903	252371	291798	281024
	10	150530	129545	146478	142185
	5	82829	74824	104371	87342
	1	46014	42162	49641	45939
	0.5	46719	42197	42620	43845
	0.1	34687	32361	31991	33013

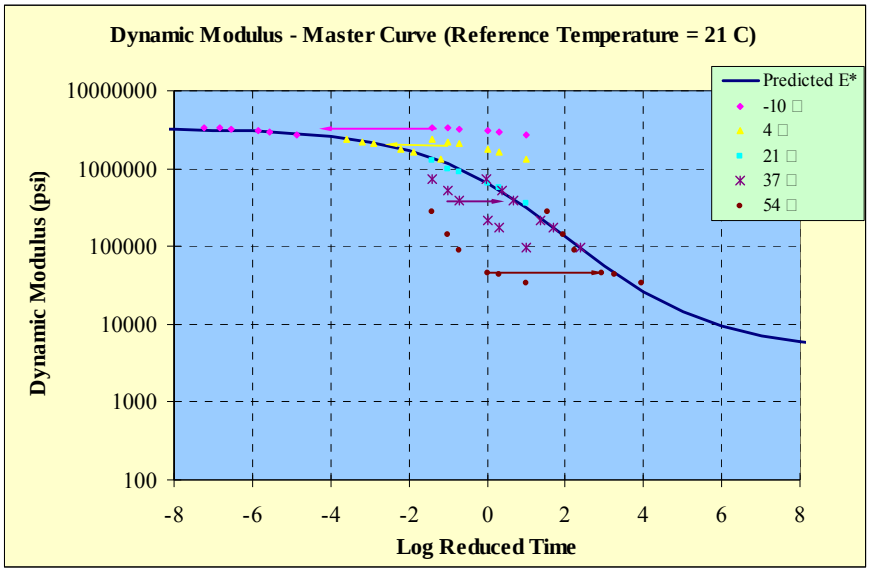

Figure B23 19.0L/G67-22, N85

Table C24 19.0L/G76-22, N85

Temperature, °C	Frequency, Hz	Dynamic Modulus, psi			
		A	B	C	Average
-10	25	2971337	3754954	2955335	3227209
	10	2920033	3572905	2831693	3108210
	5	2856994	3453443	2765743	3025393
	1	2664024	3221678	2594587	2826763
	0.5	2572948	3095566	2506482	2724999
	0.1	2323132	2798367	2247843	2456447
4	25	2060484	2507711	1998470	2188888
	10	1893987	2313922	1821684	2009864
	5	1773398	2161773	1721071	1885414
	1	1487091	1811267	1461951	1586770
	0.5	1354278	1651916	1335886	1447360
	0.1	1065224	1296830	1048031	1136695
21	25	1100648	1205898	1024085	1110210
	10	826071	986220	803293	871861
	5	736389	857317	692084	761930
	1	511315	592873	472774	525654
	0.5	427207	495000	385649	435952
	0.1	262772	308841	236546	269387
37	25	518733	579109	501284	533042
	10	331674	370490	305937	336034
	5	218790	255061	194996	222949
	1	139037	161575	123350	141321
	0.5	113472	131258	99718	114816
	0.1	74353	86347	64287	74995
54	25	264562	275047	233662	257757
	10	136493	134808	118076	129793
	5	69105	76280	61442	68943
	1	52904	59083	47031	53006
	0.5	47690	54042	42402	48045
	0.1	38312	44401	34066	38926

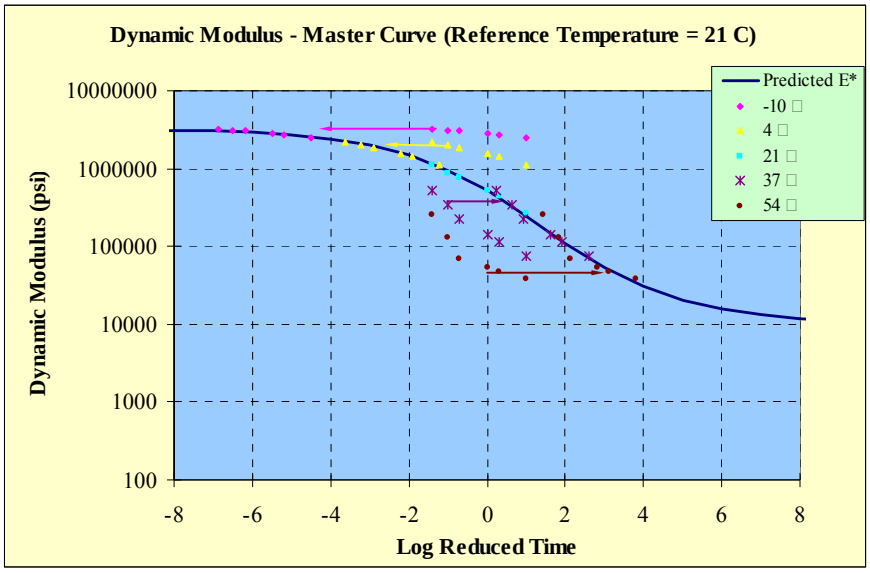

Figure B24 19.0L/G76-22, N85

Table B25 19.0GR67-22, N50 3%

Temperature, °C	Frequency, Hz	Dynamic Modulus, psi			
		A	B	C	Average
-10	25	2523419	2746261	2484936	2584872
	10	2470531	2629027	2283974	2461177
	5	2415275	2545163	2181034	2380491
	1	2215676	2331924	2087787	2211796
	0.5	2147219	2236698	2011592	2131836
	0.1	1941118	2000620	1814572	1918770
4	25	1929937	2055436	1913104	1966159
	10	1771723	1888519	1768571	1809604
	5	1645021	1768217	1645420	1686219
	1	1343722	1470083	1355061	1389622
	0.5	1219775	1347370	1226618	1264588
	0.1	941066	1050128	933642	974945
21	25	925724	1099457	795561	940247
	10	736681	884282	786782	802582
	5	632810	763159	666480	687483
	1	418446	515523	442622	458864
	0.5	343378	424709	355157	374415
	0.1	216793	261320	205475	227862
37	25	386086	475436	374749	412090
	10	264113	327583	225154	272284
	5	179285	224504	154548	186113
	1	101364	116552	87207	101707
	0.5	82062	96703	67372	82046
	0.1	51391	57377	41254	50007
54	25	163115	173525	132277	156306
	10	96894	116211	72219	95108
	5	61340	59274	39804	53473
	1	34104	33179	28860	32048
	0.5	NA	NA	NA	NA
	0.1	NA	NA	NA	NA

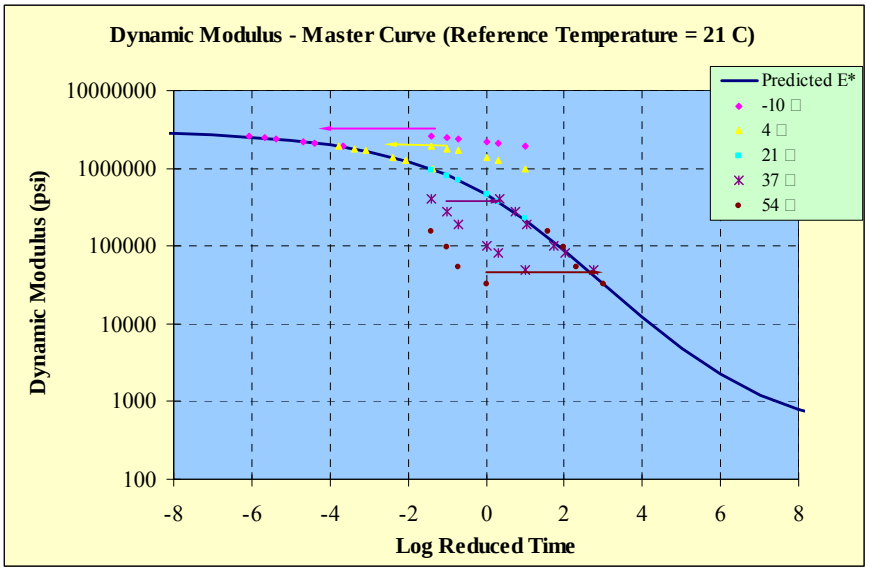

Figure B25 19.0GR67-22, N50 3%

APPENDIX C

ASPHALT PAVEMENT ANALYZER RUTTING GRAPHS

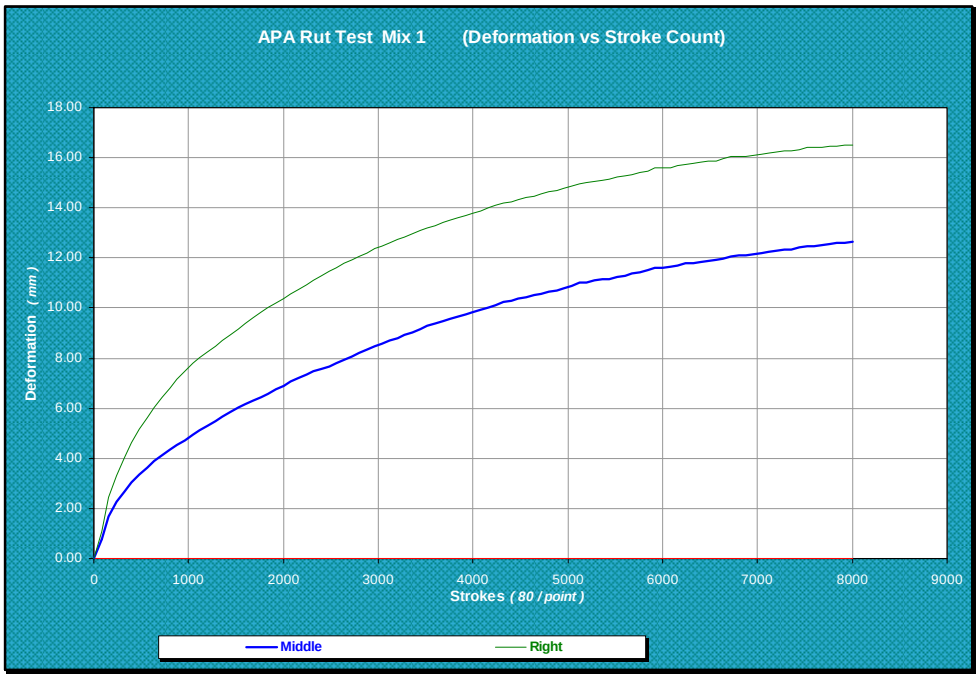

Figure C1 9.5GR67-22, N50

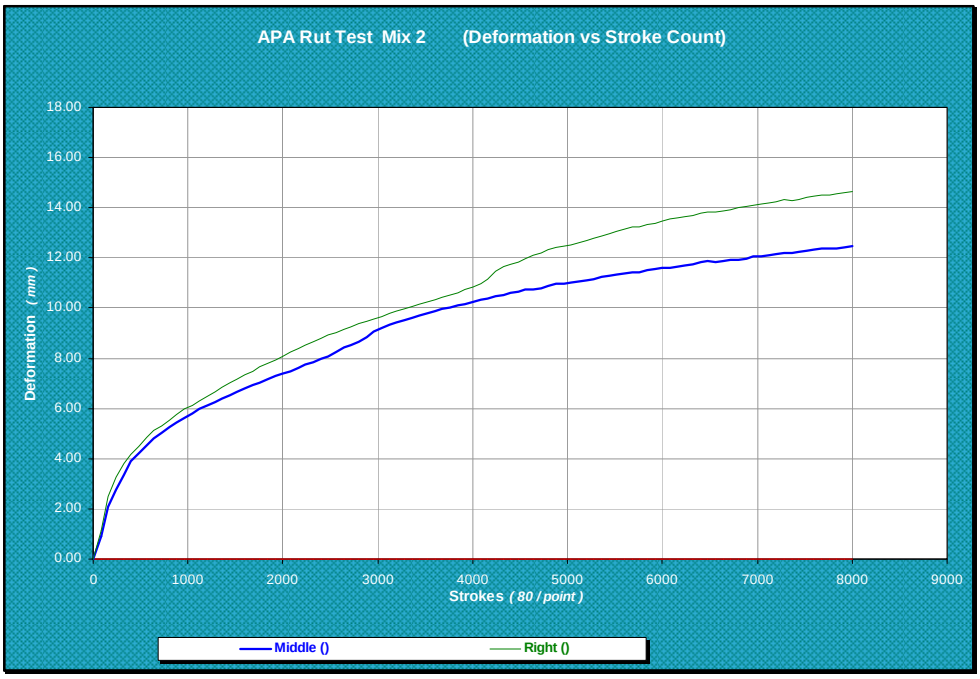

Figure C2 9.5GR67-22, N65

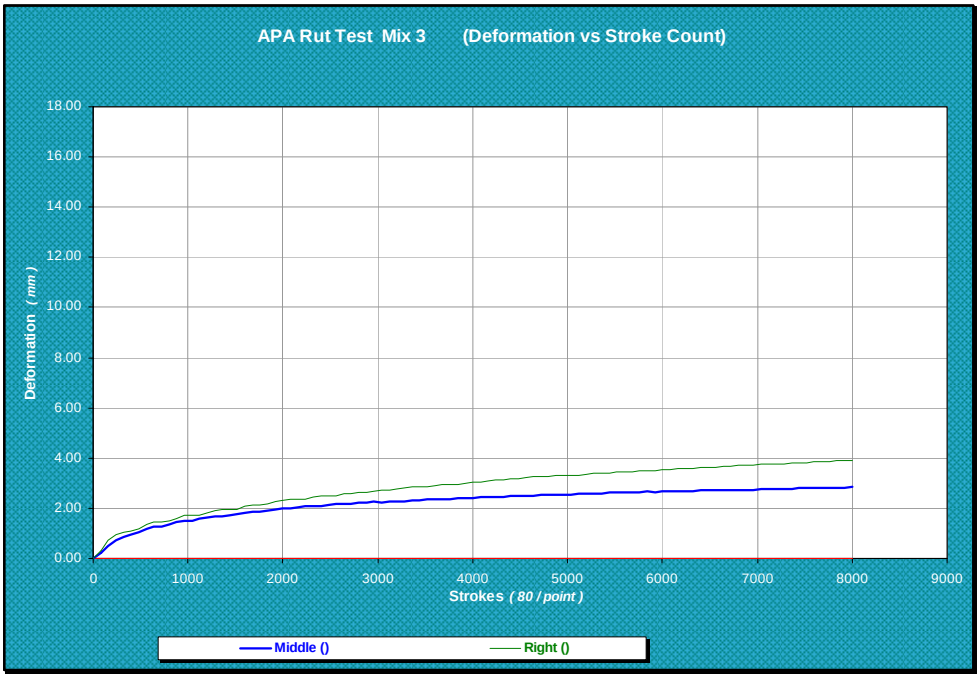

Figure C3 9.5GR76-22, N85

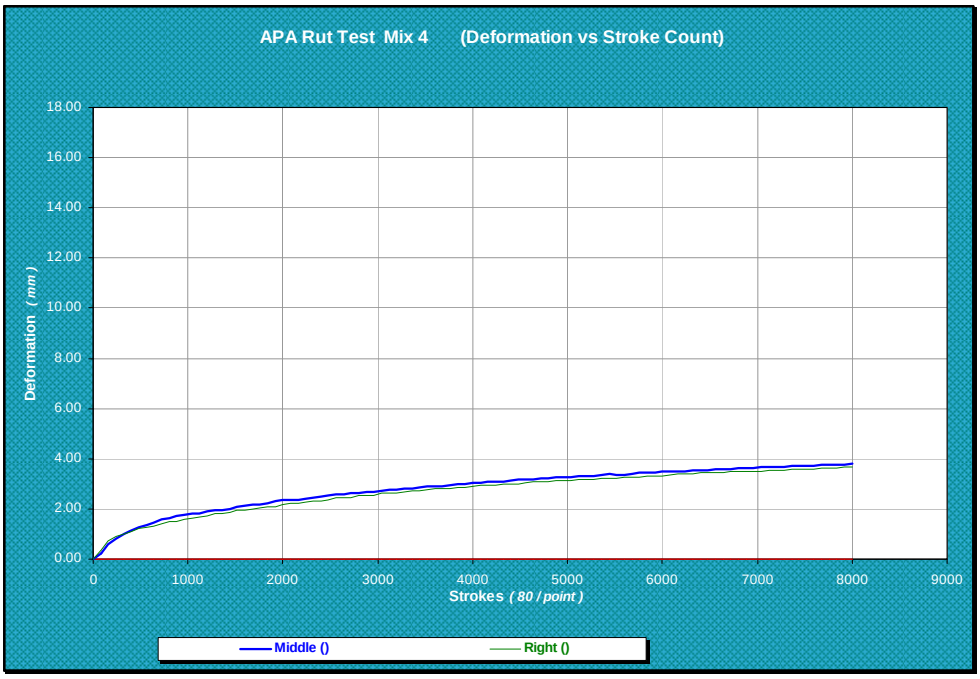

Figure C4 9.5GR82-22, N85

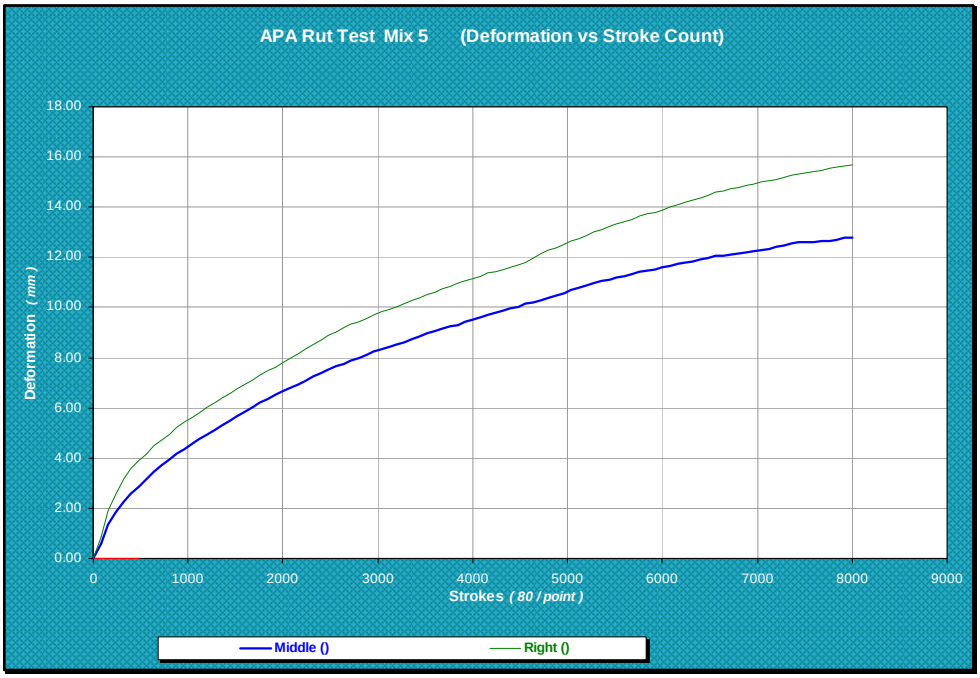

Figure C5 12.5GR67-22, N50

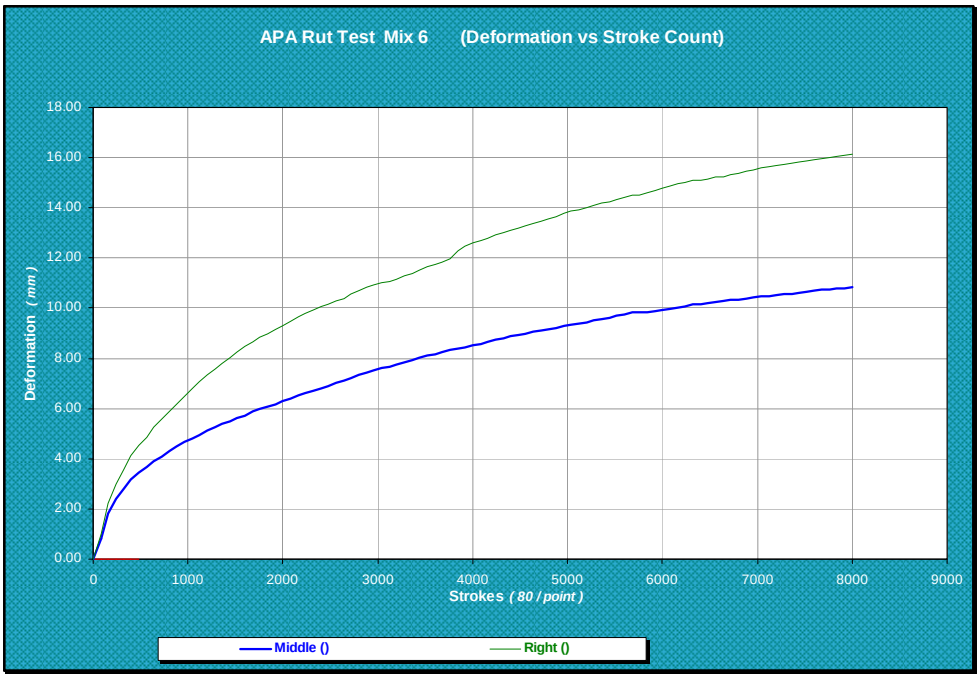

Figure C6 12.5GR67-22, N65

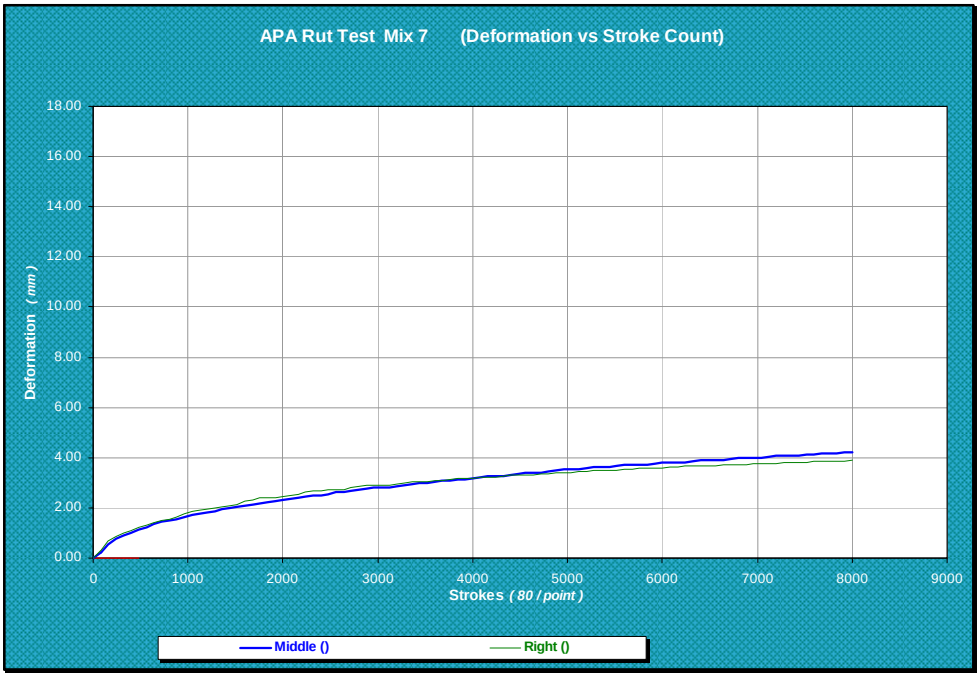

Figure C7 12.5GR76-22, N85

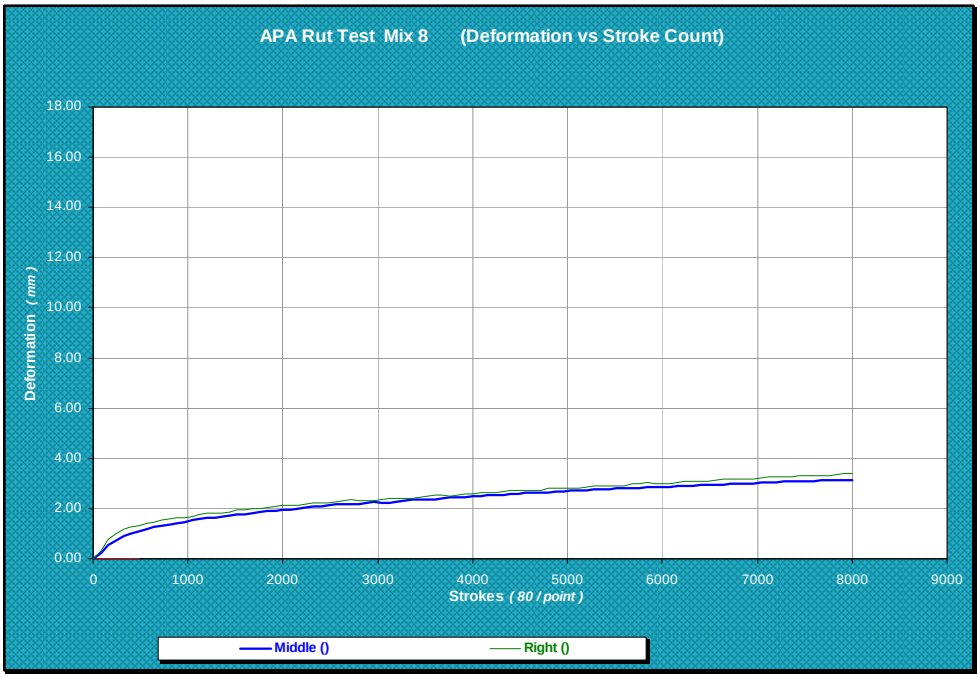

Figure C8 12.5GR82-22, N85

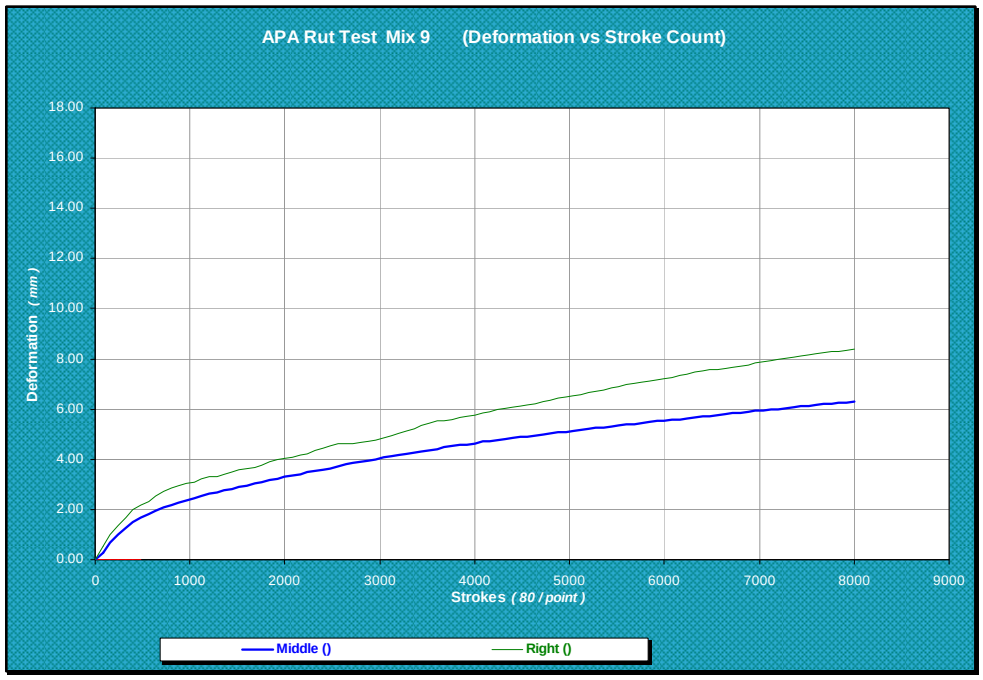

Figure C9 19.0GR67-22, N50

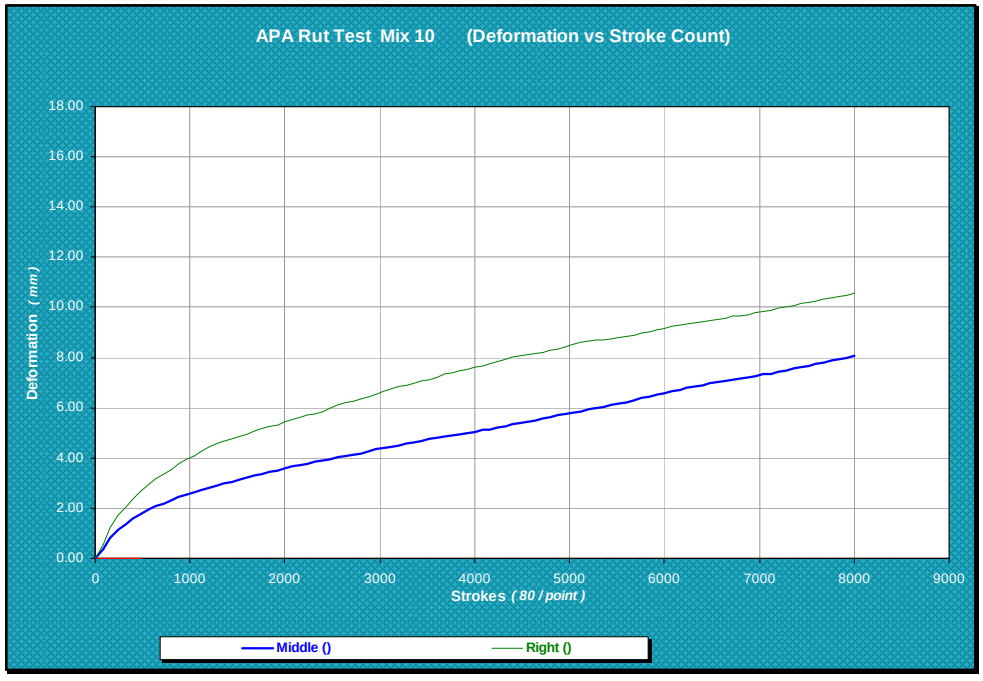

Figure C10 19.0GR67-22, N65

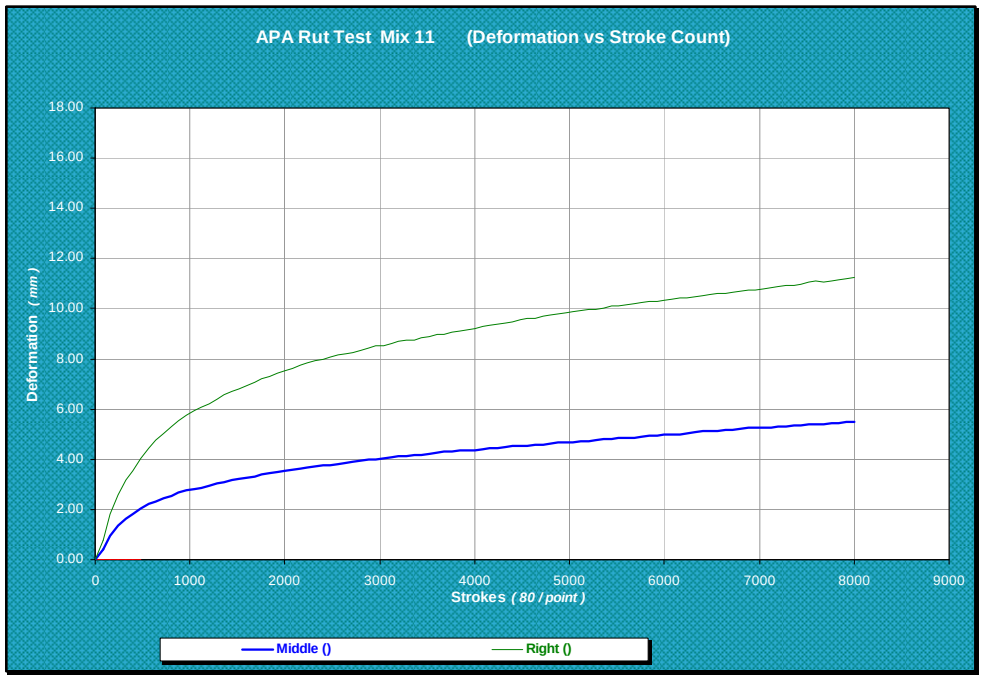

Figure C11 19.0GR67-22, N85

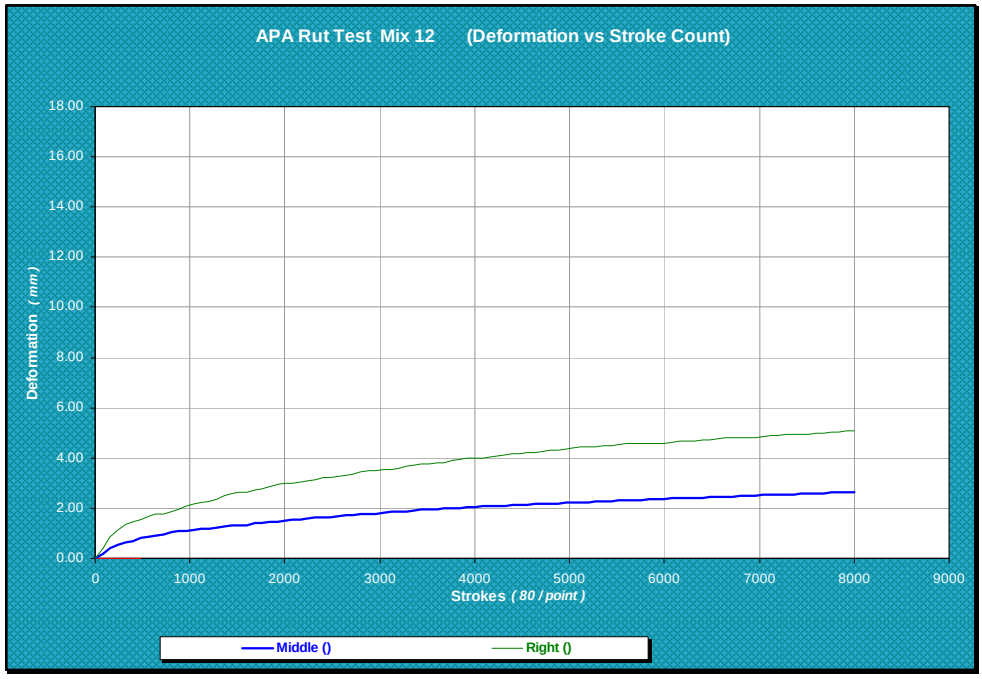

Figure C12 19.0GR76-22, N85

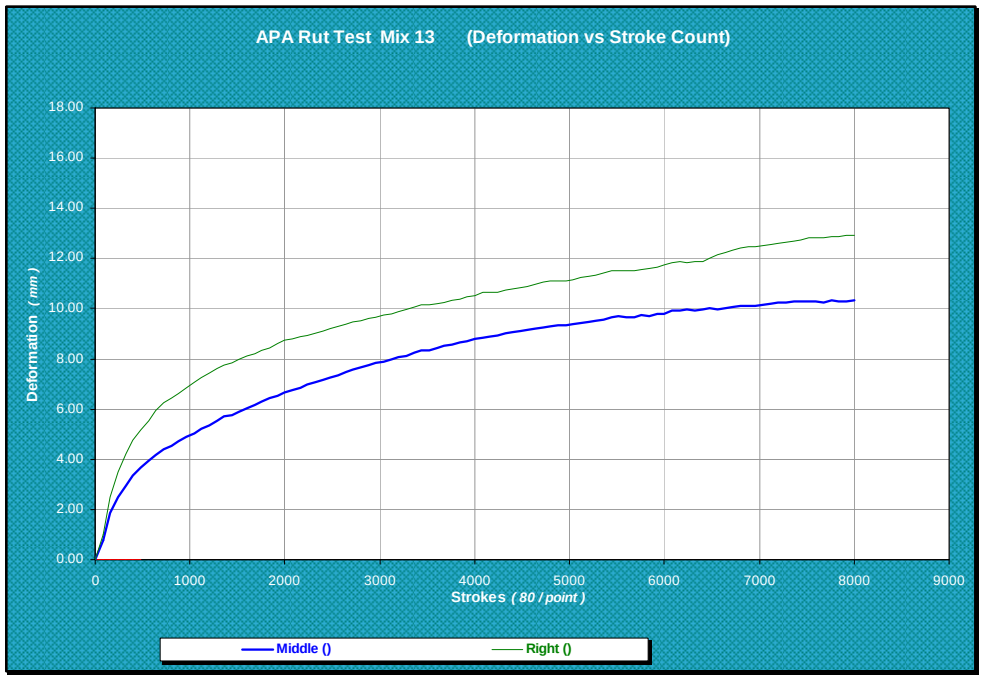

Figure C13 9.5L/G67-22, N50

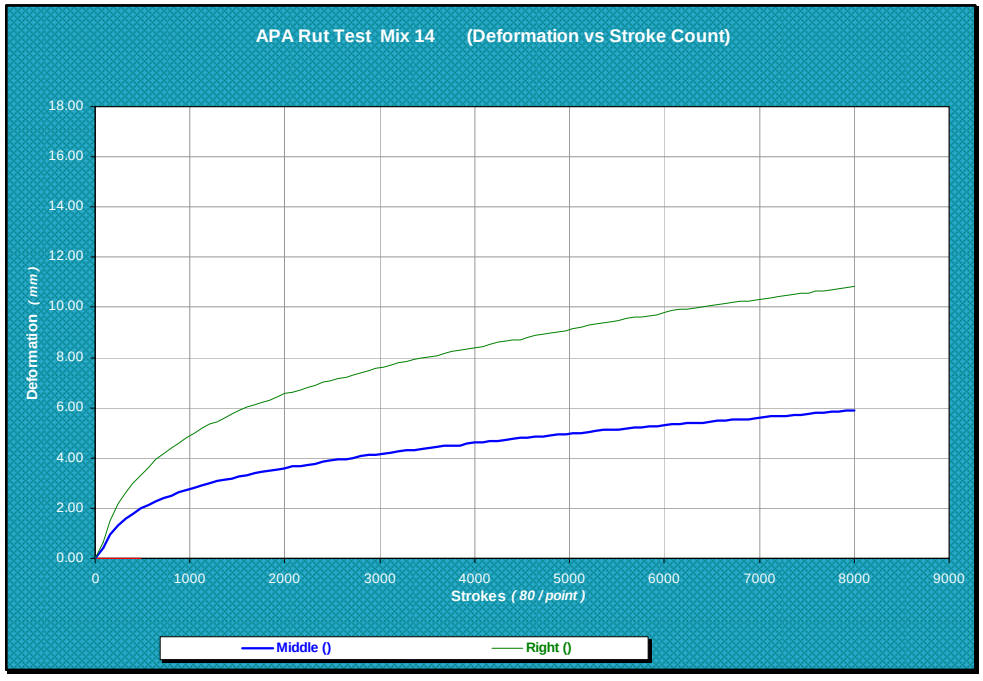

Figure C14 9.5L/G67-22, N65

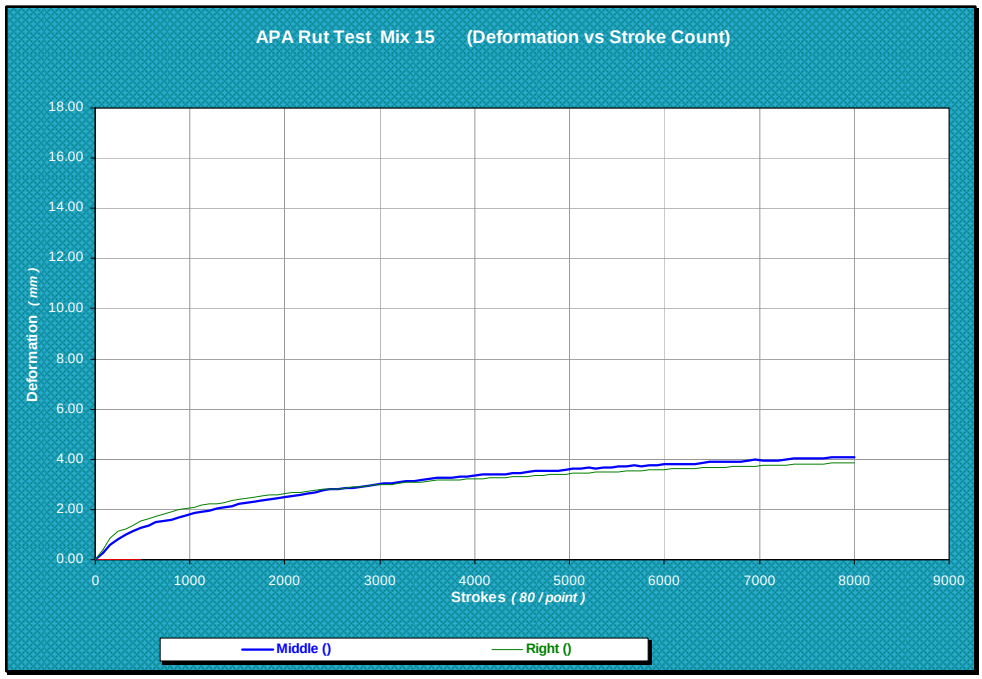

Figure C15 9.5L/G76-22, N85

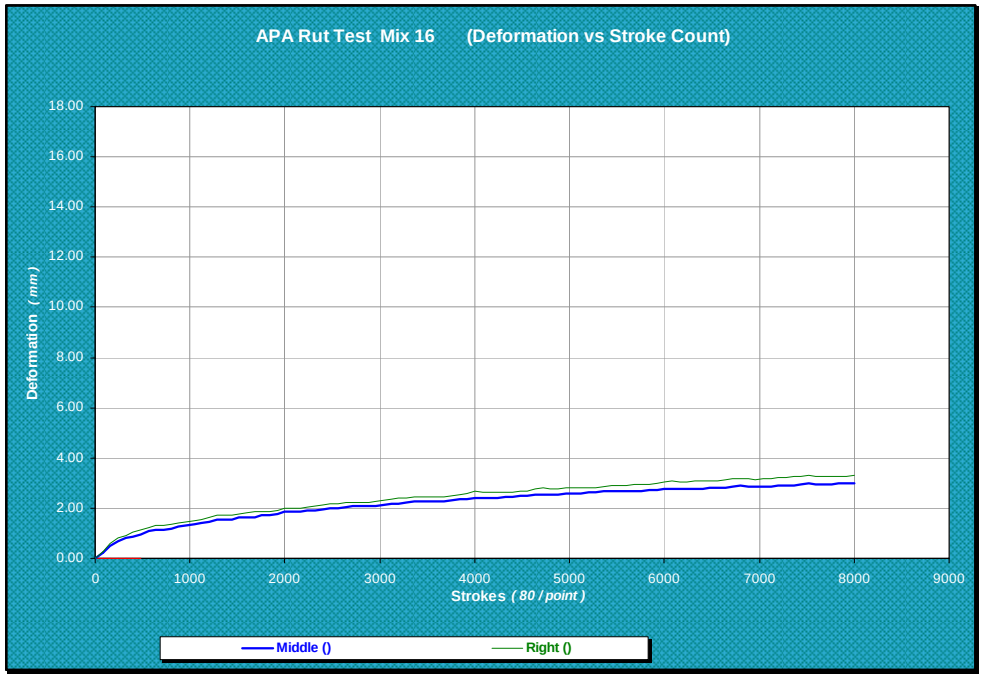

Figure C16 9.5L/G82-22, N85

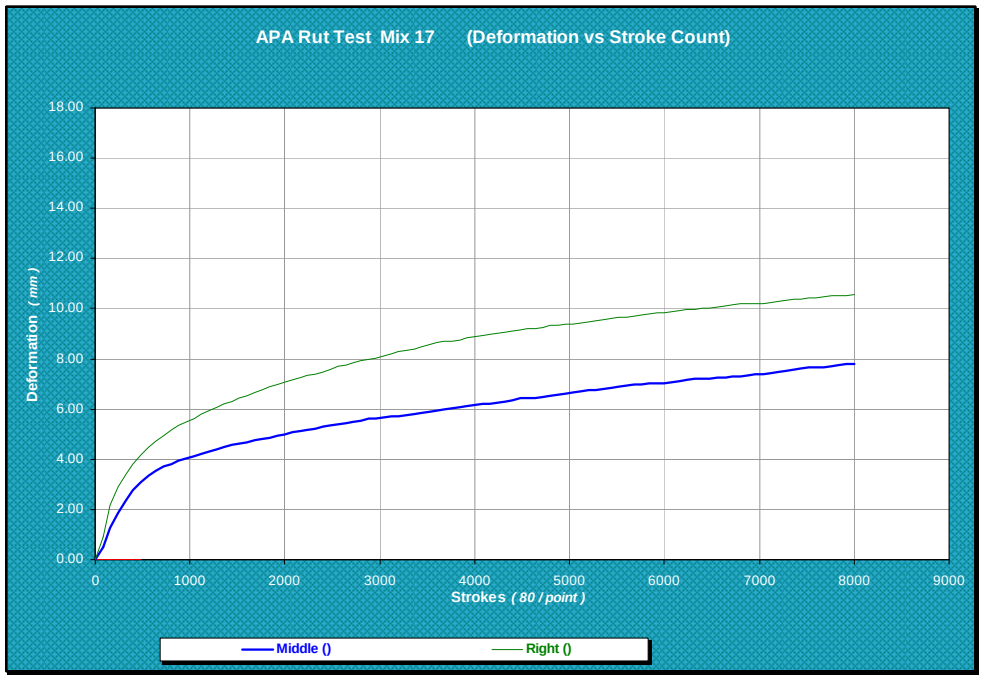

Figure C17 12.5L/G67-22, N50

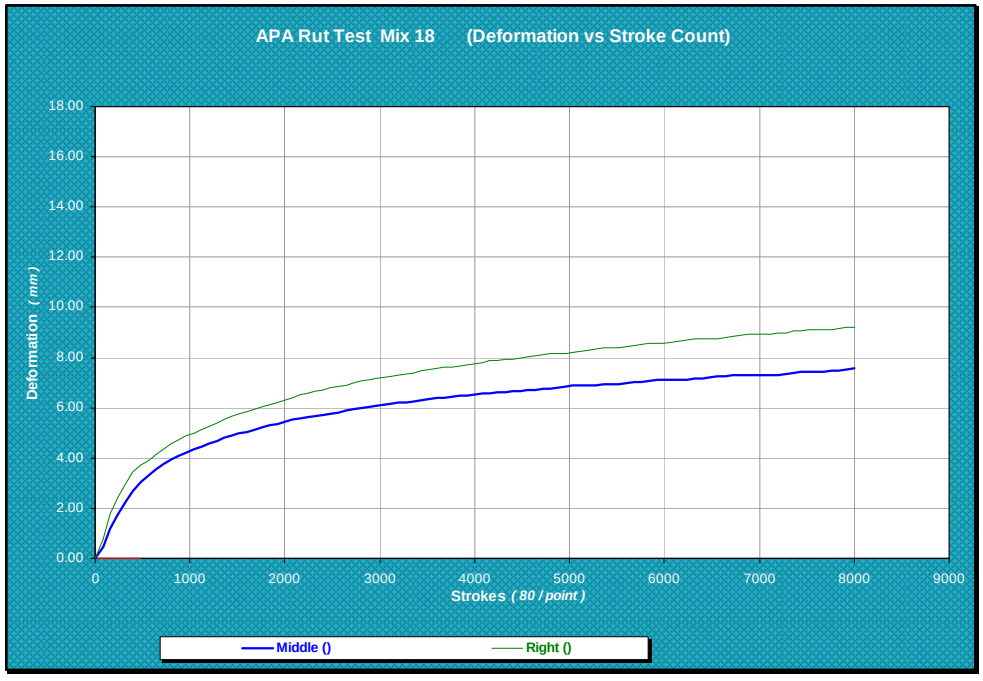

Figure C18 12.5L/G67-22, N65

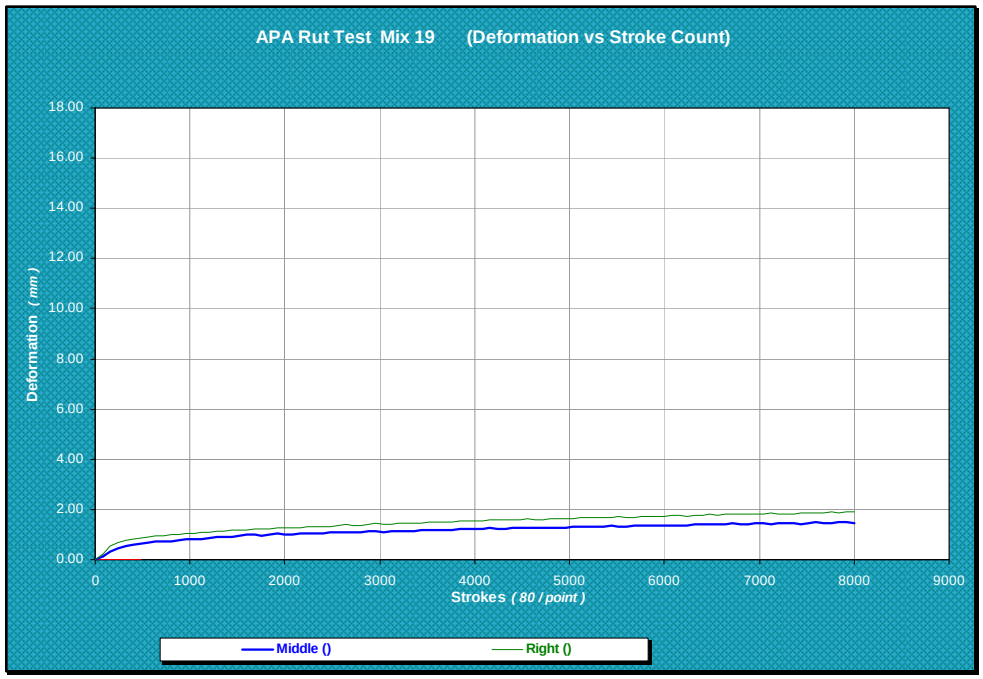

Figure C19 12.5L/G76-22, N85

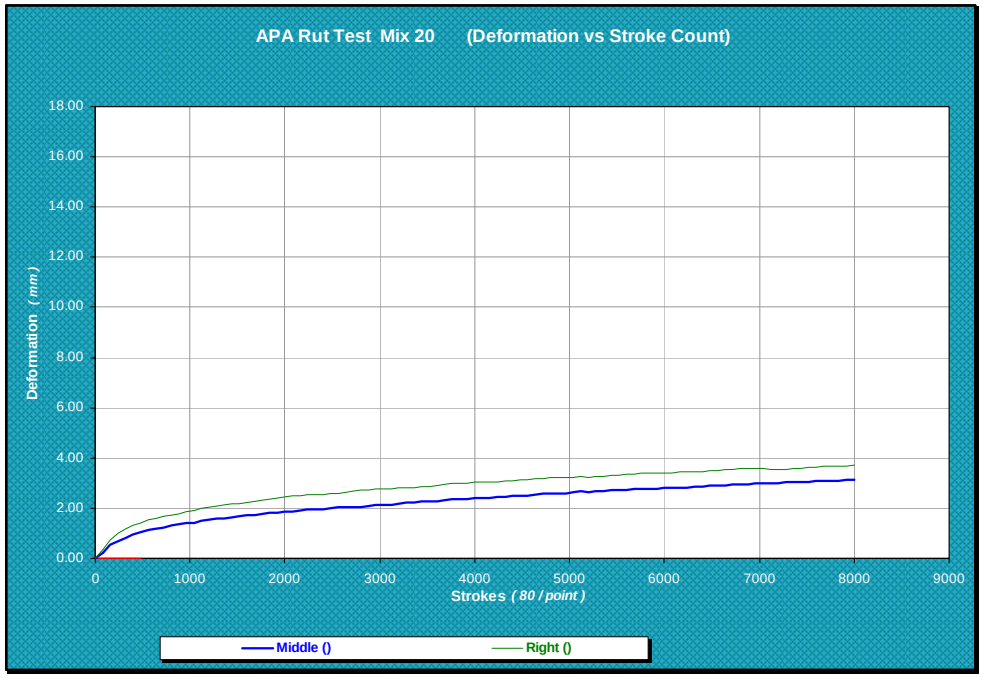

Figure C20 12.5L/G82-22, N85

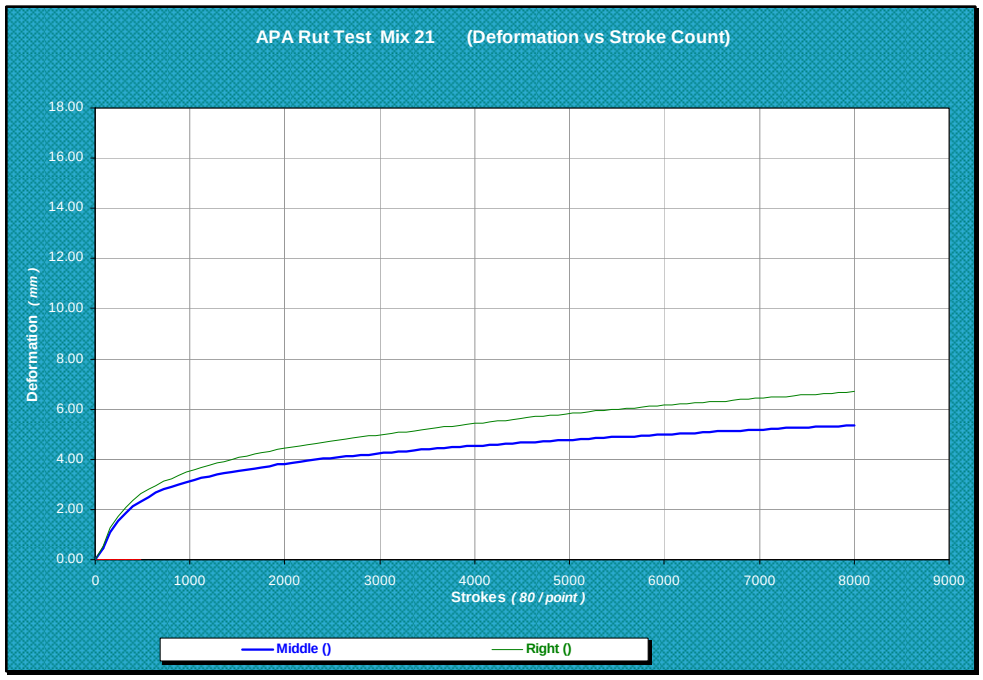

Figure C21 19.0L/G67-22, N50

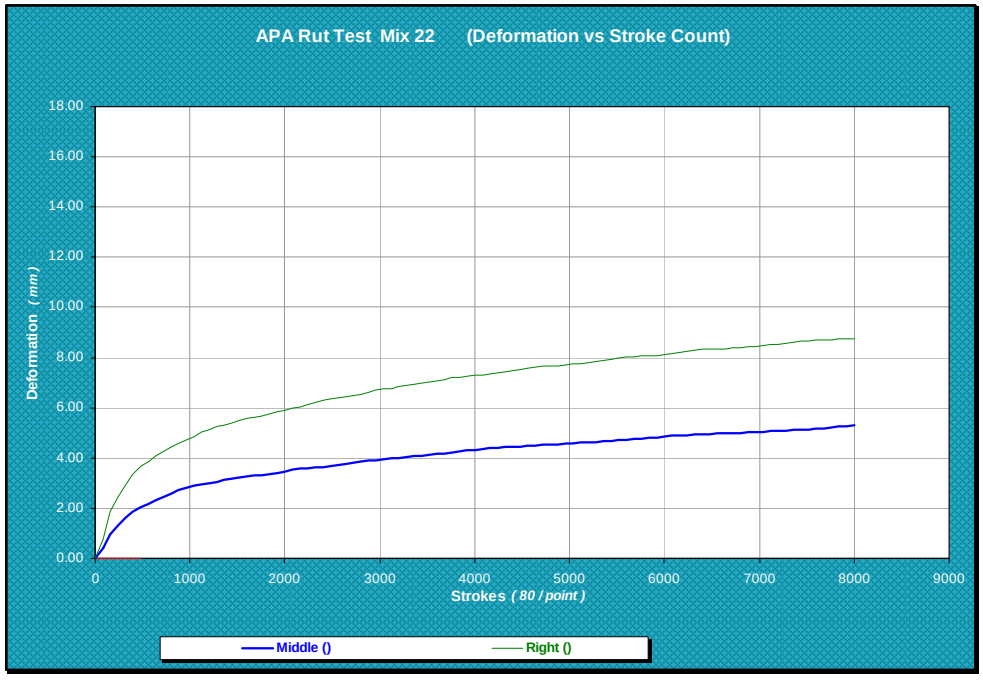

Figure C22 19.0L/G67-22, N65

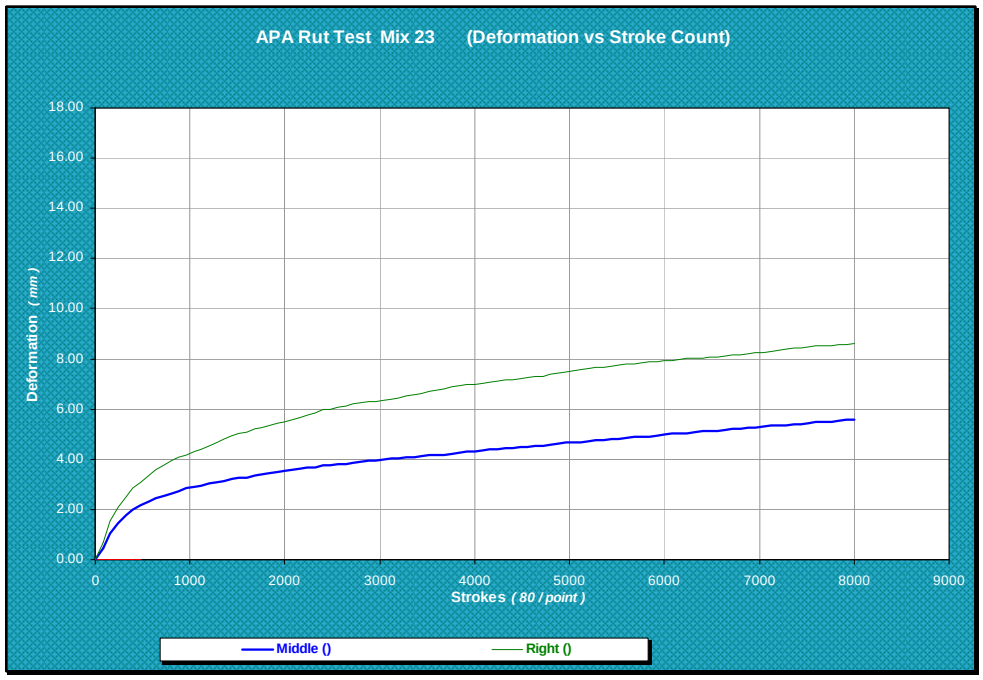

Figure C23 19.0L/G67-22, N85

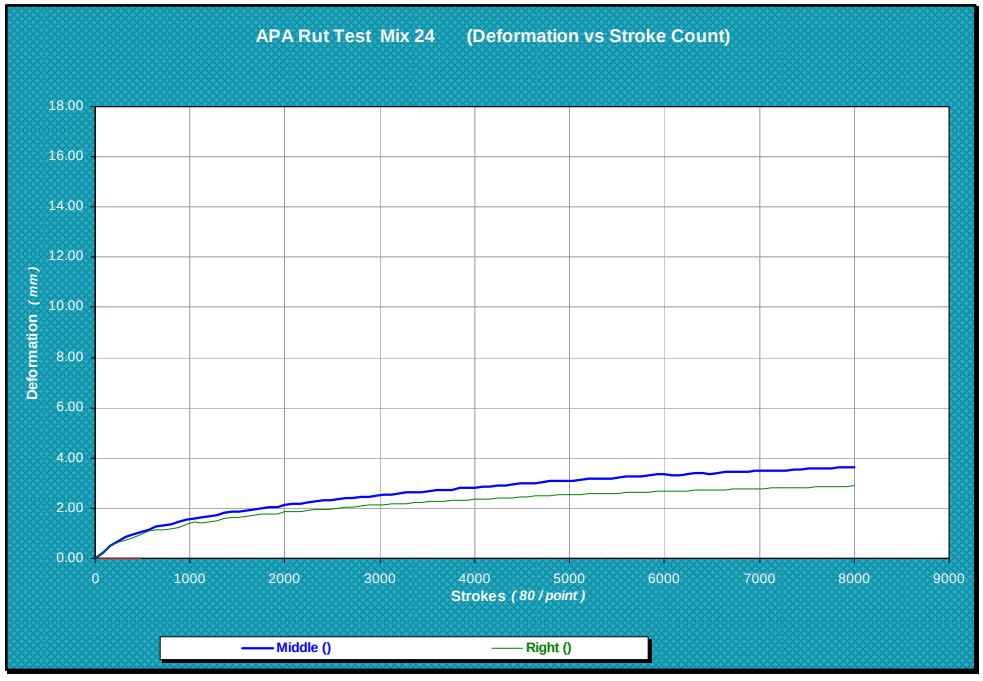

Figure C24 19.0L/G76-22, N85

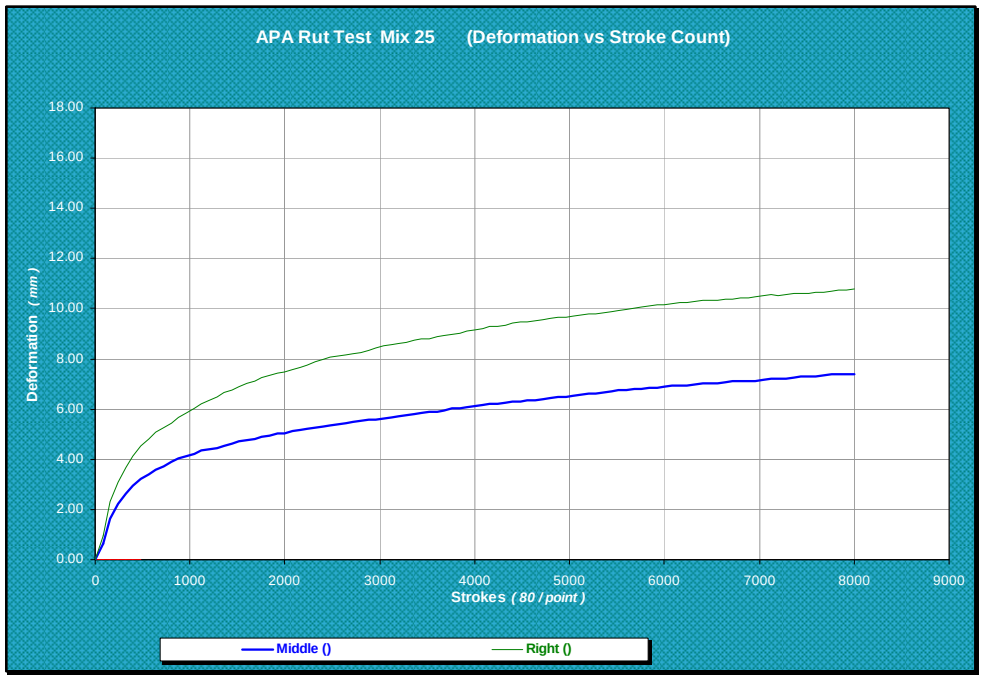

Figure C25 19.0GR67-22, N50